the automatic train speed control, allowing headways down to 60 seconds at the top speed of 72 km/h[171]. High thrust and deceleration were possible since force transmission did not rely on the steel wheel on rail interface.

Following successful system evaluation it is planned to build two lines in Toronto, both about 6km long, one linking Union station with southern Toronto, and the other connecting industrial and residential zones in Hamilton.

2.5.1.6 Brush-British Rail Mickleover Tests

Brush Electrical Machines produced an experimental axial flux LIM under contract to the Department of Industry[157,172-3]. The machine, which could generate up to about 3kN of thrust was tested on the British Rail Research site at Mickleover near Derby, in 1976, with Brush and British Rail cooperation. 240 metres of aluminium reaction rail were laid on the top cheek of a steel I beam placed between a conventional duorail. The stator weighed 263kg and was supported on load cells to a bogie of a self powered two car rail set. On board conditioning consisted of a Brush 375kVA twelve pulse voltage fed inverter, with a resonant power controlled chopper to vary the dc link voltage. Tests could be performed with the train set running at a constant maximum speed of 80 km/h, and the motor taken through motoring, plugging and regenerative braking by setting the slip through the inverter frequency control. Machine details are given in Table VI.

A variety of track joints were tested to investigate their importance on the eddy current patterns in the secondary. Forced air cooling was employed to give up to three times the power output from an uncooled stator. Maximum apparent efficiency at 12mm air gap was 0.31.

2.5.2 Linear Synchronous Motors

The LSM in this section all have passive iron secondary track structures, with iron cored primaries carrying one or two superimposed windings. The

homopolar inductor and heteropolar linear synchronous machines (HLSM and HELSM) both have an ac and a dc winding which allows a theoretical unity power factor operation, as far as any on board converter is concerned. The linear reluctance motor (LRM) and its variants use the track saliency to provide reluctance interaction with a single ac primary winding. The LRM has a low power factor, since air gap magnetization is derived from the ac supply, but its overall performance is theoretically superior to a LIM. The existence of substantial normal forces have suggested that these LSM and the LRM may be used as combined suspension and propulsion systems.

2.5.2.1 Heteropolar Linear Synchronous Motors

The original HELSM was proposed by the North American Rockwell Corporation[174]. The "Nadyne" track structure consisted of the claw-pole arrangement, where alternate north and south polarized blocks were connected to outboard longitudinal rails as shown in Figure 7. The dc magnetization was produced by a field winding establishing a transverse flux into the side rails. Within the field C core an axial flux armature winding produced the ac mmf wave linking the alternating north and south claws, and provided the closing path for the field flux. The machine consequently has a relatively long magnetic path, and a doubling of the air gap length.

Claw-pole machines were supplied by Rockwell to Disney World for a synchronous low speed operation. Due to difficulties with drift of the analogue control system the machines could not be made to operate synchronously so the dc winding was left unenergised and a reaction rail built in to allow induction motoring. It was hoped that at a later stage digital control would enable the inverters to track the vehicle motion successfully.

US DOT funding since 1973 prompted Levi to include the claw-pole machine as a more promising alternative to SLIM for high speed ground transport propulsion[175-8]. In the preliminary study the claw-pole showed a

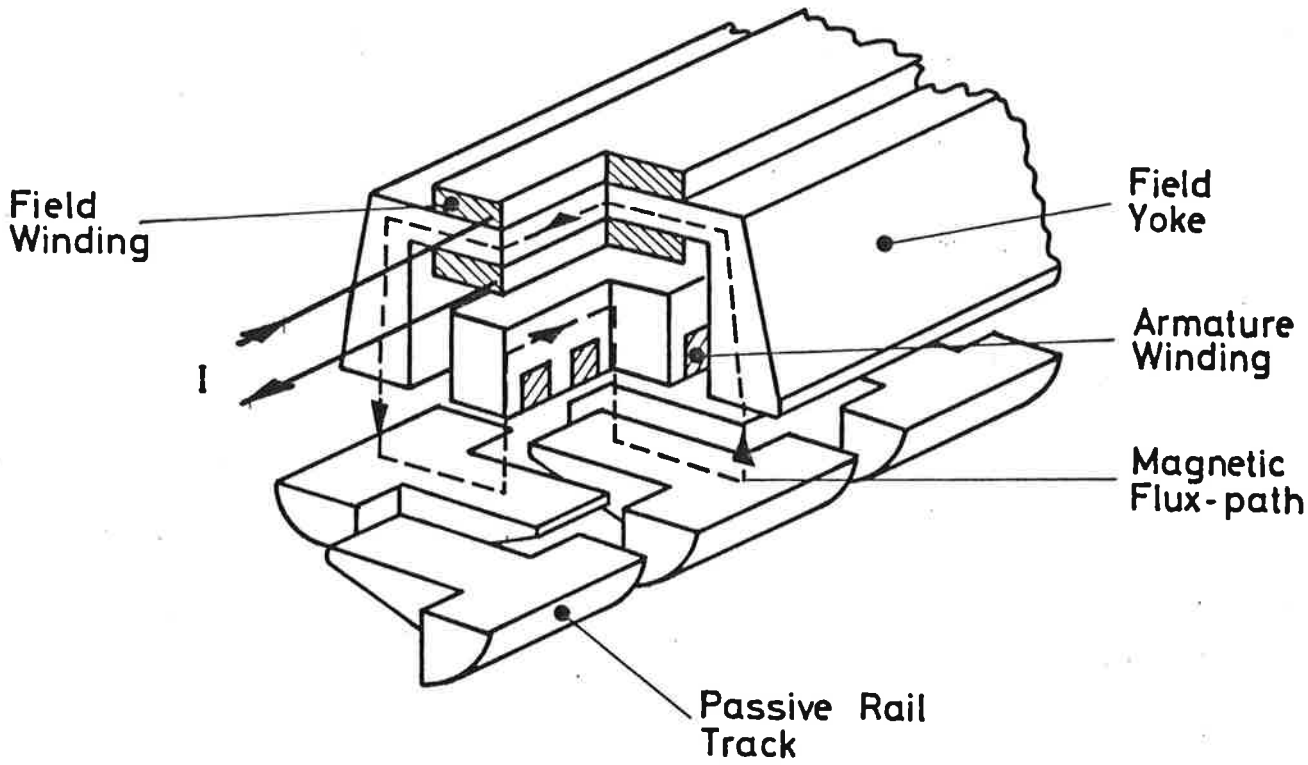

FIGURE 7. CLAW POLE MOTOR

power to weight ratio of 5.5 compared to 3.7 for HLSM and 2.5 for SLIM (kW/kg). A further 30 month exploratory study by General Electric for a 400 km/h, 5000hp comparison[179] suggested that this ratio should be modified to HELSM 0.48, HLSM 2.9, SLIM 0.9. For this reason the HELSM development ceased, and emphasis was placed on the HLSM in USA.

Levi also considered another form of heteropolar machine, in which the field windings and the armature windings produced fully longitudinal fluxes (Figure 8)[178]. The track members are more simply made, but now require a fine lamination because they see high frequency alternating flux as the vehicle passes. This configuration only received a cursory examination before it was discarded as unsuited to ground rail transportation, because of increased track complexity.

Eastham designed a modified heteropolar machine based on a transverse flux core[180], where both the ac and dc winding fluxes were strictly transverse (Figure 9). The track structure then became simpler, being only staggered slabs of iron without side rails. A laboratory static model was built, followed by an arch motor mounted on a drum. Initial tests[181] suggested that a fixed torque angle of 90° provided maximum output at near optimum efficiency, and that pole shaping and coarse lamination could improve power factor by reducing the longitudinal edge effect.

Brush built two motors based on Eastham's transverse flux principle but, to ensure mechanical rigidity used an axial flux longitudinally laminated core and side limbs with keyed in transverse laminated back iron carrying the dc winding[172]. The linear motor had 5 poles and ran at a 10mm gap on the 80m test track at Brush[182] (Table VI). Several different pole shapes were tested as well as the original rectangular design, including T's and trapezoides. The trapezoidal poles attempt to maximise the useful plan area of the air gap, decreasing the effective reluctance at both the edges and centre. Search coils indicated that the flux paths were not wholly transverse as expected, and that a partly axial path was followed.

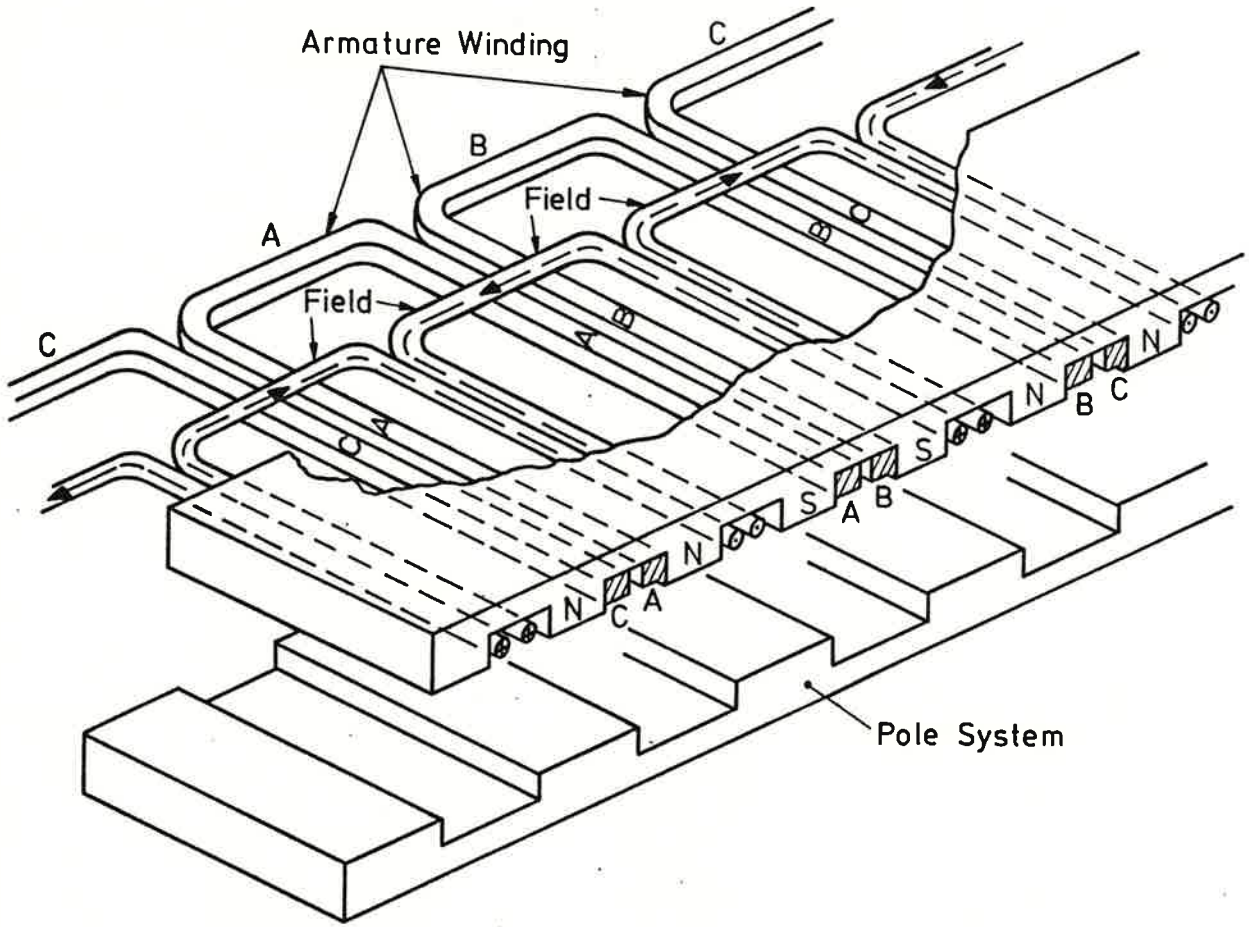

FIGURE 8 HETEROPOLAR INDUCTOR MOTOR

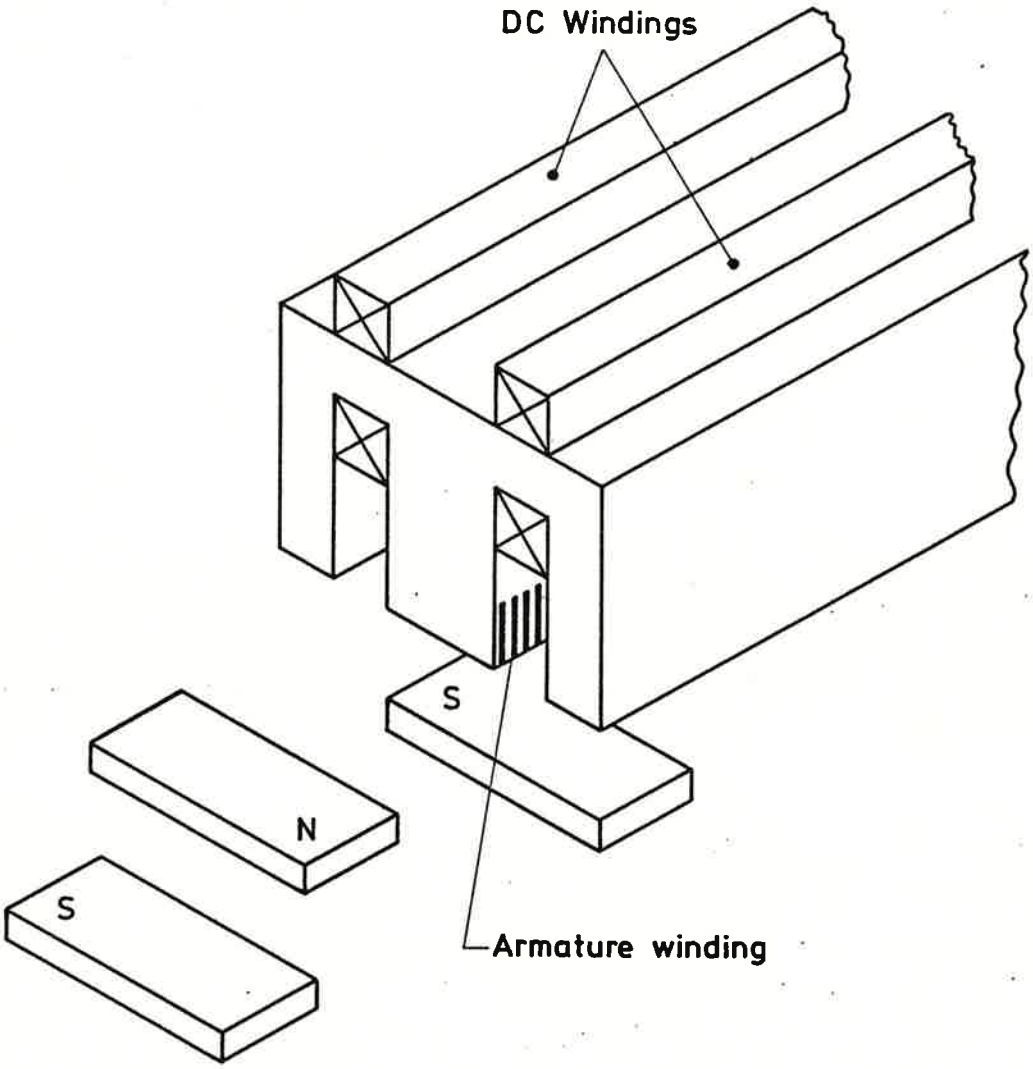

FIGURE 9 ABERDEEN TRANSVERSE FLUX HETEROPOLAR MACHINE

An improved core design with pole face windings on the outer limbs for the dc magnetization, solid back iron and axial flux centre limb was suggested for future designs.

The rotary version was tested at Nottingham University, and was built as a six pole arch motor reacting on a 1.1 metre drum (Table VII). It showed up the weakness of the design in that only about 11 percent of the dc coil flux reached the slotted armature core[183]. Computation and test allowed pole shape optimization to be performed, with final close agreement between experiment and calculation. Work continues at Nottingham to design and test a HELSM which combines levitation with propulsion, to meet the Science Research Council Advanced Ground Transport Panel's specification for a 72 km/h, 3 tonne vehicle.

2.5.2.2. Homoplar Linear Synchronous Motors

Kemper's scheme for combined levitation and propulsion was based on a HLSM[11]. The track consisted of an iron rail with side staggered poles which were cross magnetised by a dc winding on the back of an axial flux parallel pair of armature laminations (Figure 10). The armature slots were filled by straight through windings. Separate guidance magnets reacted against a vertical iron plate placed above the main rail. Nearly two decades later, Leitgeb at Siemens followed on the development with double sided designs for combined propulsion and guidance, which had the advantage of a very simple rectangular block track structure[184,185]. The LSM was to be used on an urban vehicle H-Cabinen. The field winding could be either on a yoke straddling the vertical track, or split and placed behind each armature block (Figure 11 a,b). In the later case one half of the machine resembled Kemper's design. Leitgeb also suggested a single sided version in which one armature block reacted with an array of rectangular blocks mechanicly supported by thin backing iron[186].

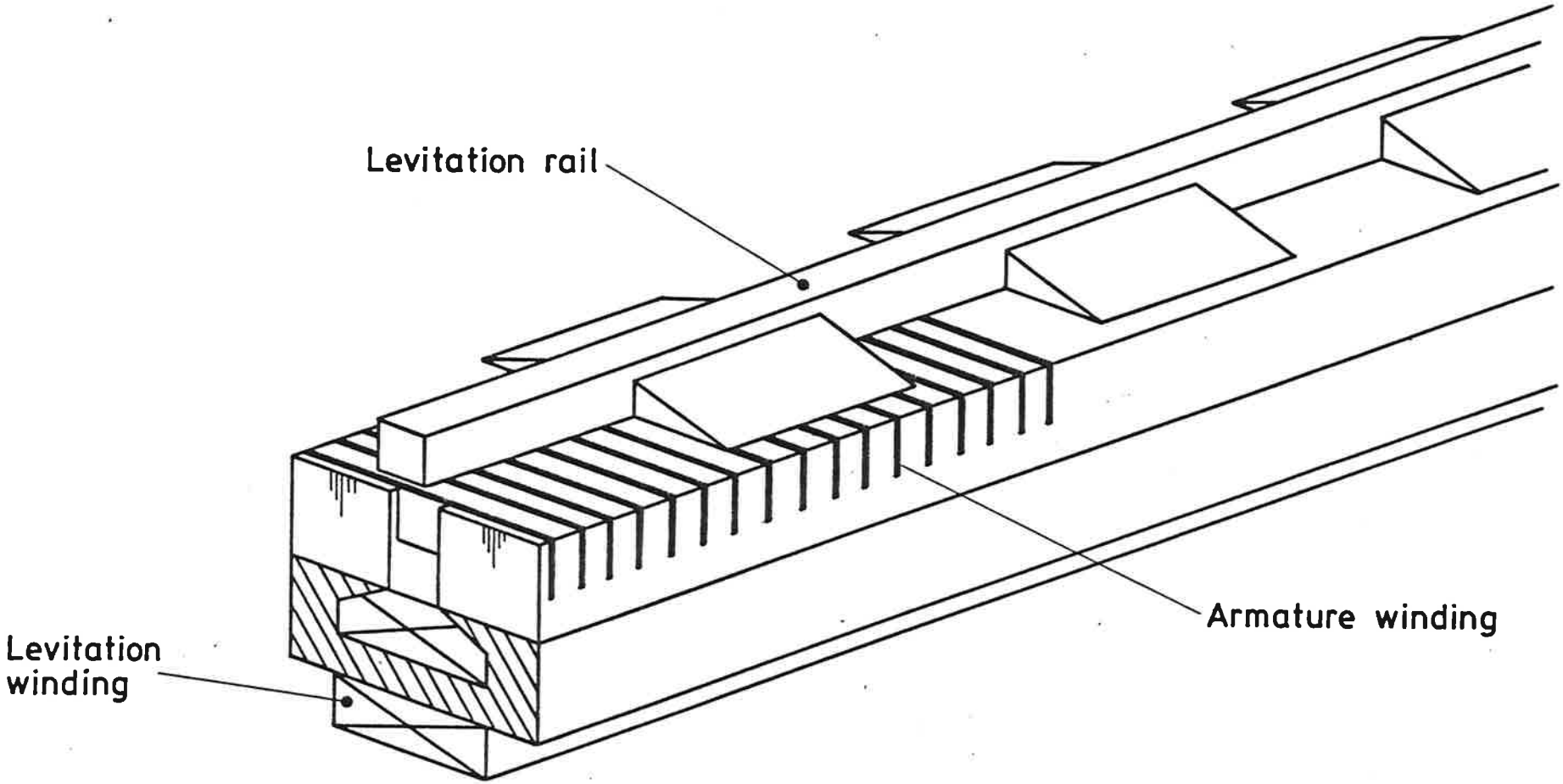

FIGURE 10 KEMPER'S HOMOPOLAR MACHINE WITH LEVITATION

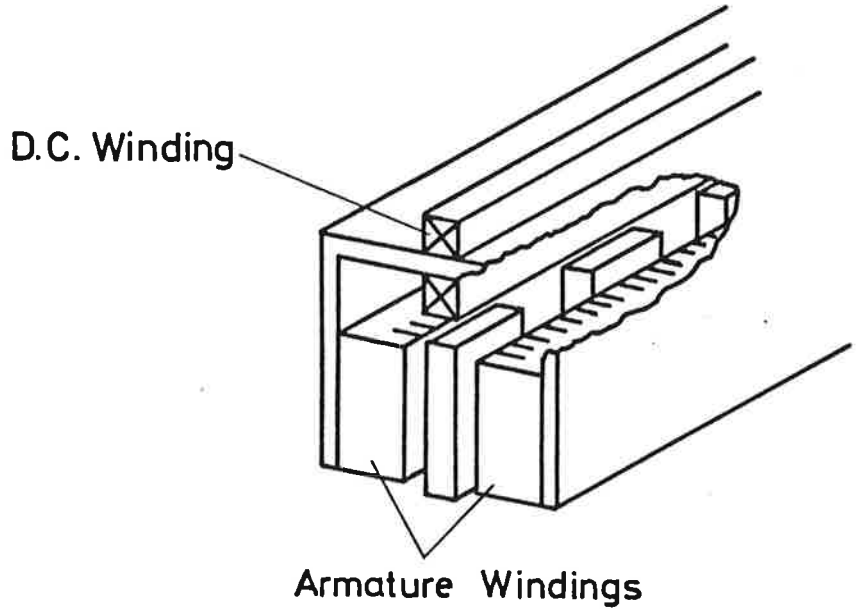

FIGURE 11a. DOUBLE SIDED HLSM WITH YOKE

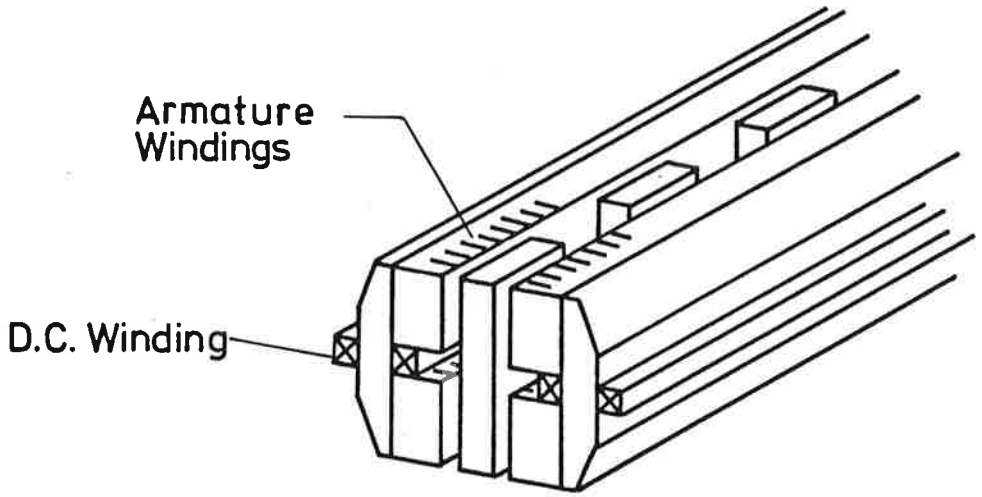

FIGURE 11b DOUBLE SIDED HLSM

An analysis of Leitgeb's yoked double sided HLSM was performed by Rummich[187], and this formed the basis of calculation by Levi in his performance comparisons of LSM with SLIM for the US DOT[175-178]. The study showed that both HELSM and HLSM design were flux density limited rather than thermally limited as was the case with SLIM. Higher possible airgaps and improved power to weight ratios despite the increased track complexity prompted continued study by Levi and also General Electric. Eastham had described a variation in winding topology for transverse flux cores in 1973[188] where the laterally adjacent but pole pitch offset similar windings were interconnected twisted coils. This winding could be used to produce a transverse flux homopolar machine[180] where the track structure resembled Leitgeb's single sided design without the thin backing iron (Figure 12). This new interconnection (as opposed to the straight through winding) was analysed by Ooi[189] as part of the General Electric programme, and employed dynamic circuit theory representation of the electromagnetic coupling and force generation. Levi analysed the staggered pole HLSM (Figure 13), using a 2 step Schwartz-Christoffel transformation to determine the effects of salient pole shaping[190]. At the same time, General Electric worked through full-scale designs (400 km/h, 3.75MW) for HELSM and HLSM. Because of the predicted high power to weight and thrust to weight ratios for the HLSM (approximately three times the values for SLIM, and six times HELSM) of 2.9 kW/kg and 25.8 N/kg, a self controlled current fed inverter excited HLSM was built rated at 112kW ([179,191]. The 5 pole machine covered 70° of arc on a 1.4 metre diameter wheel (Table VII), which could run at speeds up to 402 km/h. The first tests used staggered poles and the progresssive figure of eight transverse flux armature winding proposed by Eastham. Saturation was apparent in the rotor saliencies, and also in the armature teeth adjacent to the saliencies. Levi adequately explained the effects on the open circuit measured voltage, and the leakage flux fringing modeling

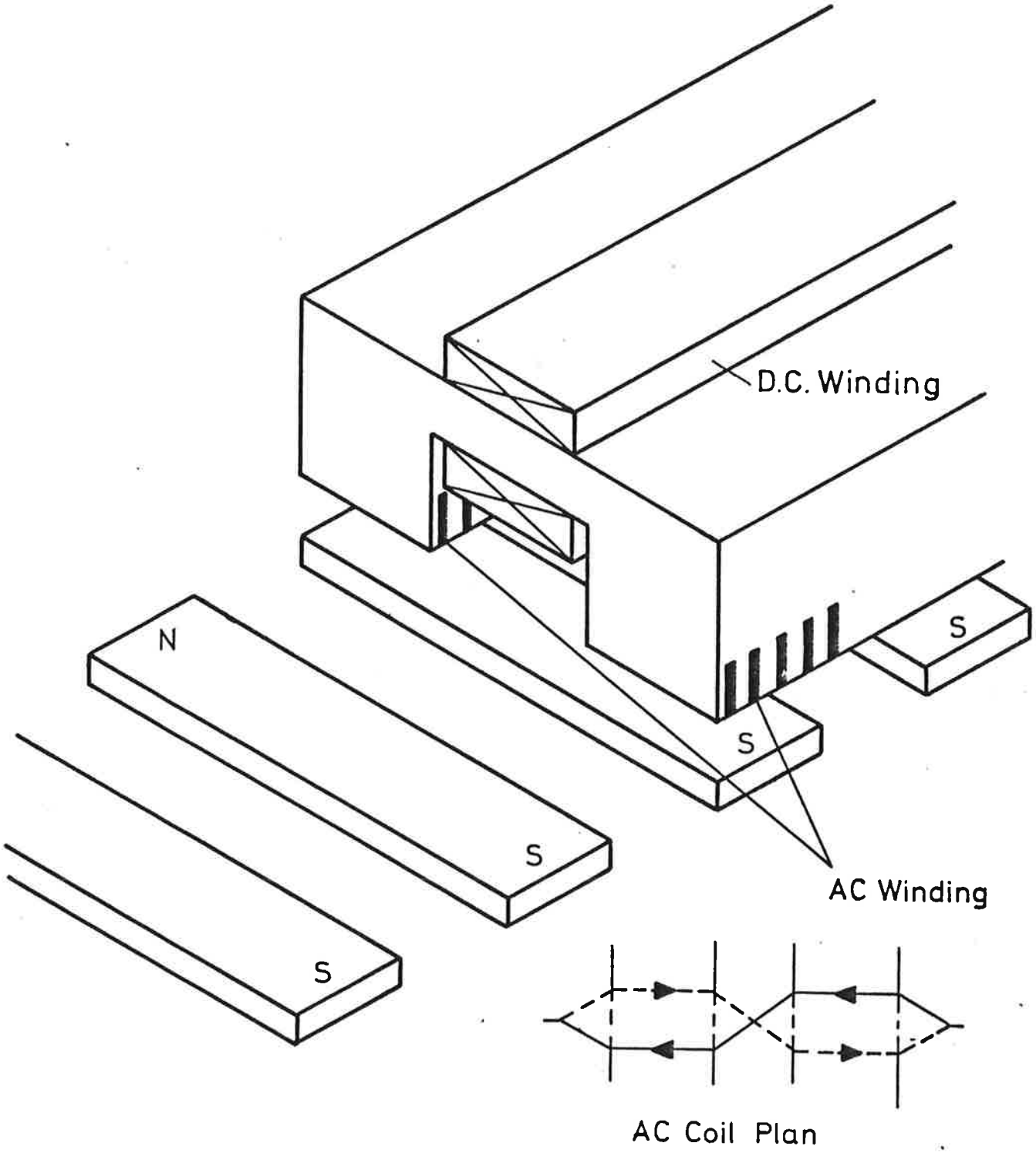

FIGURE 12. ABERDEEN TRANSVERSE FLUX HOMOPOLAR MACHINE

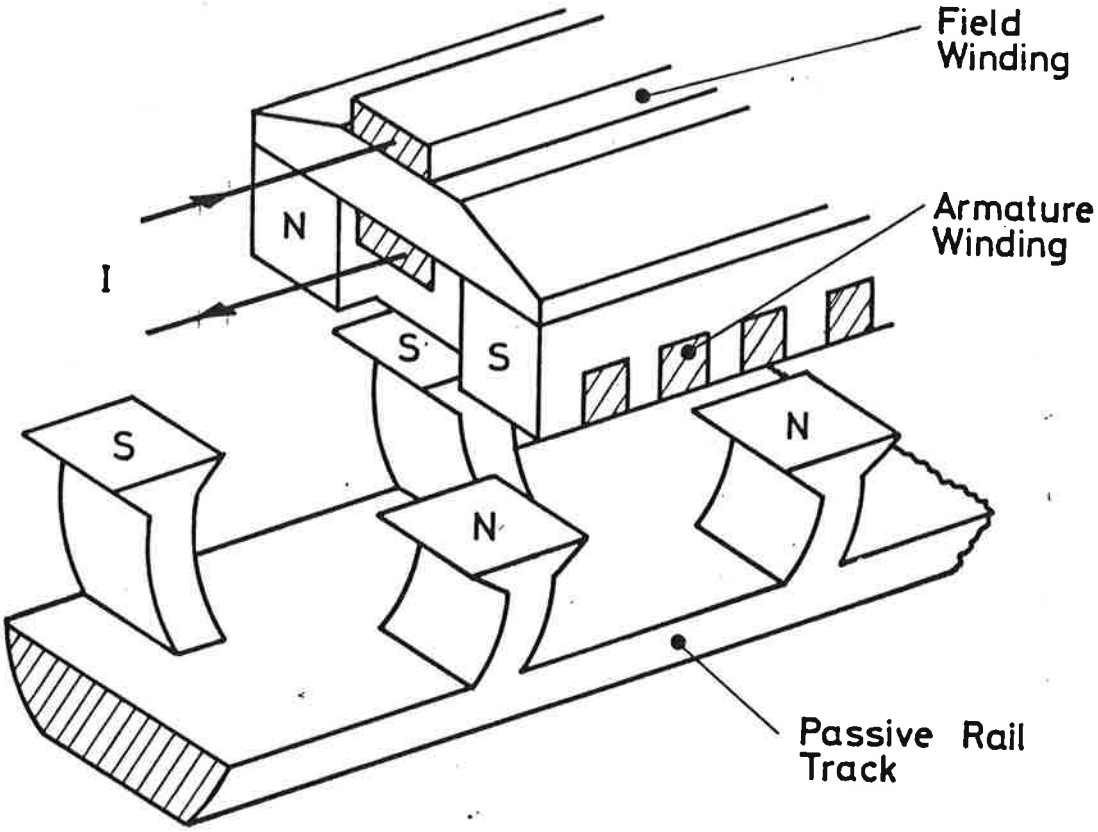

FIGURE 13. HOMOPOLAR INDUCTOR MOTOR

correlated experimental and calculated air gap lines[190].

Levi further examined the control of HLSM fed by current source inverters, and showed that power output maximum could be achieved by running at a unity power factor operating angle[192]. The consequence was that a minimum size machine was possible. Slemon tested a small HLSM on a 2 metre diameter wheel at Toronto, to establish its suitability for urban vehicles[193]. Table VII lists machine details. A current source inverter using the techniques developed for EDS LSM control, drove the armature, and open and short circuit tests together with force mesurement suggested that the very simple current and voltage fed equivalent circuits could be used to predict machine performance.

2.5.2.3 Linear Reluctance Motors

The ROMAG system[158] in its simplest form constituted a LRM, in that a polyphase vehicle armature winding reacted against a notched or castellated track magnetic rail. Boldea and Nasar analysed this configuration[194,195], and identified a further machine variant in which the track was constructed from blocks of ferromagnetic material embedded in a non-magnetic material (e.g. concrete). The segmented secondary LRM could therefore show a much improved track cost compared to the conventional notched rail motor. By the addition of thrust angle feedback, it was possible to achieve controlled thrust and normal forces sufficient for urban vehicles, with motor primaries mounted at each corner. Pole face damper windings were considered necessary to provide induction starting, but a superior method would be to use a variable voltage and frequency inverter which could track the vehicle position.

The group at the University of Sussex examined the segmented track LRM as the subsequent stage in their urban vehicle research, having successfully operated an EMS vehicle with LIM propulsion. Edwards and El-Antably proposed a uniform airgap model with which the field components could be obtained in a closed form, and the normal and traction forces could be

evaluated through a conventional equivalent circuit[196]. Airgap reactance coefficients for the direct and quadrature axes were calculated from fundamental flux per pole values and were found to be close to experimental values, once segment end flux leakage is included.

Chahal at Brush developed an alternative LRM configuration which used a transverse flux armature core and a ladder secondary. A disadvantage of this system is that the pole flux has to traverse two air gaps for a given mmf, and so has a reduced power to weight ratio compared to a straight axial flux LRM. A further development was the hybrid flux linear reluctance motor (HFLRM) which again used a ladder track, but a conventional axial flux primary. The direct axis flux now follows a hybrid path of longitudinal direction in the primary and the secondary end rings, and transverse in the secondary pole. The quadrature flux is longitudinal in both the primary and secondary[197,198].

One main problem with LRM is that they exhibit load angle instabilities at speeds or frequencies below the rated values. It is not sufficient to run the machines in closed loop with just a speed following phase locked loop. The Sussex Group examined this problem on their test rig (Table VII) and provided negative damping into the feedback loop to remove the instabilities. Test rig results also confirmed the adequacy of the large uniform airgap model used to derive calculated performance[199-200].

Several versions of LRM have been built acting as linear stepping motors, and Finch at Newcastle University has investigated vernier LRM. Although the linear stepper has been applied to a conveyor drive, producing 400N thrust on a 250 kg load travelling at 4 km/h[195], a full size transport version has not been constructed.

2.5.3 Linear DC Motors

An urban vehicle drive which used a double sided track slot lined with permanent magnets, was proposed by the Aerospace Corporation. A vehicle mounted coil array ran in the slot and the coil switching was digitally

synchronized with the relative position of the array to the magnets. A one sixth scale model was built, but the idea was not continued because of the track complexity and cost[202].

Japanese National Railways have persued the development of a DC linear motor (DCLM), in parallel with their EDS LSM research,since 1971. The basic system is outlined in a UK Patent[203], and in more detail by Amemiya[204] and Matsui[205,206]. Essentially the track coils are air cored and potted into a vertical fin to give sufficient rigidity and mechanical protection. The vehicle coils are formed onto an iron cored field structure, and are normally conducting (i.e. not cryogenically cooled). The track coil switching is accomplished by "super-forced" commutation, whereby the coil feeding thyristor is force commutated by a reverse voltage some order of magnitude greater than the back emf of the vehicle. A short commutation time is important because of the interrelationship of coil transit time to coil size and the rate of current rise and fall within the coil.

As might be expected, the machine cannot be adequately operated on open loop control. The vehicle motion can be expressed as a second order oscillatory system, with a very small damping coefficient, and the commutation angle oscillates until it breaks past the synchronous point; the machine has only a small margin to prevent stepping out. By applying velocity feedback, the damping coefficient is effectively stabilized at a higher value, providing an efficient operating regime.

To check the operational characteristics of DCLM, a 500 km/h rotating disk and a 500 metre linear test track were built, as well as a 100 metre diameter track used to establish control strategies[207,208]. Tables VI and VII give the main details of the facilities. The rotating disk was constructed out of fibre reinforced plastic and the preformed coils were moulded in. A short time rating of ten minutes was necessary to avoid excessive temperature rise in the disk. The 100 metre diameter track was

used as a control system model to establish that a correct control strategy had been chosen, and a branch with turn out was also included to investigate switch transitions. The 500 metre linear track carried a 3.3 tonne vehicle which could produce a thrust of 2.2 tonnes, or roughly that of two cars of the Shinkansen. The design top speed of 200 km/h is reached in a 240 metre acceleration section, a 70 metre test section being followed by electric and then mechanical braking. Eight field magnets with airgaps of 85mm run at 0.9 Tesla peak, and are energised through a power collecting roller[209,210]. Later tests on pantograph behaviour at high speed provided alternative power pick up, before the track was reconfigured to give both levitation and propulsion with the same coil arrangements, but at the lower speed of 80 km/h[211].

The track coils are driven by a constant current source through a flip flop type inverter. Position indication is usually by means of a cross wire inductive system. An onboard oscillator and antenna links track mounted wires which fed a signal back to the local control of commutation within the flip flop inverter. There are two options for power feeding, the first being 'multiphase feeding' where multiphase square wave currents feed from a substation to the flip flop inverters at each feeding section. The second method is direct current feed, where dc is fed from the substation to each flip flop inverter at the feeding sections. Commercial systems will use dc feed since it is most ecomomical, in terms of lower phase inductance, inverter capacity, and number of feed lines.

Proposed commercial systems are designed for two operating speeds of 300 and 500 km/h, around the conventional JNR train set arrangement of 16 cars, with 100 seats per car. The 300 km/h system would use tyres to provide guidance and some lift, although the majority of lift and the propulsion would come from the DCLM. The 500 km/h system would be fully non contacting (except for current pick up) with the DCLM providing all the lift and propulsion, and an electromagnetic guidance system using null flux

guidance from a controlled current saddle magnet running over a coil array. Expected power levels are 35.1 and 15.6 MW for the two train sets.

In order to reduce the weight and power loss in the vehicle magnets, redesign of the magnetic circuit and an enhancement of the current density were accomplished. The choice of cooling was between air, water through hollow conductors, or boiling fluid. Boiling fluid cooling was selected as having the most promise and experimentation determined the optimum dimensions of the coil, tank and condenser circuit[212]. A fluorinated oil was chosen as the refrigerent, as it had similar physical properties to Freon 113, but its vapour pressure is approximately a quarter of Freon's, resulting in reduced tank wall thickness and a 20-30% weight saving. A trial magnet showed a current density of 4.5 A/mm^2 in aluminium wire, and a mmf of 100 kA. Using this as a base, the weight of magnets that could lift and propel a 22 tonne vehicle could be reduced from 9.6 tonne/vehicle to 4 tonne/vehicle, with an excitation power of 285kW/vehicle.

2.6 Future Near Term Development

Although the final outcome of the tests at very high speeds at Emsland and in Japan by JAL and JNR will not be known for some time, it is likely that progression to a totally levitated system will be slow, because of world recession and Government reluctance to enter into large capital projects. It is therefore reasonable to expect that the emergence of hybrid systems, namely fairly conventional duorail vehicles with linear motor propulsion, will offer near term advantages over existing methods of propulsion, but not require totally new infrastructure development with all the associated land acquisition cost and environmental impact problems. For urban vehicles, the Toronto ICTS is an example, and Slemon has suggested a permanent magnet LSM propulsion unit for a similar capacity 8 tonne vehicle, where the field is an array of samarium cobalt magnets with iron backing and the track is an air cored three phase winding excited in 200 metre block lengths[213].

SLIM's have been used in Japan as booster/retarders in a classification yard since 1974 on a regular basis[214], and can produce significant savings in reduction of damage resulting from uncontrolled end impacts, and considerably reduce noise levels in the yards. In the USA, it is estimated that remote switch motors and controlled decelerations could save $6.5 billion (1975 dollars) in the period 1980-2000[162].

For propulsion units suited to conventional high speed trains, the choice is dependent on whether cryogenic systems can be engineered to meet railway operational conditions. Abel has suggested that a magnet pack containing an isochoric cryostat and a multimagnet array could be simply supported under the power car of an APT type vehicle[137-9]. At terminii the magnet pack could be replaced with a freshly charged pack to provide a quick turn around. The unsprung mass of the driven axles would no longer be a design constraint, and sufficient propulsive power and braking obtained with a meander air cored track winding could extend the speed range to 300 km/h, and beyond, depending on wheel wear rates.

Similar studies by Nondahl at General Electric were based on SLIM or HLSM drives, the main feature being passive track structures[215]. Five operating modes were chosen, with ratings of 200, 450, 1200, 2400 and 3735 kW, the designs representing vehicles ranging from a New York City subway car (112 km/h) to a High Speed Locomotive (400 km/h). The designs were optimized to produce minimum track weight with similar magnetic and electrical loadings. The main conclusions were that the HLSM worked at a higher power factor, produced greater restoring forces for track misalignments, and gave lower track heating than the SLIM. The SLIM advantages were that there was no need to synchronise train speed and frequency, the machine was easier to construct, lower copper weight, a more easily anchored track structure. Generally, when the output power and available frequency are low the HLSM track is lighter, and similarly, the SLIM track is lighter at higher powers and frequencies. Both schemes

suffer the same disadvantage in that a power collection system is required, whereas an air cored LSM needs no pickup. The ACLSM can further be implemented with cryogenically cooled coils and small airgaps, since there is no requirement for levitation. The air gap field harmonics can be picked up by the vehicle and used to produce on board power when the vehicle is in motion.

Another option is cryogenically cooled coils driven by a dc busbar power collection as part of an ACLSM propelled urban vehicle. These hybrid applications are discussed in a later section.

Kolm and O'Neill have suggested using a basic ACLSM as an electromagnetic launcher. Primarily research has been aimed at lunar transport of materials, and shuttle pay load launching. One novel application has been the suggestion of nuclear waste disposal into deep space, and the inevitable use as an electromagnetic gun has also been investigated[216-218]. However, these systems require energy compression ratios of about 60:1, and suitable energy delivery equipment. The most promising arrangement is a homopolar generator feeding pulsed power into the armature system. For space payload launching, an evacuated 7.8km tube can house a 1 tonne vehicle, which would emerge through a vacuum lock at 12.3 km/s, having been accelerated at 1000 gee, Launch time would be 1.5 seconds, and would require 76 GJ. More reasonable applications include short take off assistance for conventional aircraft: 20 kg vehicles launched at 400 km/h would reach a 600 metre altitude and then act as gliders. Typical launch ramps would be 5m long, and 100 gee would require 0.12 MJ delivered in 0.1 second.

Since 1977, AGT system development has been generally on the decline, with the exception of the German and Japanese effort. The emphasis has changed from that of high speed at low cost (which marked the aspirations of work in the late 60's) to adequately high speed transport at reasonable energy

efficiency, compared to the alternative modes. This has acted against the development of EDS since the aerodynamic drag power doubles on a vehicle going from 400 to 500 km/h, and EDS is more effective at the high speed than EMS. The LIM has been given a reasonable top speed of 300-400km/h when used as an EMS propulsion or as part of an ISPS. LSM have proved to be the preferred propulsion unit,long stator iron cored for EMS vehicles, or air cored for EDS and pehaps high speed duorail trains. HLSM and HELSM show slight improvement over LIM and LRM, but both require current pickup which is likely to preclude their use at high speed. The Japanese DCLM is a serious alternative for a maglev system, but again, requires a current collection system to supply the on board electromagnets.

The three main contenders for AGT propulsion all have track windings which are block supplied, in short lengths approaching the vehicle length in the case of the DCLM, several times the vehicle length for the iron cored LSM, and many times the vehicle length for the cryogenic LSM. The latter two cases do not rely on current collection through brushgear and either use an on board power supply or effectively pick up the air gap harmonics to top up on board battery supplies. Because of the advantages that these machines show over conventional rotary machines driving power wheel sets with the attendant problems of unsprung mass, wheel and rail wear through the adhesion interface and limited acceleration and deceleration rates, it is to be expected that they will be the focus of continued research and development. The final outcome will be a design for a prototype with substantially improved performance compared to a conventional duorail vehicle, and extended speed capability with low initial infrastructure cost and minimal maintenance requirements.

CHAPTER THREE

PERFORMANCE CHARACTERISTICS OF LSM

3. Performance Characteristics of LSM

3.1 Equivalent Circuit Representation

3.1.1 Basic Requirements

If machine performance over a wide range of conditions is to be accurately predicted, it is necessary to formulate a suitable model. Invariably, for electromagnetic devices, an equivalent circuit is used as the basis for investigating performance in terms of either imposed operational constraints, or parameter variation and system sensitivity. The component parts of the circuit should be readily identifiable as relating to particular aspects of the real machine (for example phase resistance, leakage inductance etc) and must, if possible, include all mutually induced effects from other similar linked circuits.

The LSM can be represented by lumped parameters in a representative phase. The representative phase is that identifiable single winding representation of a polyphase armature winding whose magnetomotive force (mmf) coincides with that of the whole polyphase armature sheet mmf. Although it is tempting to split the phase into sections which either link the main field flux or are distant from the vehicle[219], there is no particular advantage in doing so. In the simple equivalent circuit shown in Figure 14, phase current passes through the phase impedance and is driven by the difference in terminal voltage E_T and the induced back emf E_B. The phase impedance is made up of a resistive term and a reactance based on the overall phase inductance, excluding field linkages. The phase inductance is therefore essentially a leakage inductance, and itself can be decomposed into two terms, a winding self inductance, and a mutual term, formed by the representative phase net mutual linkage with the rest of the armature windings.

The back emf E_B represents the mutual linkage between the armature representative phase and the field winding array. E_B although reflected into the terminals is only induced in the few turns per pole per phase

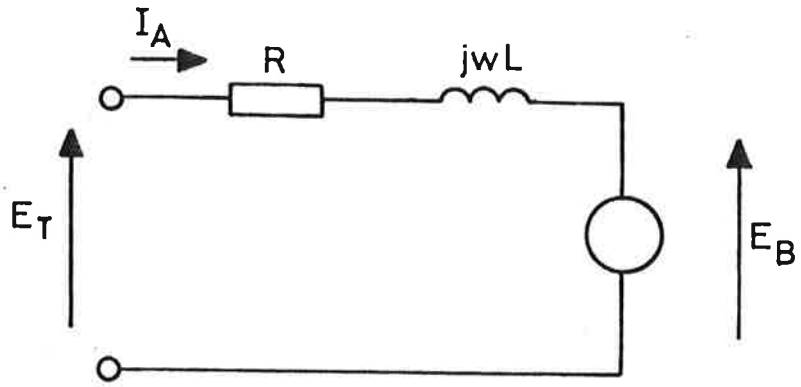

FIGURE 14. VOLTAGE FED EQUIVALENT CIRCUIT

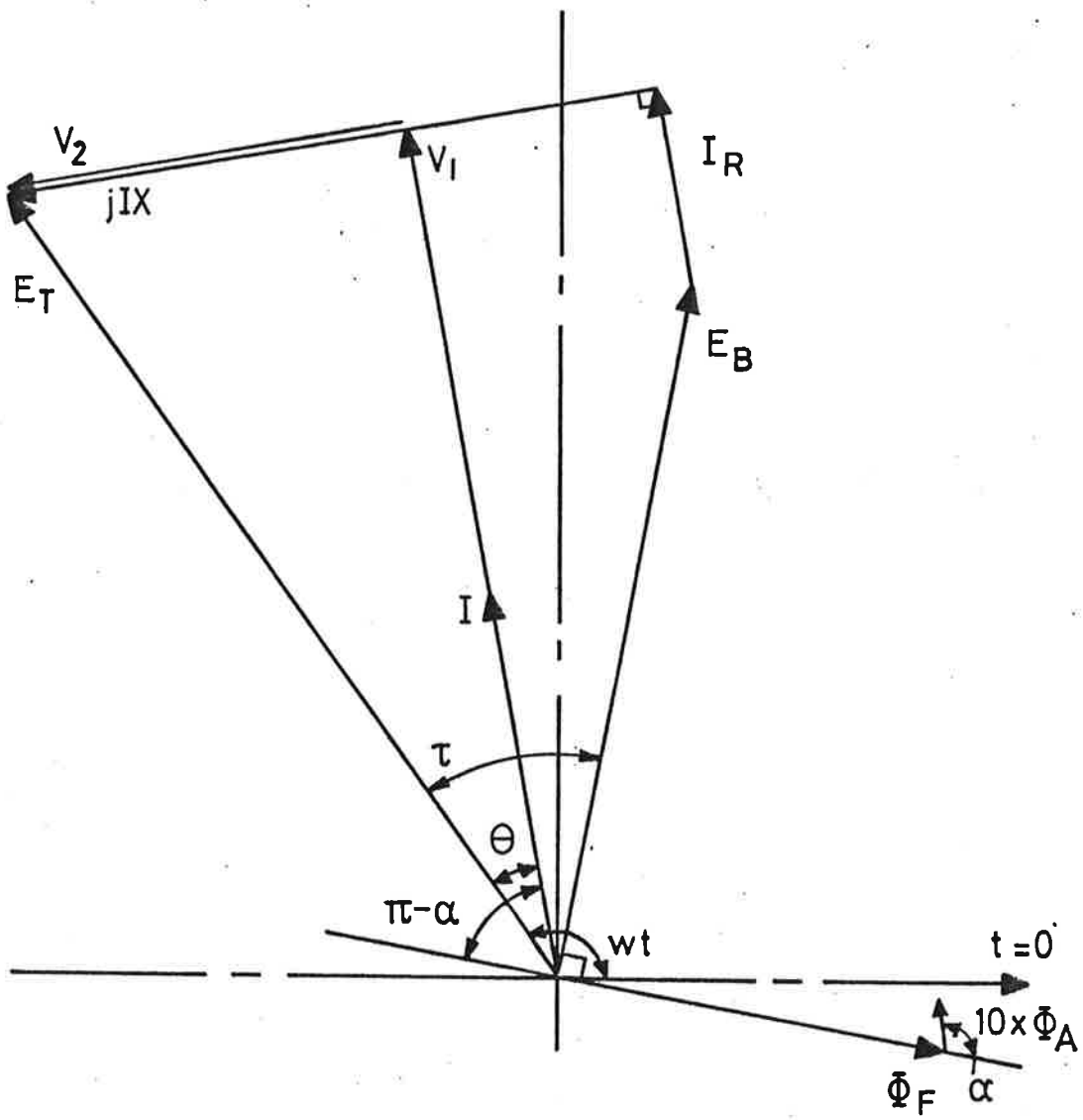

FIGURE 15. PHASOR DIAGRAM FOR REPRESENTATIVE PHASE.

over the short section of the energised armature linking the vehicle field coils. Because the superconducting magnets have such high ampere turns (three orders of magnitude greater than the armature) the field strength at the track level is such that the armature reaction is relatively small, and E_B can approach the terminal voltage even when considerable amounts of power are being transferred.

The field and armature windings are air cored and generally can be broken down into the simple configuration shown previously as Figure 1. Non linearities which are usually associated with conventional iron cored machinery are therefore absent for ACLSM. The track level flux density is generated by a regular disposition of finite coils, and if the coil height to pole pitch ratio is low, multiple harmonics in the induced emf will occur. Each harmonic can be treated separately in the equivalent circuit, and the net effect evaluated, with no loss of generality, or the need to introduce additional components.

Figure 15 shows the representative phasor diagram deduced from the equivalent circuit. The armature flux Φ_A is driven through the machine airgap by the phase mmf. In the machine air gap directly below the magnet coil array the field winding flux Φ_F lags behind the armature flux by a force angle α (also known as the current angle). Φ_F induces in the phase windings the back emf E_B, and this leads the Φ_F phasor by $\frac{\pi}{2}$. As will be seen later, the optimum operation of the machine occurs with $\alpha > \frac{\pi}{2}$, in a region that is normally unstable for synchronous machines without either fast acting AVR's or other auxiliary closed feedback loops in the excitation or terminal control. The back emf lags on the terminal voltage by the load angle τ; on no-load operation there would be no net current flow, τ would be zero, and the back emf would be exactly balanced by the terminal voltage, E_T. This situation is unreal for LSM; the nearest equivalent would be an evacuated tube vehicle with low drag, or alternatively when the machine is braking and passes through the $\tau = 0$ locus before regenerating.

The phase current I lags on the terminal voltage by the power factor angle θ, and is of course in phase with Φ_A.

3.1.2 Load Angle Derived Equations

A load angle derived equation set is particularly easy to formulate, and so will be introduced first to establish basic relationships. Using phasor representation of the phasor diagram, with the terminal voltage as the time reference,

$$\bar{E}_T = E_T + j0$$

then $$\bar{E}_B = E_B \cos\tau - jE_B \sin\tau$$

and $$\bar{I} = I\cos\theta - jI\sin\theta$$

the equivalent circuit gives a solution for the current phasor,

$$\bar{I} = \frac{\bar{E}_T - \bar{E}_B}{R + jX}$$

since $$I = |\bar{I}| = (\bar{I}\bar{I}^*)^{1/2}$$

$$I = \left[\frac{E_T + E_B - 2E_TE_B\cos\tau}{R^2 + X^2}\right]^{1/2} \qquad (1)$$

At the terminals, the instantaneous input power S_T for a machine with m phases is given by

$$S_T = m\bar{E}_T\bar{I}^* = P_T + jQ_T \qquad (2)$$

P_T and Q_T are the average power and reactive volt amperes (reactive power)

The magnitude of S_T is given by

$$S_T = \frac{mE_T\,[E_T^2 + E_B^2 - 2E_TE_B\cos\tau]^{1/2}}{(R^2+X^2)^{1/2}} \qquad (3)$$

Similarly the machine output S_B is given by

$$\bar{S}_B = m\bar{E}_B\bar{I}^* = P_B + jQ_B$$

Taking the real part of $\bar{S}_B$ gives P_B, the mechanical output power,

$$P_B = \frac{mE_B}{R^2 + X^2} \left[R(E_T \cos\tau - E_B) + XE_T \sin\tau \right] \qquad (4)$$

The expressions for the remaining input and output magnitudes can also be written, which allows the linking terms of power factor $\cos\theta$, efficiency, η and power factor-efficiency product $\eta\cos\theta$ to be evaluated

$$\text{Power factor,} \quad \cos\theta = \frac{P_T}{S_T} = \frac{\frac{R}{X}\left(\frac{E_T}{E_B} - \cos\tau\right) + \sin\tau}{\left(1 + \frac{R^2}{X^2}\right)^{1/2}\left(1 + \frac{E_T}{E_B}\left(\frac{E_T}{E_B} - 2\cos\tau\right)\right)^{1/2}} \qquad (5)$$

$$\text{Efficiency,} \quad \eta = \frac{P_B}{P_T} = \frac{\frac{R}{X}\left(\cos\tau - \frac{E_B}{E_T}\right) + \sin\tau}{\frac{R}{X}\left(\frac{E_T}{E_B} - \cos\tau\right) + \sin\tau} \qquad (6)$$

$$\text{Product,} \quad \eta\cos\theta = \frac{P_B}{S_T} = \frac{\frac{R}{X}\left(\cos\tau - \frac{E_B}{E_T}\right) + \sin\tau}{\left(1 + \frac{R^2}{X^2}\right)^{1/2}\left(1 + \frac{E_T}{E_B}\left(\frac{E_T}{E_B} - 2\cos\tau\right)\right)^{1/2}} \qquad (7)$$

Equation (7) is important since it provides the link between the mechanical output power P_B and the required total instantaneous power at the terminals, S_T. If the machine is running at a steady synchronous speed v, then the traction force or thrust F_B is simply given by

$$F_B = \frac{P_B}{v} \qquad (8)$$

The current angle α is directly linked to the power factor angle and load angle by

$$\alpha = \frac{\pi}{2} - \theta + \tau \tag{9}$$

as can be seen from the phasor diagram. Equations 5 to 9 are plotted in Figures 16 and 17 for a typical value of $\frac{E_B}{E_T}$ of 0.75 and two representative values for $\frac{R}{X}$ of 0.3 and 0.6. It is seen that although the efficiency peaks rapidly with load angle, the power factor is much less sensitive to changes. The efficiency-power factor product, $\eta \cos\theta$ has a broad maximum in the range $15° < \tau < 35°$. The value of load angle at which this maximum occurs is

$$\tau \Big|_{\max.\eta\cos\theta} = \frac{\sqrt{1 + \frac{R^2}{X^2} - \frac{E_B^2}{E_T^2}} - \frac{R}{X}}{1 + \frac{E_B}{E_T}} \tag{10}$$

As mentioned the usefulness of the load angle as a fundamental quantity for analysis is limited, since in an operating system the conditions for no load running will only occur when the machine is about to pass into regeneration while decelerating. On-load conditions make load angle difficult to measure, and the method used, for example, in the CIGGT control strategy is to provide a model to artificially create the track armature, and compare the signal generated for E_B with a real time E_T - derived signal. The vector difference is a measure of τ in the real machine. Sen's analysis of the load angle derived equations[107,220] is faulty because of an inconsistency in the sign notation used to derive the equations, and results in curious performance characteristics of a revenue vehicle design.

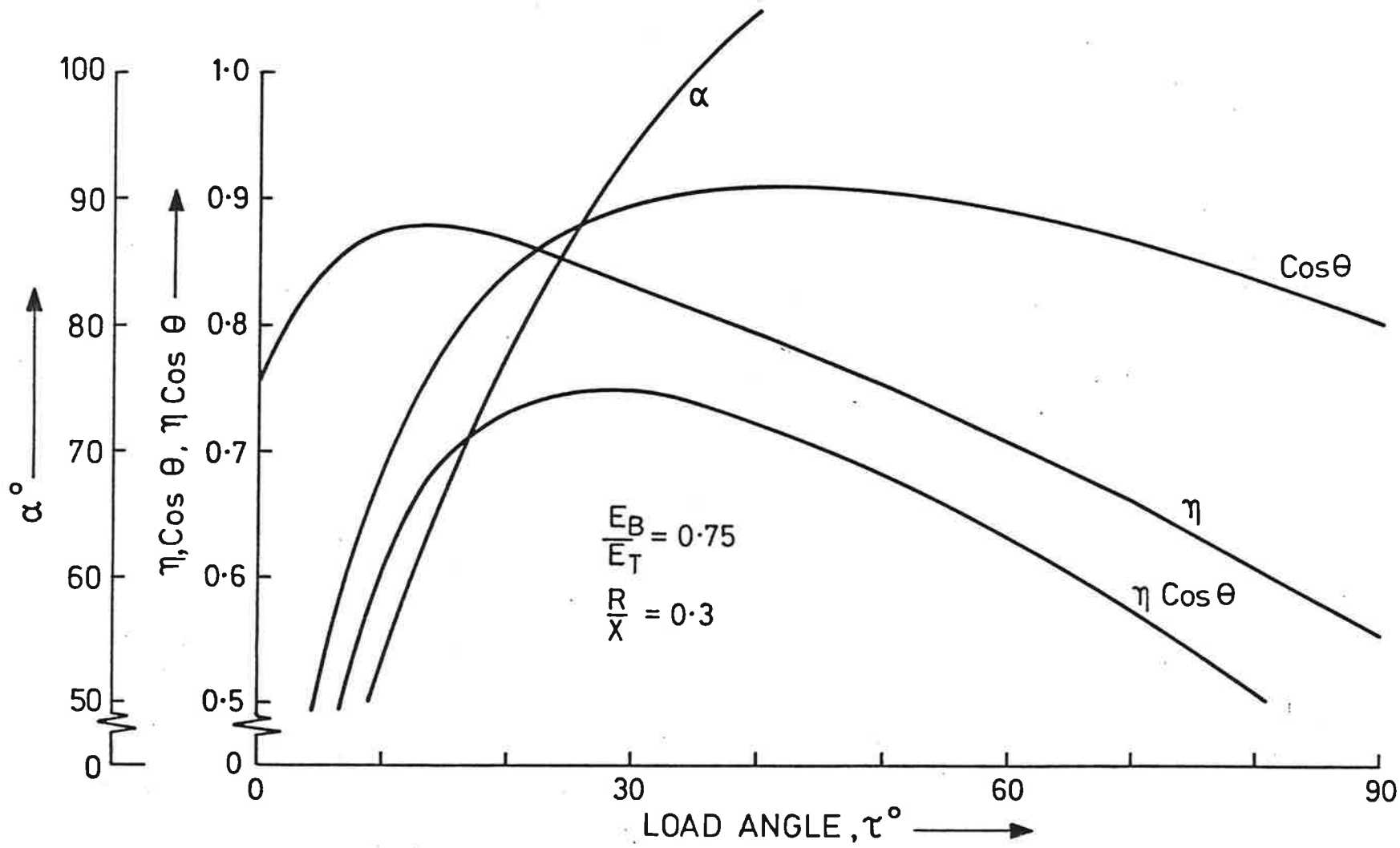

FIGURE 16. EFFICIENCY, η, POWERFACTOR, COS θ, AND ηCOS θ WITH CURRENT ANGLE, α WRT LOAD ANGLE τ

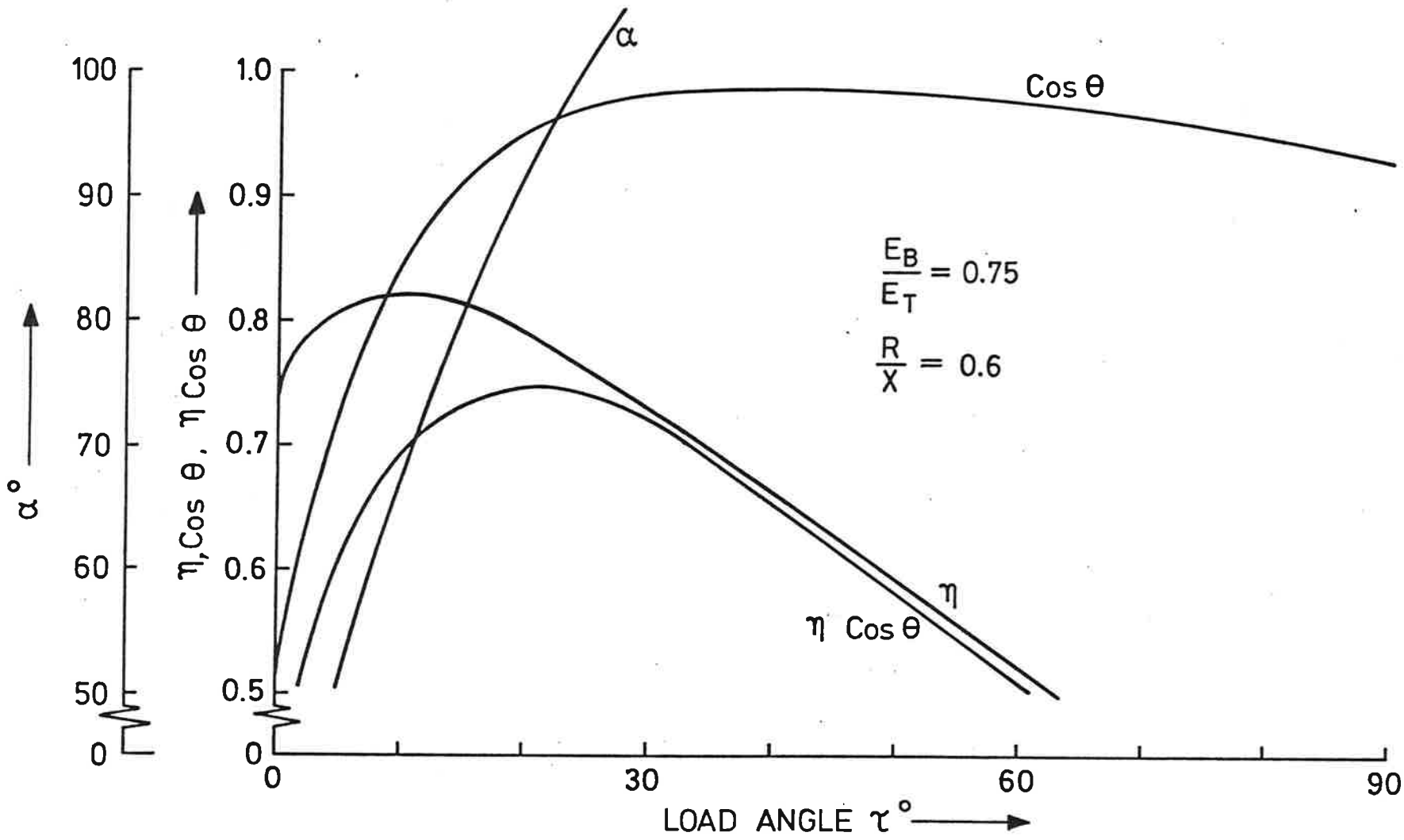

FIGURE 17. EFFICIENCY, η, POWERFACTOR, COS θ, AND η COS θ WITH CURRENT ANGLE, α WRT LOAD ANGLE τ.

3.1.3 Current Angle Derived Equations

The current angle is the linear equivalent angle between the peaks of the armature and field mmf distributions. In the phasor diagram, Figure 15, the terminal emf can be split into active (in phase with stator current) and reactive (quadrature phasing to current) components. The appropriate voltages are given by

$$V_1 = E_B \cos(\tau - \theta) + IR = E_B \sin\alpha + IR \qquad (11)$$

$$V_2 = -E_B \sin(\tau - \theta) + IX = E_B \cos\alpha + IX \qquad (12)$$

The power factor is directly obtained as

$$\cos\theta = \cos\left[\tan^{-1}\left\{\frac{V_2}{V_1}\right\}\right] = \frac{V_1}{(V_1^2+V_2^2)^{1/2}} \qquad (13)$$

and the terminal emf, E_T, is

$$E_T = [V_1^2 + V_2^2]^{1/2} \qquad (14)$$

The machine is primarily designed to provide a particular thrust-speed characteristic determined by the required acceleration and load profile. The thrust, F_B, is linked to the back emf, phase current and current angle by

$$F_B = \frac{P_B}{v} = \frac{m E_B I \sin\alpha}{v} \qquad (15)$$

Since the induced emf is proportional to speed, the developed thrust is speed independent, and can be controlled by individual manipulation of either phase current I or current angle α, at the inverter.

The machine active input power P_T is given by

$$P_T = P_B + m I^2 R \qquad (16)$$

So efficiency is

$$\eta = \frac{P_B}{P_T} = \frac{1}{1 + \frac{mI^2R}{P_B}} = \frac{1}{1 + \frac{P_B R}{mE_B^2 \sin^2\alpha}} \tag{17}$$

Using (14), (15), the total input power S_T is

$$S_T = mE_T I = \frac{P_B}{\sin\alpha}\left[1 + \frac{P_B^2(R^2+X^2)}{m^2E_B^4\sin^2\alpha} + \frac{2P_B(R + X\cot\alpha)}{mE_B^2}\right]^{1/2} \tag{18}$$

Also

$$P_T = P_B\left[1 + \frac{P_B R}{mE_B^2\sin^2\alpha}\right] \tag{19}$$

and

$$Q_T = P_B\left[\cot\alpha + \frac{P_B X}{mE_B^2\sin^2\alpha}\right] \tag{20}$$

Finally, the linking expression

$$\eta\cos\theta = \frac{P_B}{S_T} = \frac{E_B}{E_T}\sin\alpha \tag{21}$$

indicates that for a high power factor-efficiency product at a particular thrust loading, the back emf-terminal emf ratio and current angle product must be as large as possible. A typical value range of 70-85% might be achieved for a large machine, when the track installation and energy consumption optimizations are worked through into the design.

By manipulating the current angle at which the motor operates, power conditioning benefits can be achieved. Minimum phase current (equivalent to maximum efficiency), minimum terminal voltage, minimum terminal rating as well as power factor can be chosen depending on the particular requirement[221]. In most cases the minimum terminal rating option will be chosen since installed conditioning and cabling cost will be proportional to this factor. In revenue service with supply from a Utility, it may show some advantage in maximum peak demand costings to operate some of the scheduled LSMs at leading power factor to compensate the remaining LSM's operating at the more usual lagging power factor. This would ease the

stored energy MVAR obtained from the Utility Grid and any cost benefit may offset the increased superconductor and track conductor cost. Inevitably any trade off of parameters to obtain a particular result will have a detrimental effect on other parameters. In the design process the trade off effects must be understood so that specific parameters are not compromised. As LSM development has progressed, it has become apparent that more system flexibility is possible if sections are supplied by individual inverters, rather than operating the steady state cruise sections on a synchronous near-Utility tie, so that the minimum terminal rating option is likely to be made the preferred choice.

If machine parameters are fixed, a decision has to be made as to which variables should be optimised, and with what constraints. The basic fixed parameters for a certain steady state are simply track armature resistance and reactance, number of phases, and back emf. Machine thrust at the synchronous speed is a parameter which depends on the thrust-speed requirement of the vehicle, and is linked to the output power by equation (15), which effectively fixes $I\sin\alpha$ at a constant value.

For a constant thrust requirement, the value of current angle which minimises efficiency and phase current is

$$\alpha = \frac{\pi^c}{2}$$

If $$s = \frac{P_B X}{m E_B^2} \tag{22}$$

then $$E_T = E_B \left[1 + \frac{s^2}{\sin^2\alpha} \left[\frac{R^2}{X^2} + 1 \right] + 2s\left[\frac{R}{X} + \cot\alpha \right] \right]^{\frac{1}{2}} \tag{23}$$

and the minimum terminal voltage is given for a value of current angle where

$$\alpha = \pi^c - \tan^{-1}\left[s\left[\frac{R^2}{X^2} + 1 \right] \right] \tag{24}$$

Power factor may be maximised by appropriate choice of current angle, or if the back emf component in quadrature to the phase current is larger, equal to or smaller than the reactive voltage drop, then lagging, unity or leading power factor will ensue.

Unity power factor occurs when θ is zero, i.e. termial voltage and current phasors are in line, which is interpreted as V_2 is also zero. The required value of current angle for unity power factor is

$$\alpha = \frac{\pi^c}{2} + \frac{1}{2} \sin^{-1} 2s \qquad (25)$$

Maximum power factor is similarly obtained as occurring at the value of current angle where

$$\alpha = \pi^c - \cot^{-1} \left\{ \frac{X}{R} \left[\left(1 + \frac{R^2}{X^2} \left(\frac{X}{sR} + 1 \right) \right)^{\frac{1}{2}} - 1 \right] \right\} \qquad (26)$$

Maximum power factor efficiency product lies between the individual values of current angle producing the separate maxima, i.e. $\frac{\pi}{2}$ and the value obtained from (26). The value of current angle for which this occurs requires the solution of the cubic equation.

$$\tan^3\alpha + \left(r + \frac{2R}{X} + \frac{1}{s}\right) \tan^2\alpha + 3 \tan\alpha + r = 0 \qquad (27)$$

where

$$r = 2s \left(1 + \frac{R^2}{X^2}\right) \qquad (28)$$

Solving (27) is tedious, since it requires solution of a reduced equation, and the evaluation of its discriminant[221]. A range of the non dimensional parameters $\frac{R}{X}$ and $s \left(= \frac{P_B X}{m E_B^2} \right)$

for which the value of current angle giving minimum S_T hve been evaluated and are shown in Figure 18. As might be expected, an increase in loading, s, requires a reduction in current angle once a break point is reached around s = 0.6.

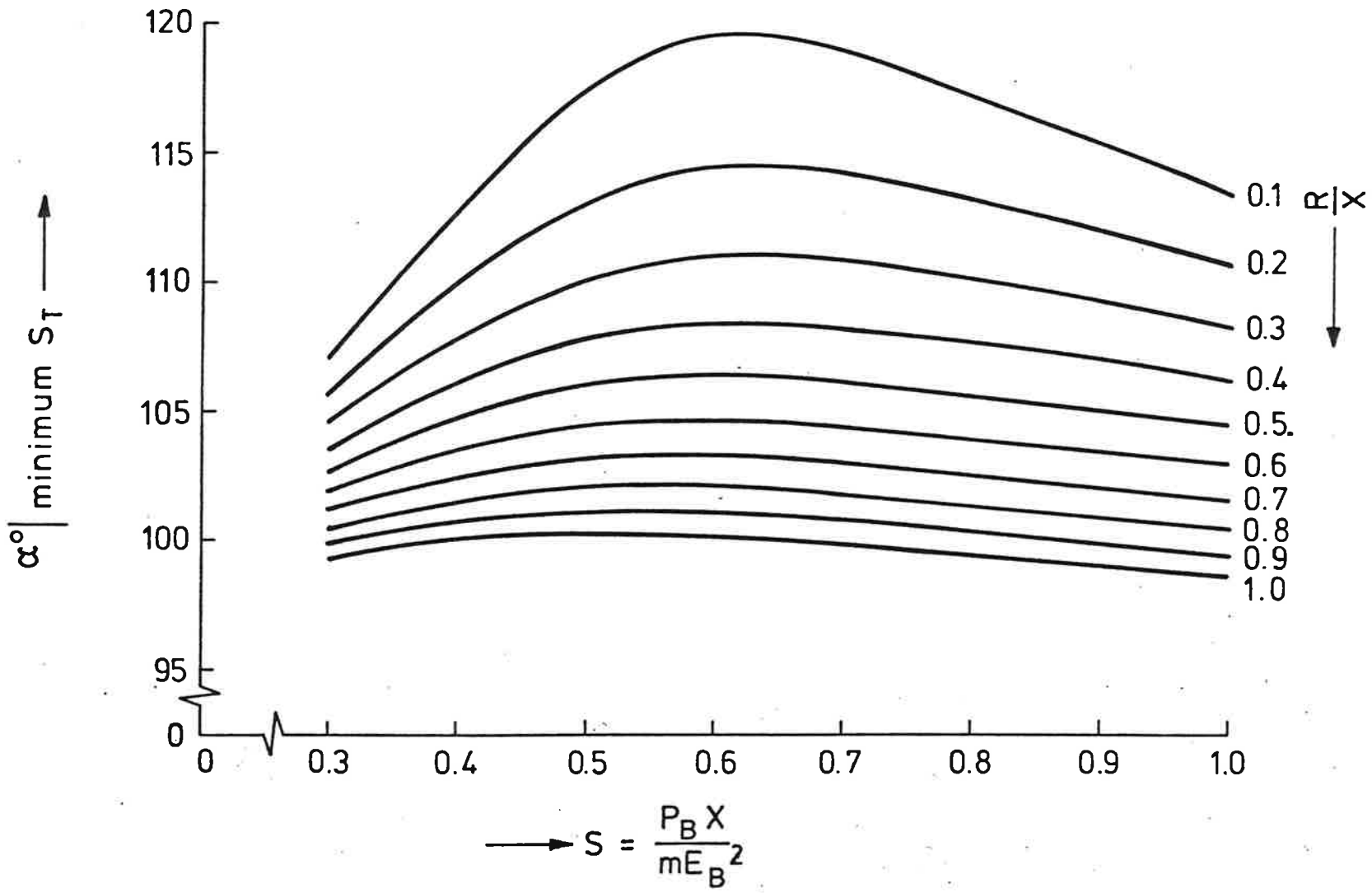

FIGURE 18. CURRENT ANGLE α° FOR MINIMUM S_T WRT S AND $\frac{R}{X}$

3.1.4 Operation at Minimum S_T

Assuming that the inverter operation is set to automatically minimise its terminal rating, to minimise total power flow, then the parameter variation for various loads should be evaluated. The results of a blanket range of calculations for efficiency, powerfactor and their product, terminal voltage, phase current and total input power with various normalizing factors are shown in Figures 19 to 23. The parameters are evaluated for the minimum S_T values of current angle resulting from combinations of the two main non dimensional factors s and $\frac{R}{X}$, over a typical design spread.

The figures are self explanatory. However it is interesting to note the fact that since for a particular track arrangement, inductance does not significantly change with increased conductor section, a low resistance track will always show overall advantage even though it degrades the power factor. Also worth noting is the high power factor efficiency products that are possible at light loadings and low track resistances.

Finally, parameter sensitivity to changes in current angle must be determined to establish any economic advantage gained from optimum running. For the CIGGT revenue vehicle, P_B = 5.4 MW, cruise speed is 480 km/h, phase resistance and reactance are 2.8 and 8.89 ohms respectively, for a 5 kilometre block length. The back emf is nominally 4kV. The minimum terminal rating value of current angle is 108°, and Figure 24 shows the terminal total power and voltage and phase current normalized about this value. Efficiency, power factor and their product are also shown for different current angles. In general the form of the curves holds for most large scale LSM designs. In going from maximum efficiency to maximum apparent efficiency operating points, the phase current increases and the terminal voltage drops. The terminal voltage reduces more rapidly than phase current increases, and in this example E_T reduces by 10% while I increases by only 5%. The implication is that the phase current affects

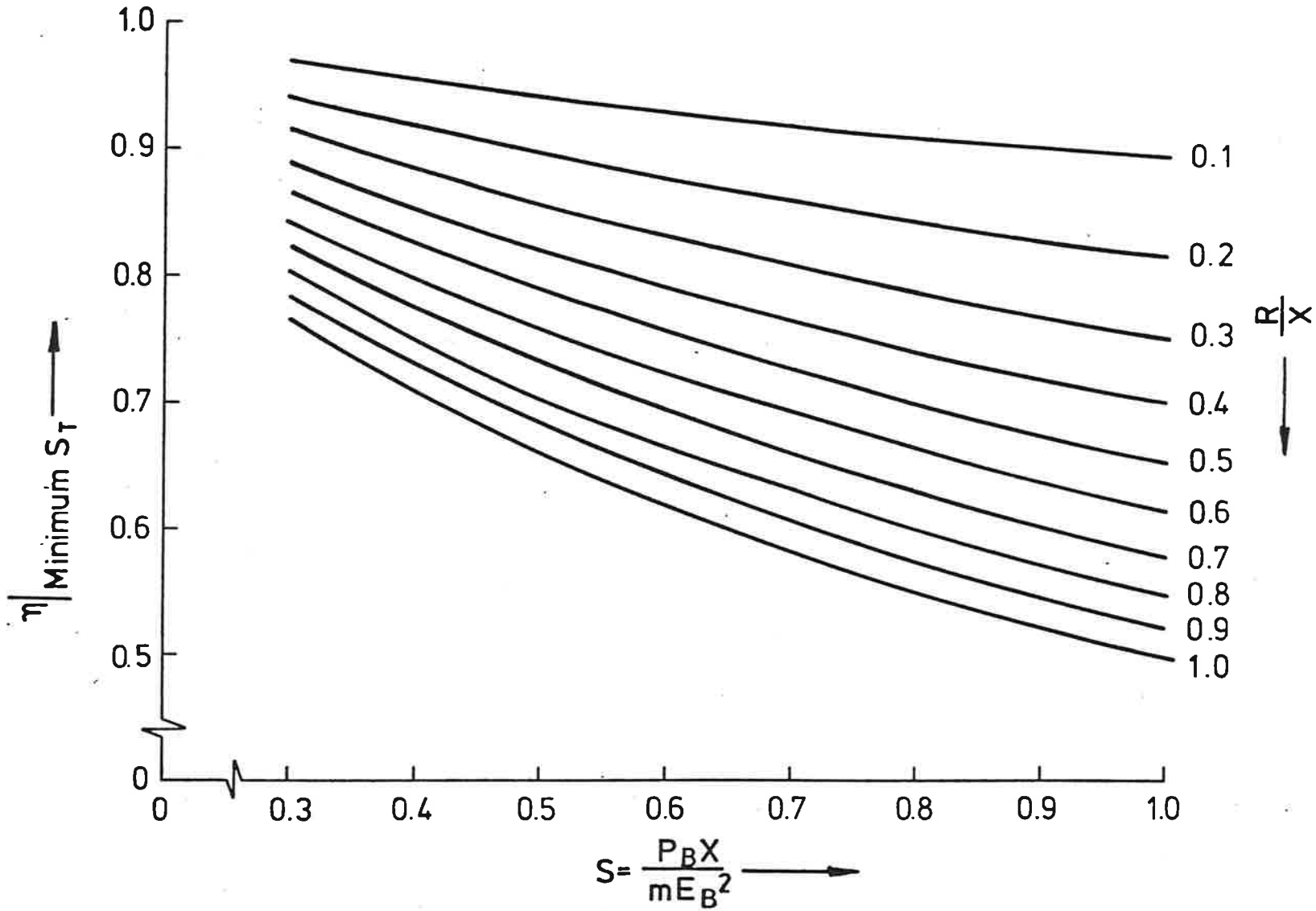

FIGURE 19. EFFICIENCY, η , FOR MINIMUM S_T WRT S AND $\frac{R}{X}$

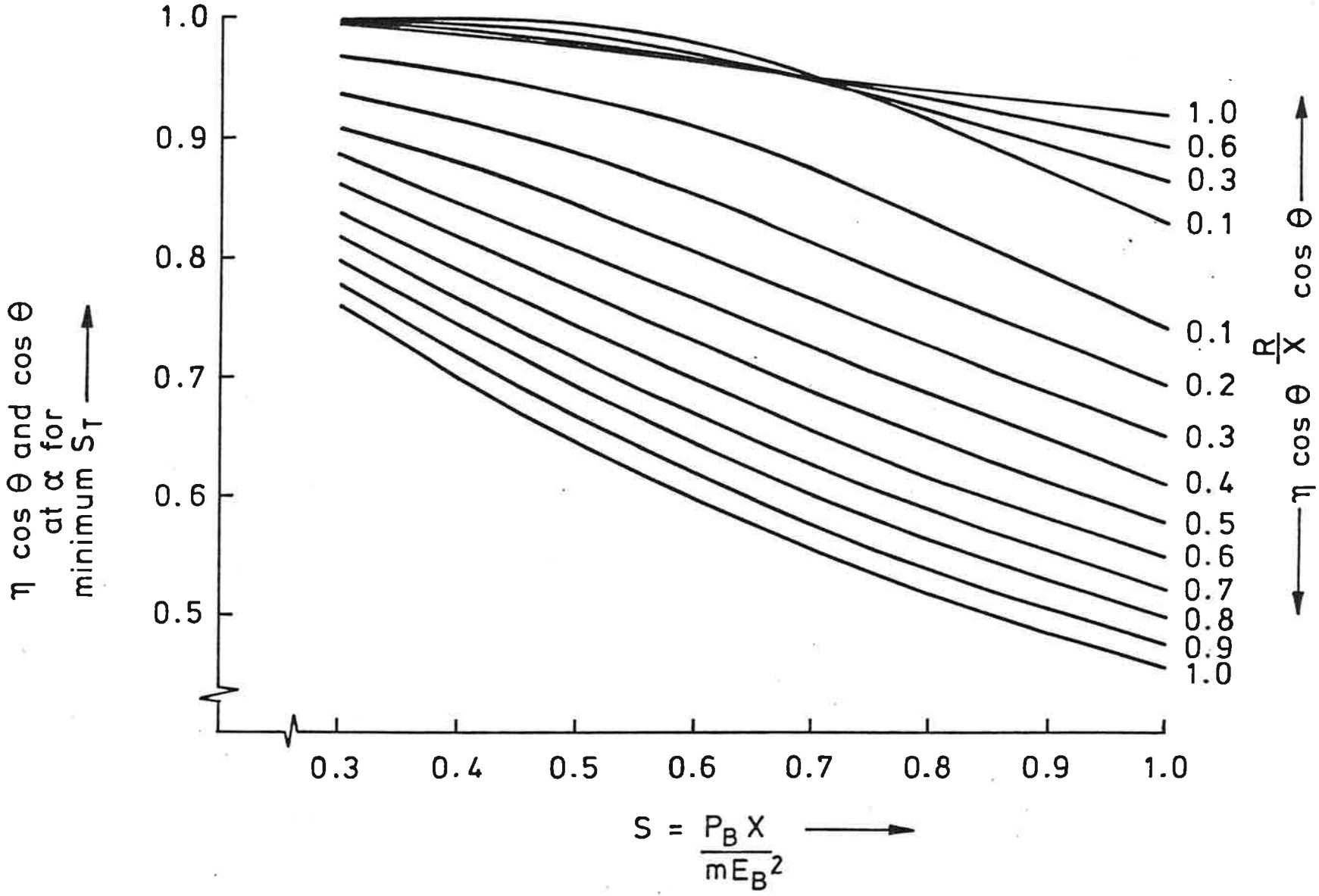

FIGURE 20 POWER FACTOR (COS θ) POWER FACTOR-EFFICIENCY PRODUCT (η COS θ) WRT S AND $\frac{R}{X}$ FOR MINIMUM-S_T α

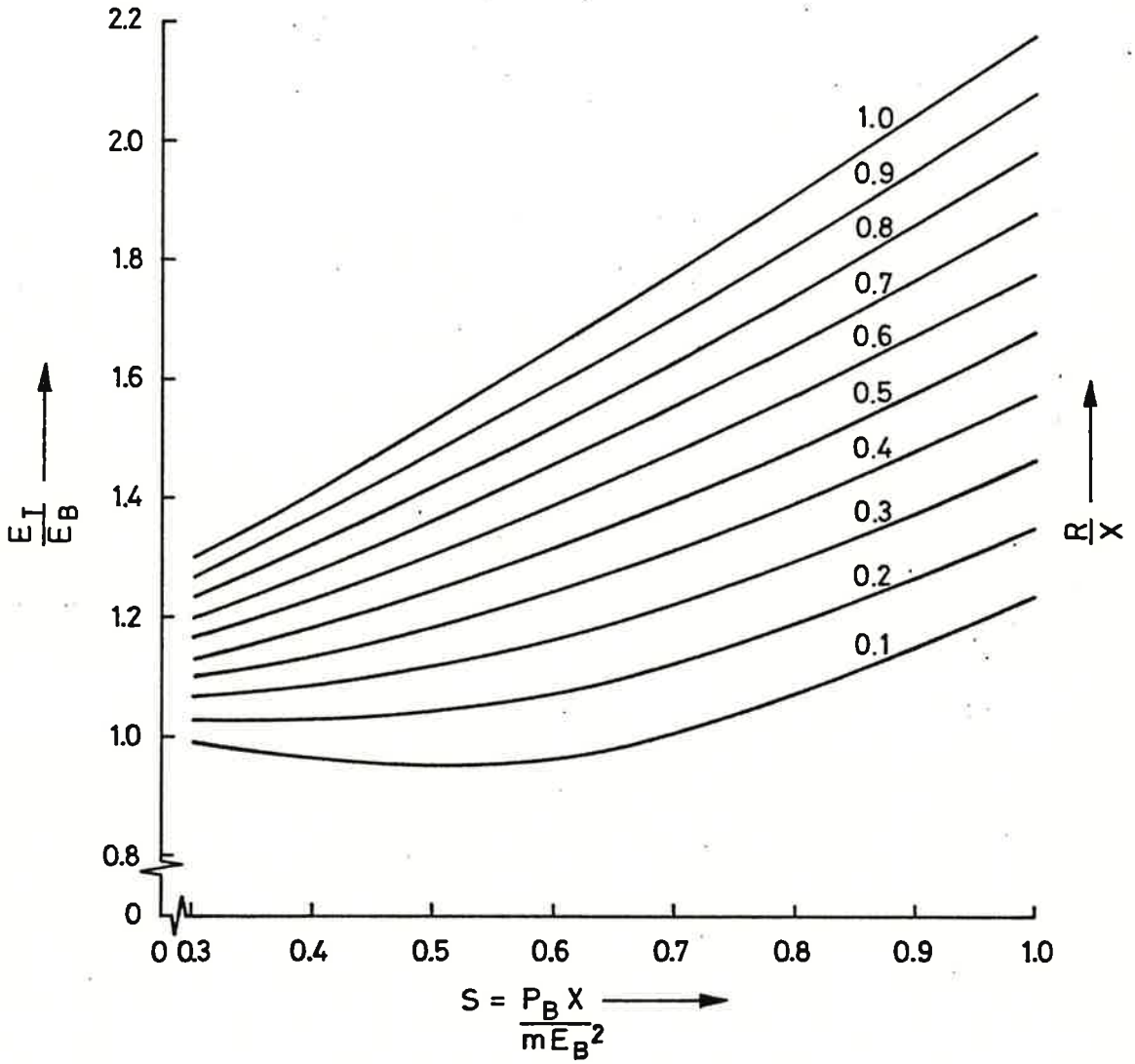

FIGURE 21. NORMALIZED TERMINAL VOLTAGE W.R.T. S AND $\frac{R}{X}$ FOR MINIMUM $-S_T$ α

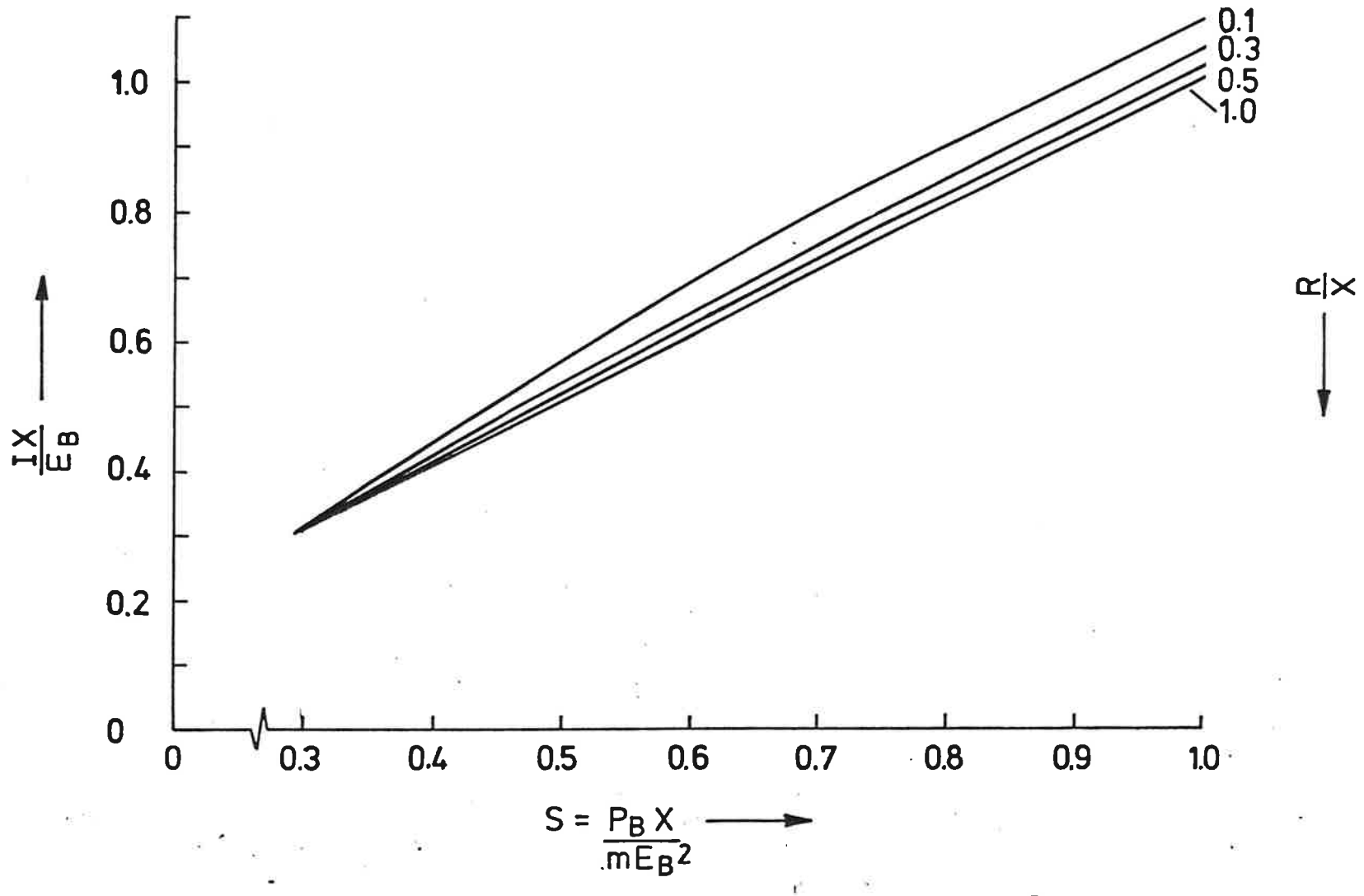

FIGURE 22 NORMALIZED PHASE CURRENT WRT S AND $\frac{R}{X}$ FOR MINIMUM $S_T - \alpha$

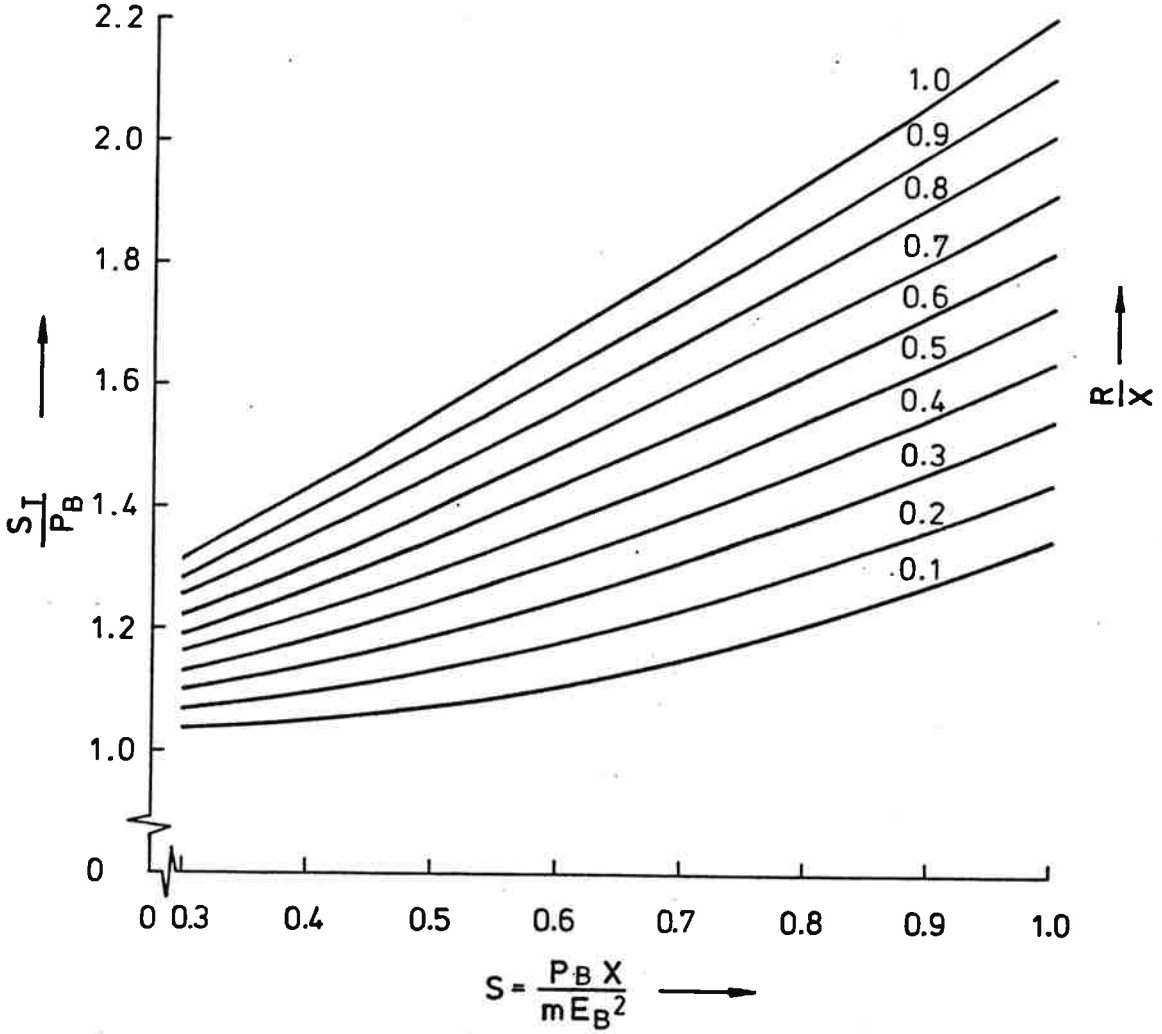

FIGURE 23. NORMALIZED POWER INPUT WRT S AND $\frac{R}{X}$ FOR MINIMUM - S_T α

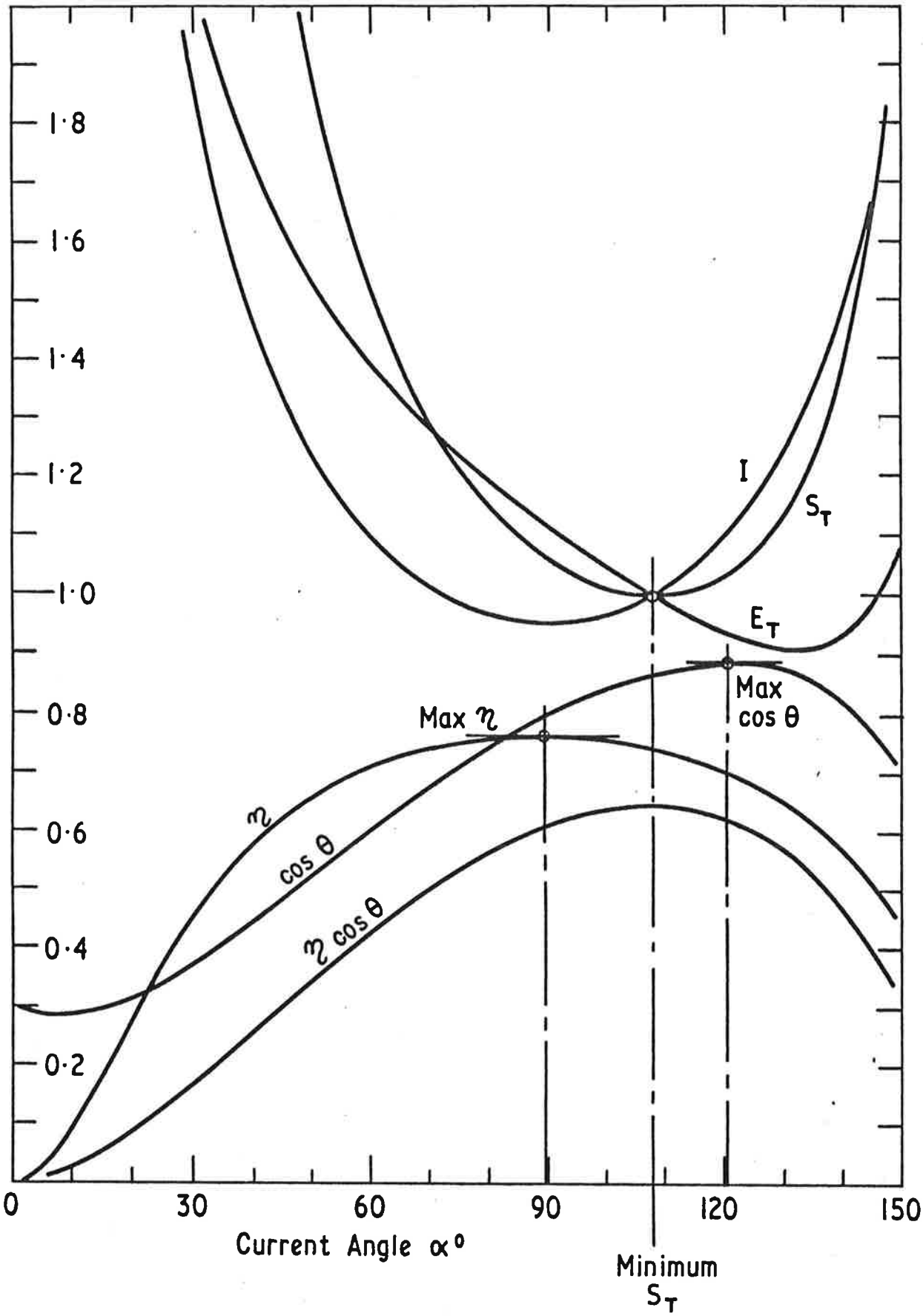

Figure24. Performance Characteristics of LSM at Cruise.

the track heating and conductor temperature rise and so determines the type of insulation and its ageing,whereas the terminal voltage affects the risk of insulation breakdown, and the inverter semiconductor required blocking voltage and the subsequent cyclical stress.

3.2 Inductance and Induced Emf Modelling

3.2.1 Mutual Inductance

In establishing the equivalent circuit model, it has been assumed that the phase inductance and back emf are known singular quantities. There are in fact force and other parameter harmonic pulsations in the model to be considered. Force pulsation occurs because of nonsinusoidal currents flowing in the armature winding, and the nonsinusoidal nature of the main airgap field. If the track windings and the field coil array are decomposed into elemental filaments, the mutual inductance between interacting filaments can be calculated (Figure 25). For LSM design, a common method of calculation is to evaluate the mutual inductance linkage for a vehicle coil and a track array, and derive the force components as gradients of force about a working point[195,219]. This involves evaluating mutual inductance six times about a common reference point. Figure 26 shows a suitable coordinate set, and identifies the convention adopted at Warwick for vehicle and track coil dimensions. The alternative solution to evaluate the forces is to lump the effects of vehicle to track linkage effectively into the back emf, E_B. Because the system is iron free, super position can be applied, so harmonics can be treated at each level separately, if required. For a particular mutual field-stator mutual inductance M_{FA}, and superconducting equivalent current i_F, the back emf is given by [107]

$$E_B = \frac{j\omega}{2} I_F M_{FA} \qquad (29)$$

An alternative to a strict application of mutual inductance formulae for offset rectangular coils, is to evaluate the line integral of a track wavelength vector potential around a vehicle loop. In this way mutual inductance is similarly defined for a unit of current flowing in the track loop. Raytheon had used this method to look at shape effects in different track and vehicle coil geometries.

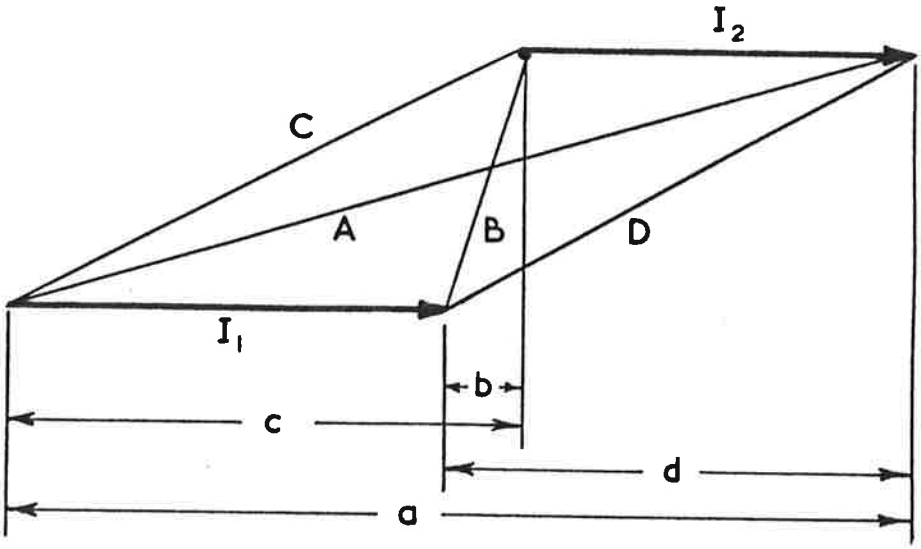

$$M = \frac{\mu_o}{4\pi}\left\{\log_e\left[\frac{(A+a)^a\,(B+b)^b}{(C+c)^c\,(D+d)^d}\right] + C + D - A - B\right\}$$

Figure 25. Mutual inductance between parallel current elements.

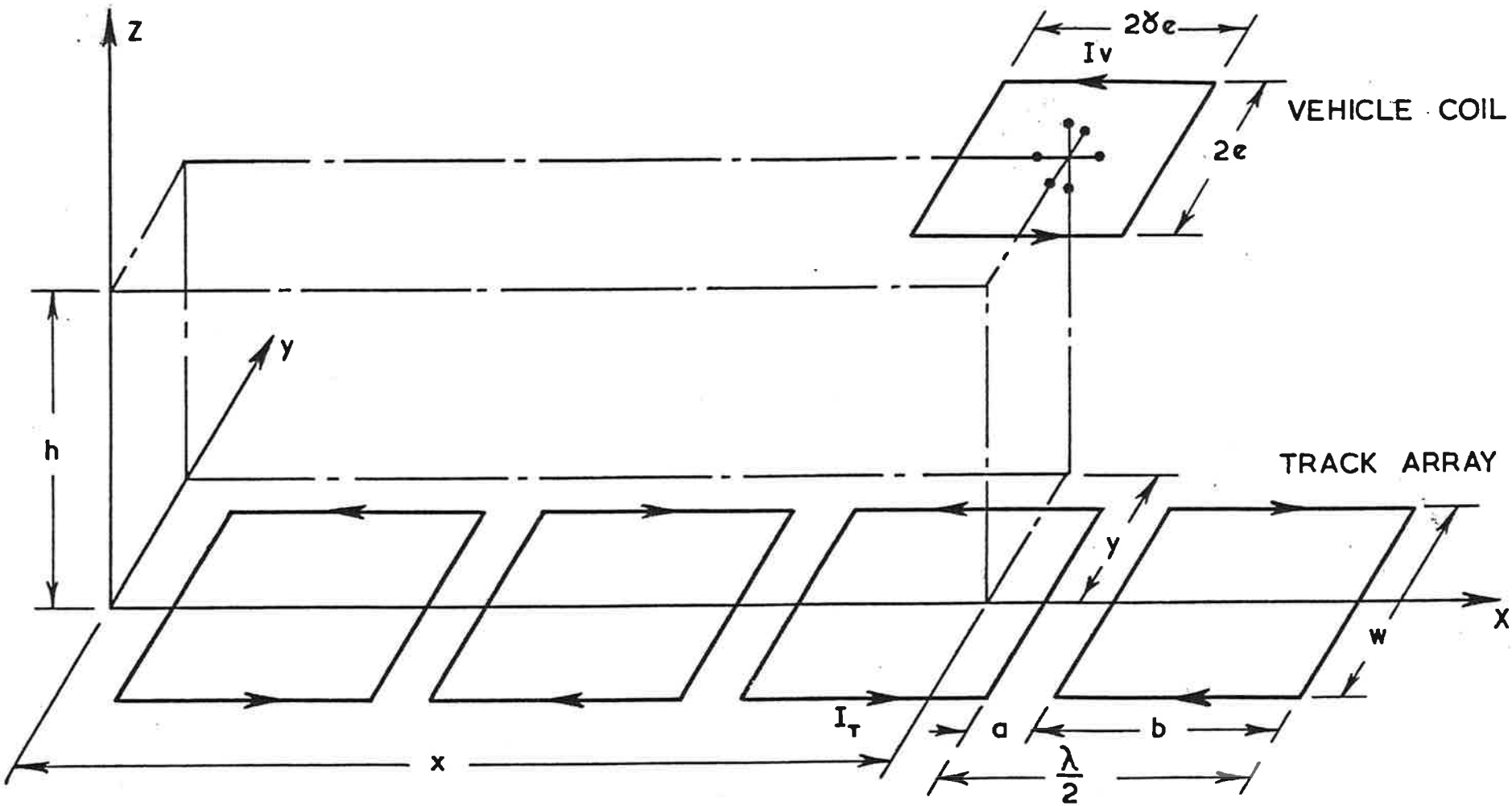

Figure 26. Coordinates for mutual inductance, vehicle coil to track coil array.

3.2.2 Track Inductance

The inductance of the meander coil type winding for the LSM is basically found to consist of two major parts. For one phase a self inductance can be established which relates to the mutual linkage of the phase winding with itself, and for a double layer winding this in fact becomes a quantity whch scales linearly with increasing winding energised length. As well as the self linkage, linkages exist with the remaining phases of the machine, and the currents in these phases set up mutual voltages in the original reference phase. These too scale linearly,for the double layer winding. Appendix III gives details of the derivation of both terms. To analyse the self inductance, the concept of an elemental inductance is introduced, being a unit of one phase which is one pole pitch long. If the whole energised phase is made up of, say, k elements, then for a particular element e_{j+1}, its elemental complement e_{k-j} must also exist, so that both have j elements outboard to themselves (Figure 27a). If the elemental inductance interacting to n, or $L_e(n)$ is defined as the self inductance of an element e, and the mutual inductance due to e and the n elements on both sides of e, by writing the contribution of e_{j+1} and e_{k-j} to the phase total self inductance, and rearranging, the total strip self inductance $L_T(k)$ is given by

$$L_T(k) = \sum_{n=0}^{k-1} L_e(n) \qquad (30)$$

For a double layer winding, an elemental pole pitch is identified, and evaluation of the elementary inductance proceeds as sequential pole pitches are added to either side of the initial element, to n increments. Figure 27b shows the way in which the terms are defined. In fact equation 30 holds for this case too. The two main terms in the total self inductance of the meander winding are termed the initial inductance, L_i, which effectively defines the physical shape of the winding conductor, and one which is a function of the geometric disposition of the conductor, and varies with the pole pitch machine width ratio, the asymptotic inductance L_a. The track phase self inductance, L for a section length G metres long is given by

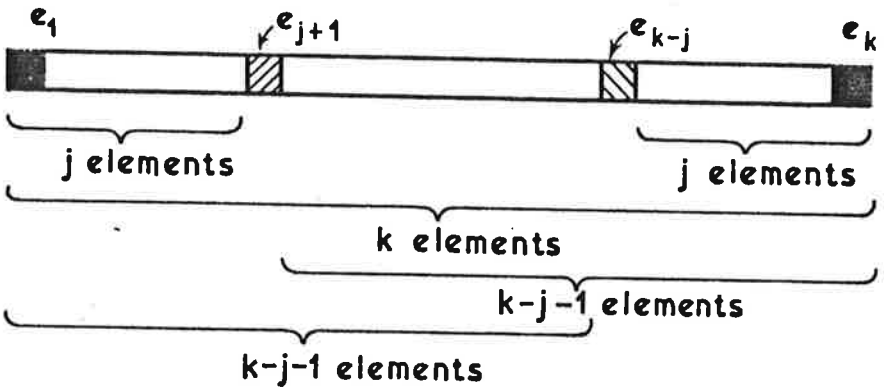

(a) Subdivision of meander winding into pole pitch elements.

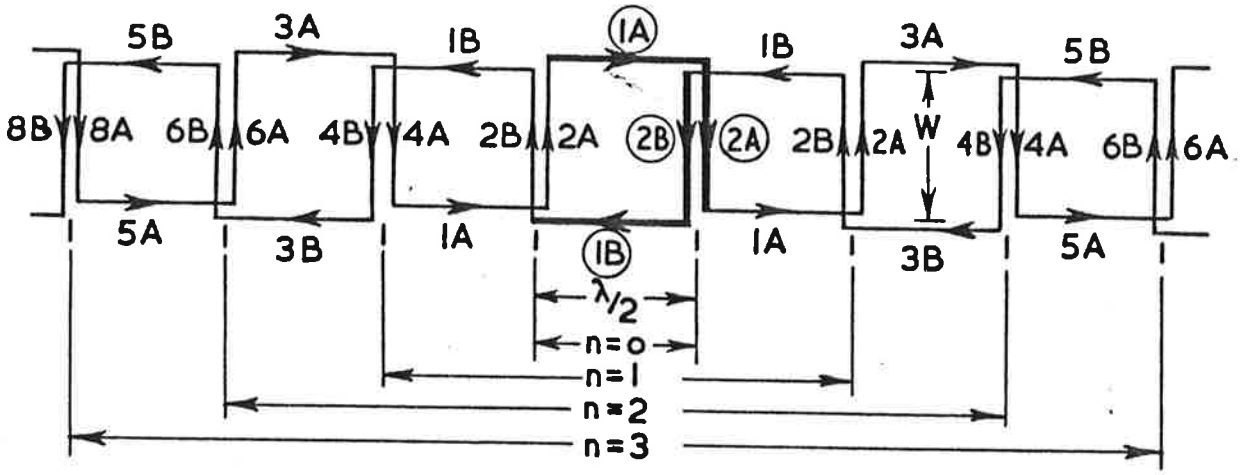

(b) Definition of limbs for self inductance calculation.

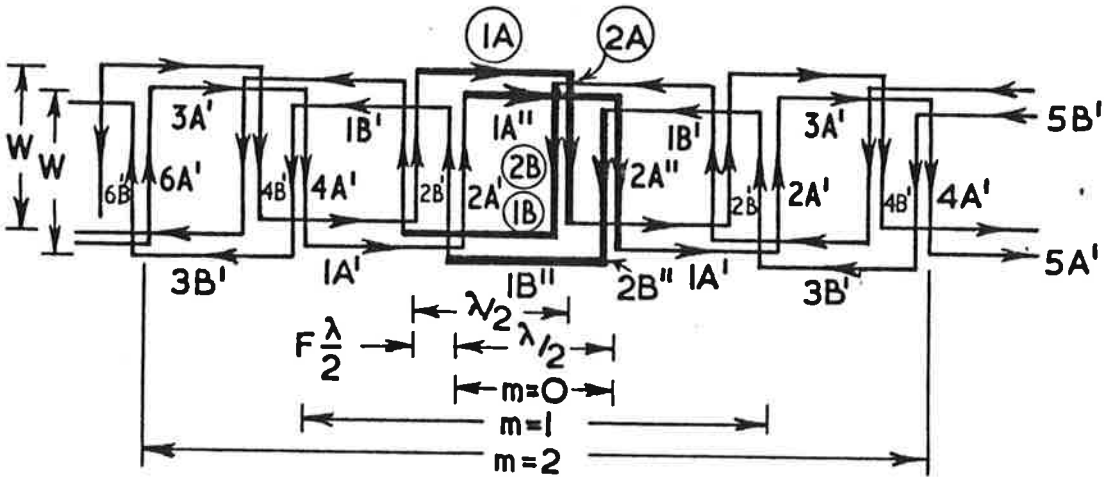

(c) Definition of limbs for mutual inductance calculation.

Figure 27. Armature winding representation.

$$L_G = \frac{2G}{\lambda}\left(L_i + \frac{\lambda}{2} L_a\right) = G\left(\frac{2}{\lambda} L_i + L_a\right) \qquad (31)$$

The mutual linkage to the remaining phases from the reference phase is calculated in a similar manner. The form of the mutual inductance must vary cyclically as the displacement between the reference phase and a second phase varies. If F is the fraction of a pole pitch that the second phase is displaced from the first phase, then

$$M(F) = M(F + 2) = -M(1+F) = M(-F)$$

$$\text{and} \quad M(\tfrac{1}{2}-F) = -M(\tfrac{1}{2}+F)$$

Figure 27c indicates the disposition of two phases. For a normal three phase arrangement, a second phase is displaced by 120 electrical degrees, or $\frac{2F}{3}$ of a pole pitch.

So $M(\frac{2}{3}) = M(\frac{1}{2}+\frac{1}{6})$

and since $M(\frac{1}{2} + F) = -M(\frac{1}{2}-F)$

$$M(\tfrac{2}{3}) = -M(\tfrac{1}{2}-\tfrac{1}{6}) = -M(\tfrac{1}{3})$$

similarly

$$M(\tfrac{4}{3}) = -M(\tfrac{1}{3})$$

If balanced operation is assumed, phase currents are equal in magnitude and the mutually induced voltages in the reference phase from the other two phases are individually the product of phase current, mutual inductance and cos 60°, so together they can be summated as a full phase current producing a voltage drop in $M(\frac{1}{3})$, for the reference winding, and three phases.

As with the self inductance, the elementary inductance $M_e(m)$ is defined as the interaction of the reference phase with the second reference elements and the m elements either side. The mutual inductance between phases G metres long is

$$M_G = G\left(\frac{2}{\lambda} M_i + M_a\right) \qquad (32)$$

where again M_i is an initial shape term, and M_a is an asymptotic value, assuming F remains constant. Figure 28 shows the variation of L_a and M_a with the width/pole pitch ratio.

For the three phase case, M_G and L_G combine to give the total phase leakage inductance, L, as

$$L = (L_G - M_G) \qquad (33)$$

and this value can be successfully used in further computation or equivalent circuits.

It is found from this type of analysis that a double layer meander winding shows significant improvement over a single layer meander winding. Essentially a single layer would have to be connected remotely, whereas a double layer allows a common terminal point for machine half phases. The effective self inductance of the phase winding is virtually halved.

3.2.3 Back Emf

The back emf, E_B has been chosen as the main linking parameter for field to armature linkage. If this value is known for a full pitched coil moving at synchronous speed, then conventional rotating machinery analysis can be used to establish the open circuit terminal phase voltage, including the effects of short pitching, transposition, and parallel and series interconnection of individual armature conductors into a phase winding. Initial analysis has assumed that the machine is fed with balanced voltages and currents, and operates under steady state conditions. Phase inbalance can in fact be accommodated by using positive and negative sequence analysis.

Taking the case of the generalized vehicle and track coil shown in Figure 29, the vehicle coil energised with I_v AT generates a track level vertical component of flux B_z. The flux linked by an elemental strip dx wide is given by

$$d\phi = \left\{ \int_{-b}^{b} B_z \, dy \right\} . \, dx$$

$$\text{i.e.} \quad \frac{d\phi}{dx} = \int_{-b}^{b} B_z \, dy \qquad (34)$$

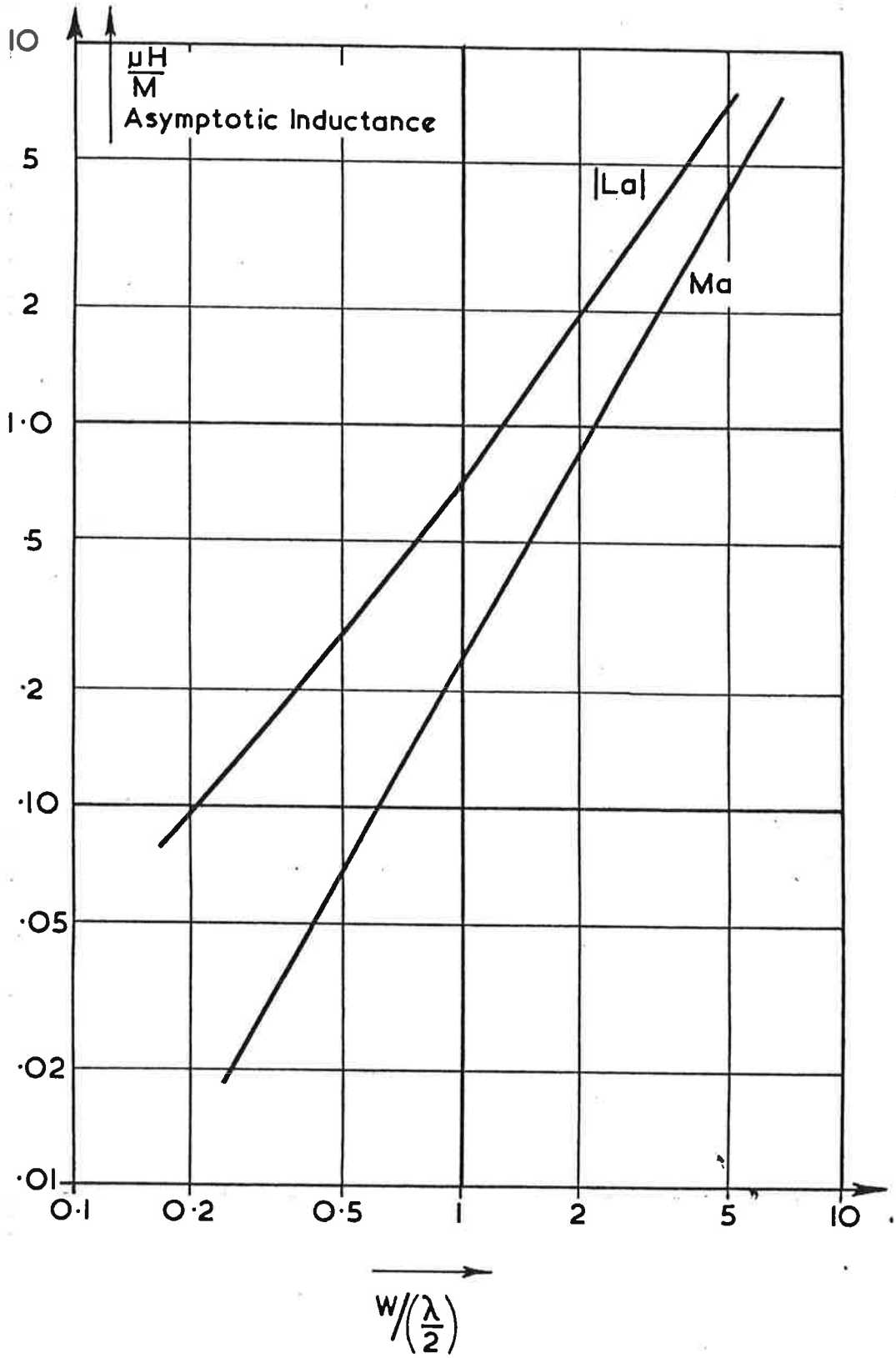

Figure 28. Asymptotic Self and Mutual Inductance as a function of width / pole pitch.

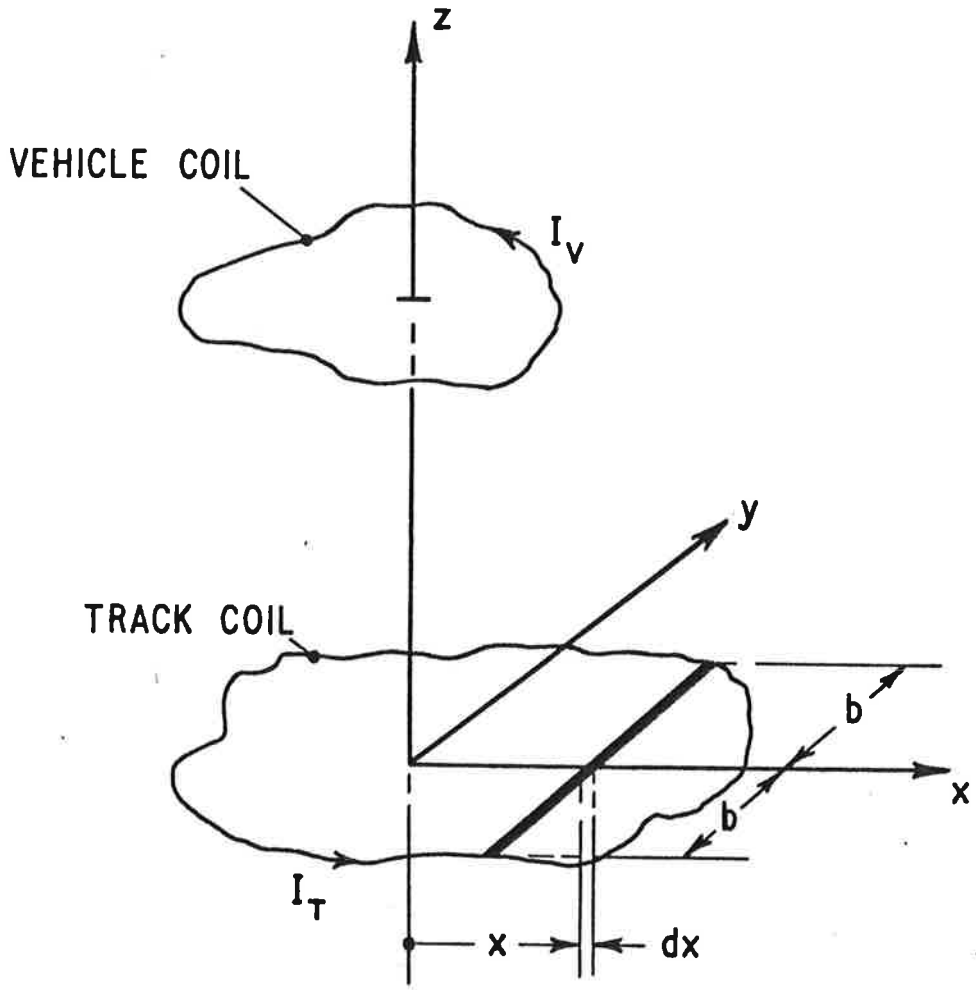

Figure 29. Generalized Vehicle and Track Coils.

The effect of having offset coils is merely to change the limits of integration. For the most common cases of tandem arranged vehicle coils, the zero offset position links the most flux. Equation 34 is valid for whatever topology of coils is finally chosen, independant of end winding geometry. The back emf induced in the track coil by the passage of a vehicle coil is simply equation 34 times the velocity.

Before attempting to evaluate 34, it is worth examining the total effect of an array of coils on the track level flux density distribution. Since the LSM is air cored, superposition can be used to sum the effects of both distant and near coils. It is necessary to establish the order of magnitude of numbers of coils to be included, to give an idea of the likely sensitivity to force calculations. By using a dipole approximation, the effect of neighbouring coils can be determined.

The external field of a current loop can be decomposed into an infinite series of multipoles. In the coil plane,

$$B(r) = \sum_{n=2}^{\infty} \frac{\mu_n}{r^{n+1}} \qquad (35)$$

μ_n is the nth pole magnetic moment, and r is the distance from the coil centre line to the field point considered. Since only far off effects are concerned, the higher orders can be neglected. The coil now appears as a dipole, and its field diminishes as the cube of the distance. For the case of the incremental contributions of 2N neighbouring coils, with for example, alternating polarities, to the total field of the reference coil, it is found that

$$B_z = \frac{2\mu_2}{(\frac{\lambda}{2})^3} \sum_{n=1}^{N-1} \left(\frac{1}{n^3} - \frac{1}{(n+1)^3} \right) \qquad (36)$$

$$n = 1, 3, 5 \ldots$$

For an accuracy of better than 0.1%, only 16 neighbouring coils need be considered. Generally, roughly ten coils give an accuracy that is sufficient for most engineering design purposes.

To establish the magnitude of the back emf, an analysis of the flux density under a coil must be made. Powell and Danby attempted to analyse a LSM with a very high harmonic content, and used a simplified expression for rate of change of flux linkage[79]. Atherton attempted to provide a complete solution for a generalised array, but similarly failed to include all the sides of a rectangular magnet in the contribution to the flux[105]. Nasar continued the application of a incomplete flux linkage solution in establishing his version of LSM theory[195]. While a solution for back emf is of course possible taking into account only the transverse field coil limbs, it can have serious effect on the evaluation of performance, especially for more compact coils where width approaches pole pitch.

A generalized expression has been obtained for the rectangular coil vertical field at an off axis position given by coordinates x, y in Figure 30[222]. Appendix IV is a copy of this Warwick Maglev Technical Memorandum. The expression includes the contribution of all four sides, and is integrated to give the flux linkage of the coil with a track elemental strip. Essentially the rate of change of flux linkage is a function of five parameters, namely

$$\frac{d\phi}{dx} = fn\ (\gamma e,\ e,\ b,\ z,\ x) \qquad (37)$$

γe and e are the vehicle coil half length and width, b is the track half width, z the levitation height, and x the off-coil centre line longitudinal displacement.

It is now possible to fully demonstrate the effect of neighbouring coils on the contribution to rate of change of flux linkage, and hence the effect on back emf. Figure 31 shows three coils from a typical (CIGGT) magnet array, with the rate of change of flux linkage of the reference coil A, and the magnitudes of the contributions of neighbouring left and right hand coils, within the half wavelength centred around A. Also shown is the total rate of change of flux

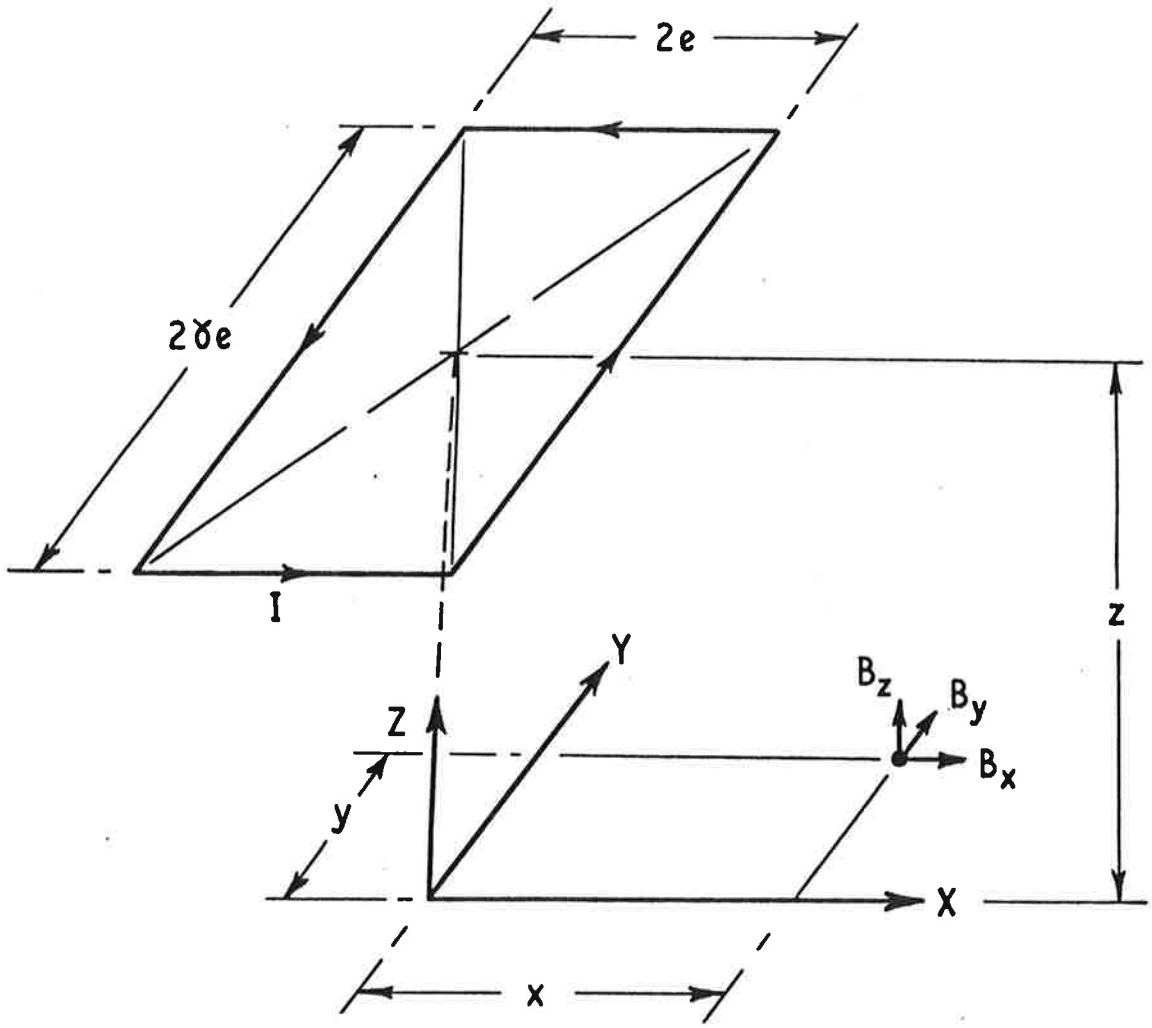

Figure 30. . Field Conventions Adopted for Rectangular Coils.

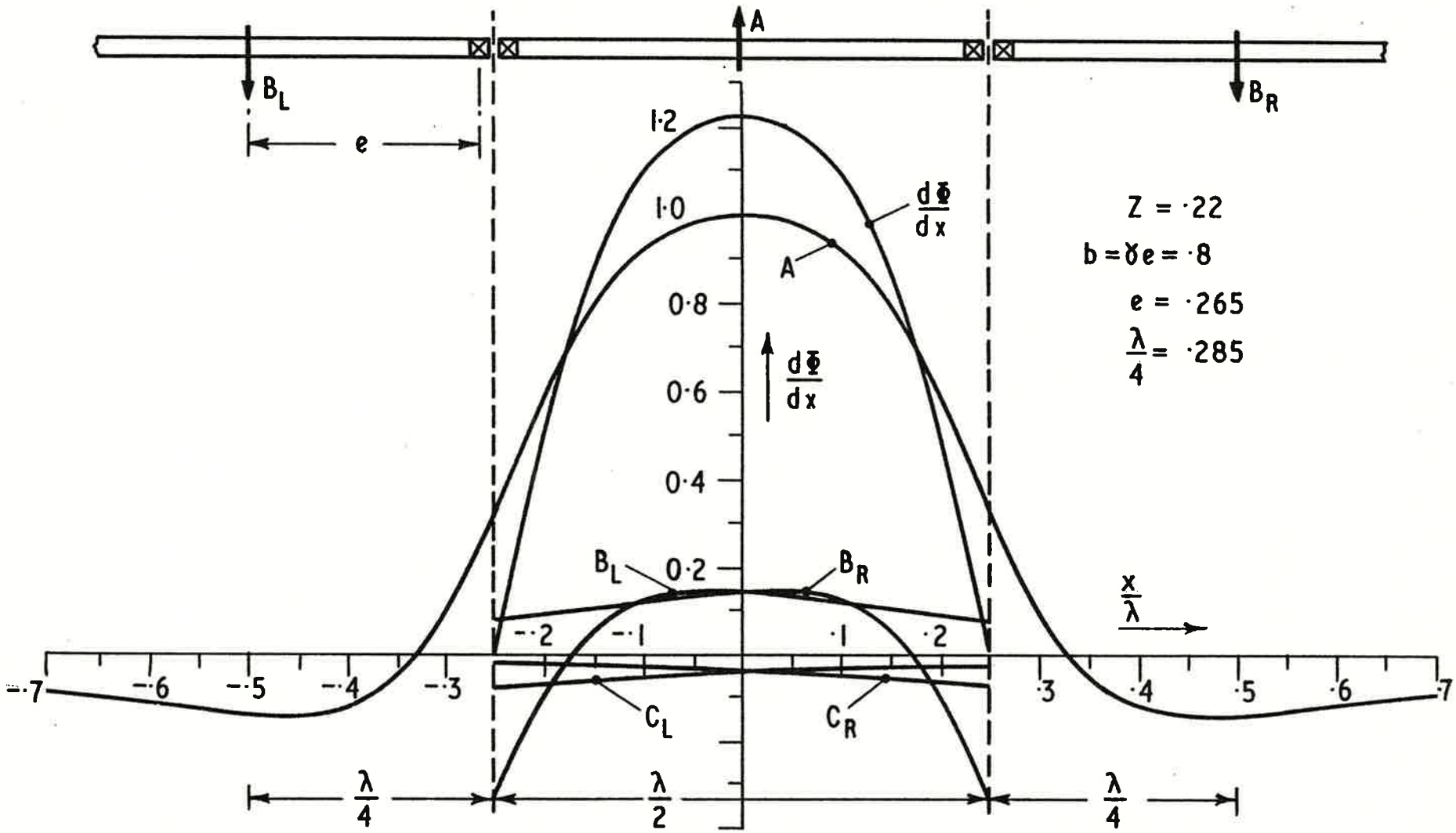

Figure31. Neighbouring Coil Contribution to $\frac{d\Phi}{dx}$.

linkage, which is forced to zero every half wavelength by conditions of symmetry. In this particular case the effects of two coils ($B_{L,R}$, and $C_{L,R}$) either side of A are included. The effects of additional neighbouring coils on rate of change of flux is shown by Figure 32. Because the case considered is for an alternating array, the successive points alternate about the final value. Also shown is a more rapid convergence, using the incremental difference of successive coil pairs. For this particular case only ten neighbouring coils (i.e. five either side of the first coil) need to be considered to give a reasonable result. The way in which the quarter wavelength value of x is rapidly forced to zero confirms the accuracy of the calculation.

Once the total rate of change of air gap flux linkage with the full pitch track coils is known, its harmonic make up can be evaluated. With the conventions shown for the x axis starting on the vehicle coil centre line, then only odd harmonics will be present in a cosinusoidal summation. Since the air gap flux is dominated by the field contribution, armature reaction will hardly affect the air gap flux distribution. This is much more marked in a linear superconducting machine as opposed to a rotary superconducting machine, where the high field winding mmf is used to increase the machine specific output and the armature reaction is similar to conventional machinery. When the flux waveform is analysed, the choice can be made to short pitch the armature winding to subvert particular harmonics, and phase spread the winding, or to simply operate with only a few turns per phase per pole, establish a star connection and allow harmonic currents to flow through the neutral to the inverter station.

In general the LSM design for Maglev vehicles will operate at an airgap to coil half width ratio near unity, which implies a near sinusoidal flux waveform at the armature. Other applications of the LSM, especially when used to propel contact guided vehicles, will imply a lower ratio, and harmonic fluxes will dominate the design procedure. For the CIGGT machine, the first harmonic has a

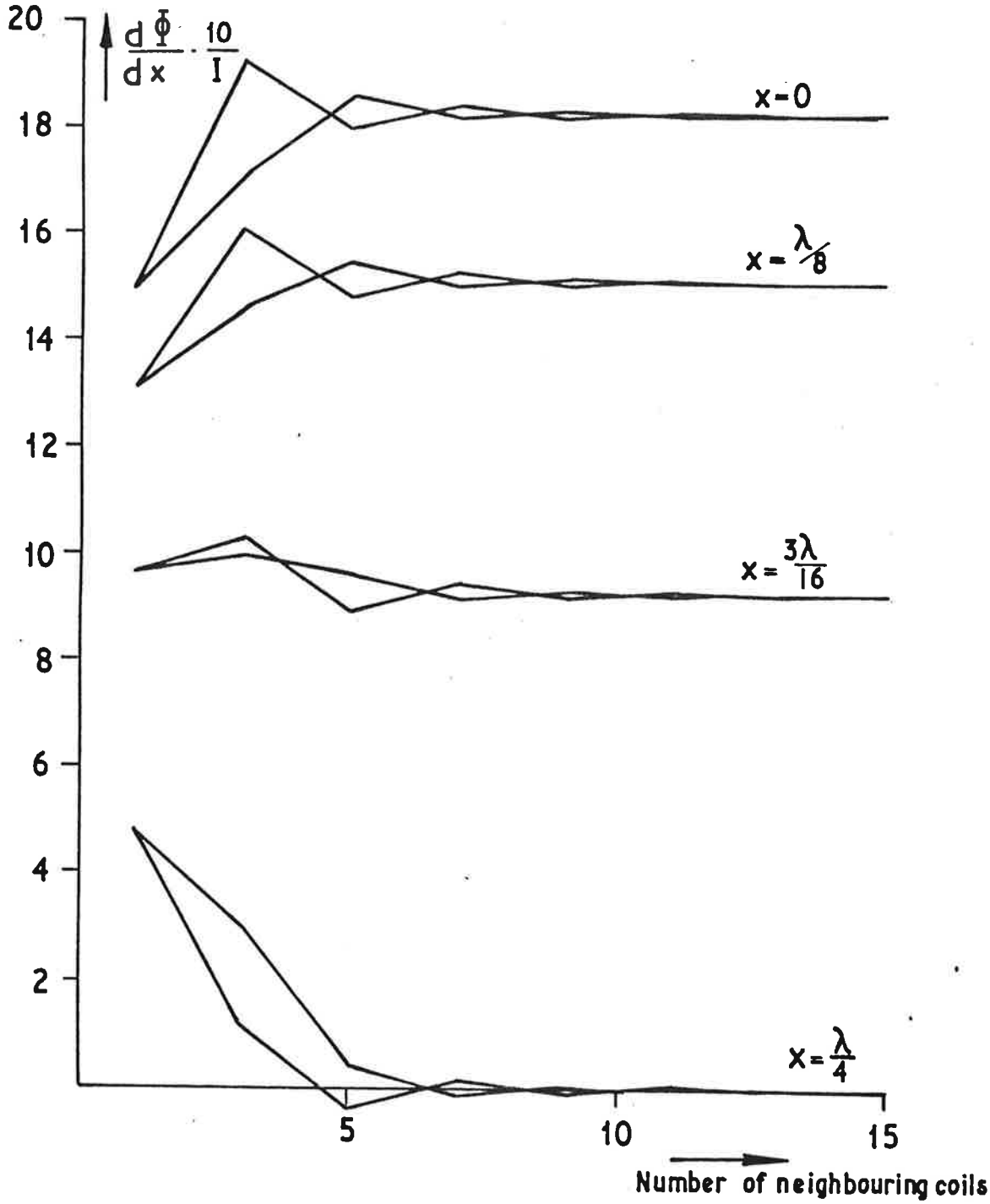

Figure 32. Effect of neighbouring coils on rate of change of flux.

amplitude of 108% of the rms value, with a 9% contribution from the third harmonic, which could be eliminated by a delta connection. There is virtually no harmonic contribution past the ninth harmonic[223].

Having only dealt with rectangular coils, the field variation at off axis positions for circular and racetrack coils must be defined. Circular coils require the solution of complete elliptical integrals of the first and second kind. Racetrack off axis positions require combinations of straight line element type formulae, with extra terms involving the solution of incomplete elliptical integrals of the first and second kind. The overall technique for solution of rate of change of air gap flux linkage is similar to that used for rectangular coils, but is computationally more awkward. When working at large air gaps an equivalent area rectangular coil can be used for first order approximation, with only a slight loss of accuracy.

Once the harmonics of the back emf are known, the force pulsations on the vehicle, and indeed the force profile can be determined by taking harmonics in turn and applying their values to equation 15. If the current has significant harmonic content, this too can be incorporated to produce the total pulsation of the parasitic harmonic forces.

3.3 Wavelength Optimization

For machine parameter optimization a more general model is required. Operational optimization in choice of a minimum power factor efficiency product working point used an equivalent circuit model. Ideally a wide track giving a long active length per pole, and a short pole pitch, to enable a large number of poles to be used might appear to be the best choice. However, track width is usually determined by the likely infrastructure and compatibility requirements with other systems, as well as vehicle width; pole pitch might be fixed by inverter or cycloconverter upper frequency limits, and cryostat and coil fabrication constraints. A simple model can be formed in which levitation height and track width are the main variable parameters, which are functions of groups of track and vehicle constants.

Thornton analysed a simple model of a finite width track interacting with a two dimensional field distribution from an effectively infinite width magnet array[91]. For this case the time averaged thrust force F_B is related to a maximum fundamental thrust force F_M by the current angle. Similarly the normal force F_N is the quadrature variation. F_B and F_N are expressed by

$$F_B = F_M \sin\alpha \qquad (38)$$

$$F_N = -F_M \cos\alpha$$

By comparison with equation 15, F_M can be related to the back emf and phase current by

$$F_M = \frac{m}{v} E_B I \qquad (39)$$

Taking a $\bar{J} \times \bar{B}$ product with the assumption of balanced phase currents and a sinusoidal current sheet representing the magnet array, with a strength of I_V AT per pole, from N poles, then,

$$F_M = 2\mu_0 N \; m \, I_v \, I_T D \; \frac{w}{\lambda} \; e^{-2\pi h/\lambda} \qquad (40)$$

m and I_T are the number of stator phases and the track per phase current, w, λ and h are track width, wavelength and coil height, and D is a dimensionless constant which expresses the meander winding end turn shape.

Two more useful parameters are P_A, the power loss in the armature per unit track length, and M_A, the meander mass per unit track length. P_A is proportional to the efficiency of the machine, and hence power consumption, and is measured in watts per metre. M_A is proportional to the amount of capital cost in installing the guideway meander conductor, and is in kilogrammes per metre.

$$\text{So} \quad P_A = m I_T^2 \cdot \rho \cdot \frac{(\lambda + 2w)}{2A\lambda} \qquad (41)$$

$$\text{and} \quad M_A = m \; (\lambda + 2w) \; \frac{A\sigma}{\lambda} \qquad (42)$$

where σ and ρ are the density and resistivity of the track conductor.

Combining 41 and 42,

$$M_A P_A = m^2 (\lambda + 2w)^2 \frac{I_T^2 \rho \sigma}{2\lambda^2} \qquad (43)$$

and eliminating the track current in (40) with (43)

$$F_M = 2 \mu_0 NI_v \frac{(2M_A P_A)^{\frac{1}{2}}}{\rho \sigma} H \qquad (44)$$

where $$H = \frac{D w}{\lambda + 2w} e^{-2\pi h/\lambda} \qquad (45)$$

H embodies width, height and wavelength in a form that can be optimised. Equation 44 contains (apart from H) items that are very often fixed by economic constraints or material conditions. For example, working the track at a particular P_A implies a choice of efficiency maximum, and for M_A, a track capital repayment cost can be inferred. NI_v is reflected directly into the vehicle cost. It is reasonable, therefore, to assume that these parameters take fixed values, and that design manipulation must be through H.

Thornton chose to maximise the thrust per pole, which implies that a vehicle thrust requirement can be met by simply adding poles. The maglev vehicle however has finite length, which is fixed at an upper limit by a tradeoff between lightness and structural stiffness in torsion and bending moment.

Abel, however chose to maximise the thrust per stator conductor length under the vehicle - stator current product, or effectively H divided by wavelength[130]. The power transferred to the finite length vehicle is maximised, which is more reasonable since usually the full vehicle length will be required for propulsion magnets, and may in fact limit the thrust capability in very high powered vehicles.

If the thrust per unit stator length-current product is found for various values of wavelength, the resulting magnitude tends to have a broad maximum, depending on the track width and magnet height. Figure 33 shows the normalized thrust,

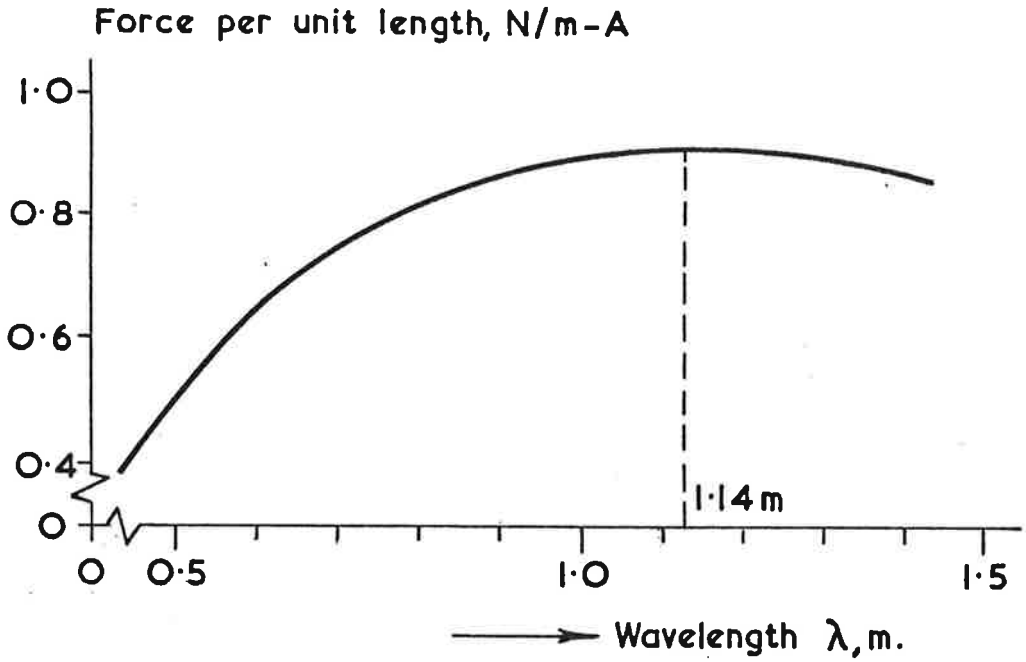

Figure 33. Thrust per unit stator length x current.

and Figure 34 shows the optimum wavelength for a range of magnet heights and track widths. Values for infinitely wide tracks are also shown. The optimum value of wavelength is

$$\lambda = \frac{w - \pi h}{2} \left[\left(\frac{1 + 8 \pi hw}{(w - \pi h)^2} \right)^{\frac{1}{2}} - 1 \right] \qquad (46)$$

resulting directly from maximising H divided by wavelength with respect to wavelength.

For the Wolfson LSM design studies, the armature fits between two levitation conductors and is fully spanned by a vehicle coil array. The assumption of a current sheet approximation for the field array is reasonably valid. For a revenue vehicle this validity breaks down, but in fact a mutual inductance derivation of various wavelengths for different track widths and magnet heights leads to similar optimum wavelength. The normal force maximum is generally greater than the thrust force maximum, since the side limbs of the magnets develop significant lift force but do not aid thrust.

3.4 Shape Effects on Coil Stress[131]

The use of superconducting magnets as the source of magnetic flux for LSM propulsion has generally been approached from the assumption that it is possible to construct tight corner radius rectangular coils. For the Wolfson design, lateral stiffness and lift to drag ratio considerations suggest that degradation of performance in levitation and guidance would occur if the proposed rectangular tandem array was made up of circular coils. In practice, it is extremely difficult to construct working magnets with tight corner radii without experiencing problems of winding migration and stress concentration at the corners. The usual method of accommodating excessive stresses is to wind circular or racetrack coils. To achieve an optimum design, it is necessary to be able to predict whether it is possible to construct coils which have tight radii at the corners and can still accept the stress levels when energised without all the attendant problems. Usually for a particular vehicle, width is at a premium. For the CIGGT design the width must accommodate the LSM propulsion cryostats as well as levitation cryostats. Propulsion magnet size is

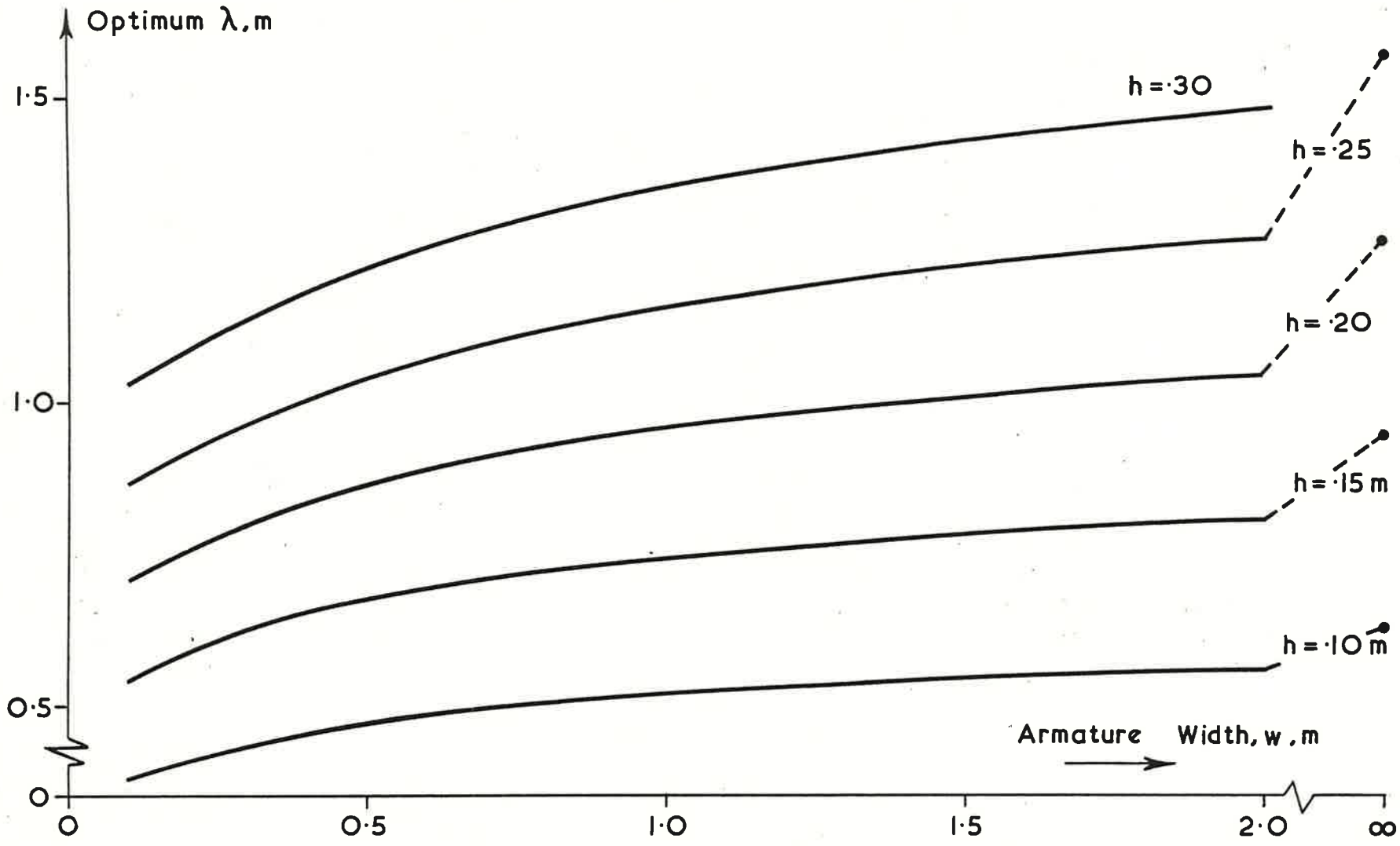

Figure 34. Optimum wavelength for machine width w, and airgap h.

determined by the thrust requirement, passenger density, and hardware costs and generally the wavelength will be in the range of 1-3 metres. For a full race track end wound propulsion coil, the linear motor active length is reduced by about half a wavelength, compared to a rectangular coil. If a dual or transverse-flux motor is adopted, then four sets of end windings will have to be accommodated in the vehicle width, with allowance for levitation magnets included.

The forces on coil systems are generally due to several sources. Mechanical stresses are induced as the coil is built. Many large superconducting coils are prestressed as they are wound, and additional clamping forces and support increase the inherent stresses. As the coils are cooled down to their working temperature, uneven material contraction can cause thermo-mechanical forces to be generated. Thirdly, as the coils are energised, magnetomechanical forces generate further stress levels. Coil stressing can be attacked at several levels of complexity. Figure 35 shows several simple elements and the way in which the Lorentz forces are generated by the interaction of an elemental current flowing in a coil part in a background field, generated either by the element itself, or an outside source. Usually coils have significant build up in three directions and a finite element solution is suitable, but requires significant computing.

For circular coils, the field level variation throughout the coil section can be evaluated using either tables or direct calculation. Appendix II gives details of the methods used in rectangular and circular solenoid design. The easiest stress analysis is to approximate the coil to a thick/thin cylinder, and model the internal stress boundary condition by a magnetic pressure. A homogeneous thick cylinder theory produces a more accurate solution. Coils are usually anistropic structures and so account must be taken of the orthotropy, as the stress tensor is evaluated. Mulhall and Prothero analysed a homogeneous anisotropic solenoid[224]

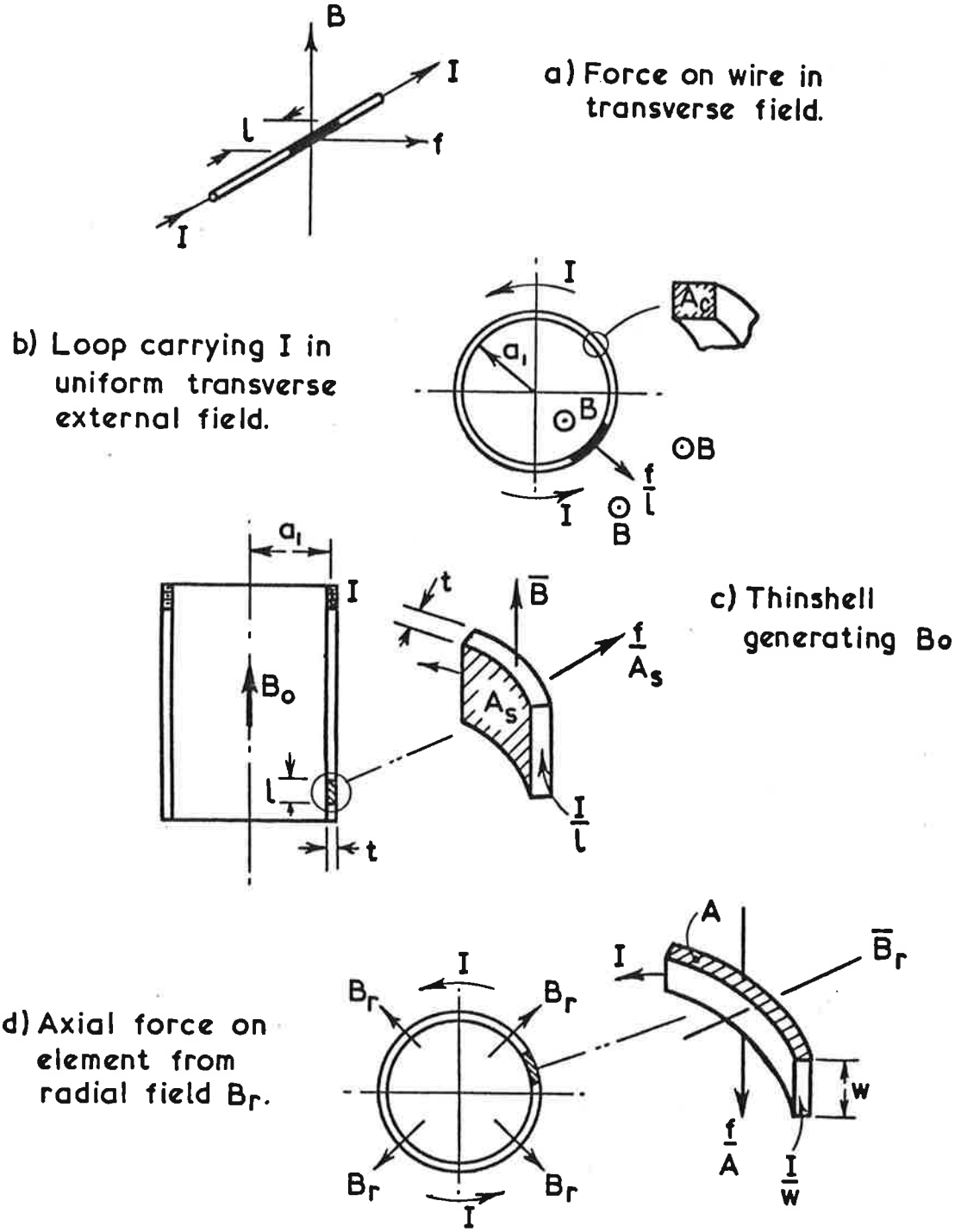

Figure35. Lorenz forces on simple elements.

by numerically integrating the field generated body force across the coil in the radial direction, to obtain hoop stress values. Abel produced a closed expression for the stress levels for the same case, using the element shown in Figure 36[225]. The body force was directly calculated since closed expressions for the radial and circumferential field are known. Montgomery has shown that for circular coils a magnetic pressure approximation approaches an exact solution if the coil build up is small compared to its diameter[226]. This condition is usually met by Maglev coils where the strength is of the order of 500 kAT for the motor magnets, and their size is of the order of 0.5-3 x 1-3 metres. If a finite element programme is available, a stress tensor relating strain to stress from equations of continuity and equilbrium would be formed. A typical element is shown in Figure 37 where the element boundary conventions are defined.

When square or rectangular coils are analysed, the exact solution without resort to finite element techniques is difficult. The most critical stress levels will always occur at the corners. A technique developed uses approximate solutions for the stress levels, by effectively matching a magnetic pressure comparison of rectangular and square tubes' stresses with equivalent circular thick walled tubes'. This methodology is acceptable because the free body diagram of sections of a corner radius and a circular coil will be identical.

For the case of a circular coil of mean radius a, winding width (radial build up) s, a magnetic pressure P_M will give hoop stresses σ_θ, radial stress σ_r and shear stress σ_s given by

$$\sigma_\theta = \left(\frac{a}{s} + \frac{s}{4a} \right) P_M \qquad (47)$$

$$\sigma_r = - P_M \qquad (48)$$

$$\sigma_s = \frac{\sigma_\theta - \sigma_r}{2} = \left(1 + \frac{a}{s} + \frac{s}{4a} \right) \frac{P_M}{2} \qquad (49)$$

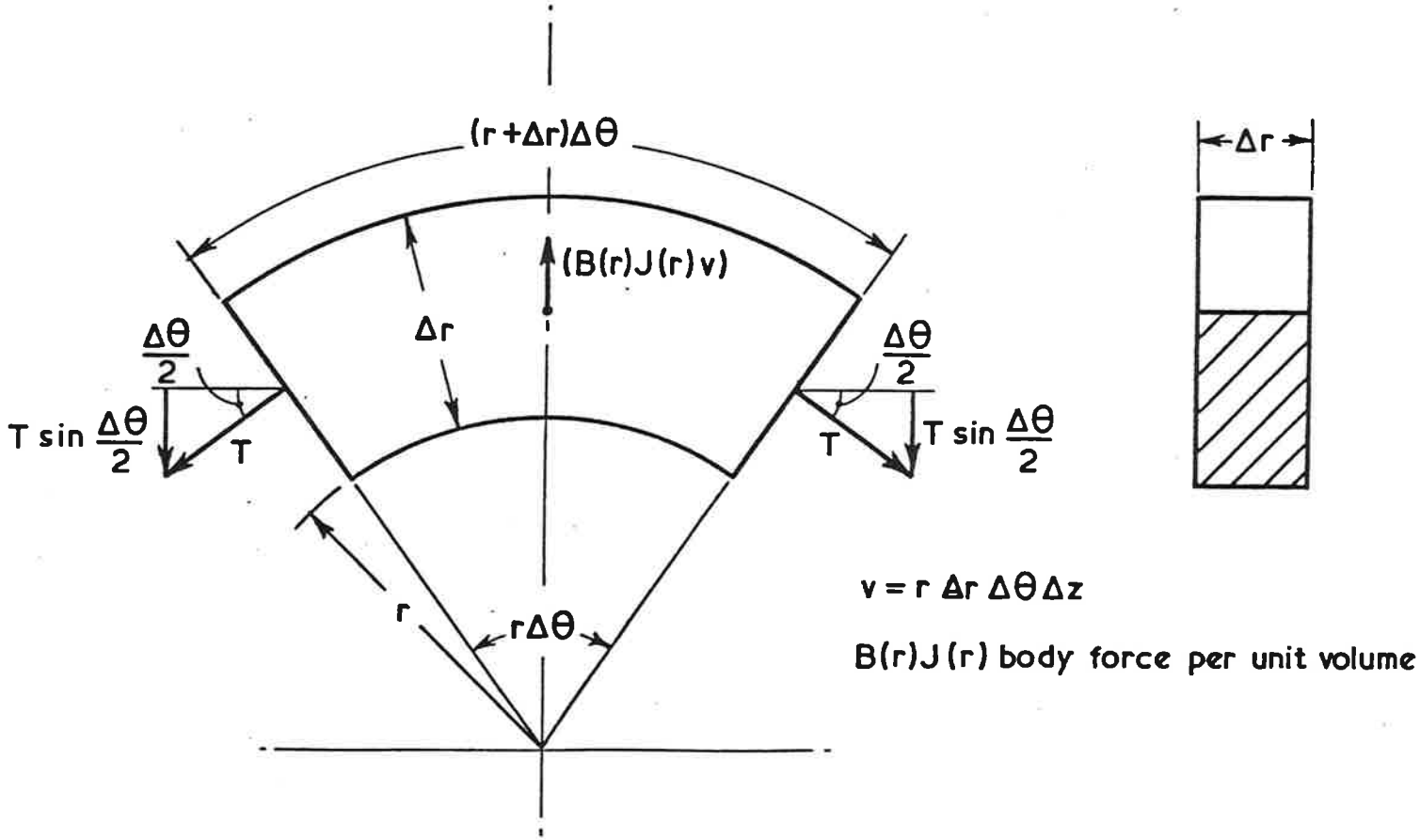

Figure 36. Balance of body forces and restraining forces.

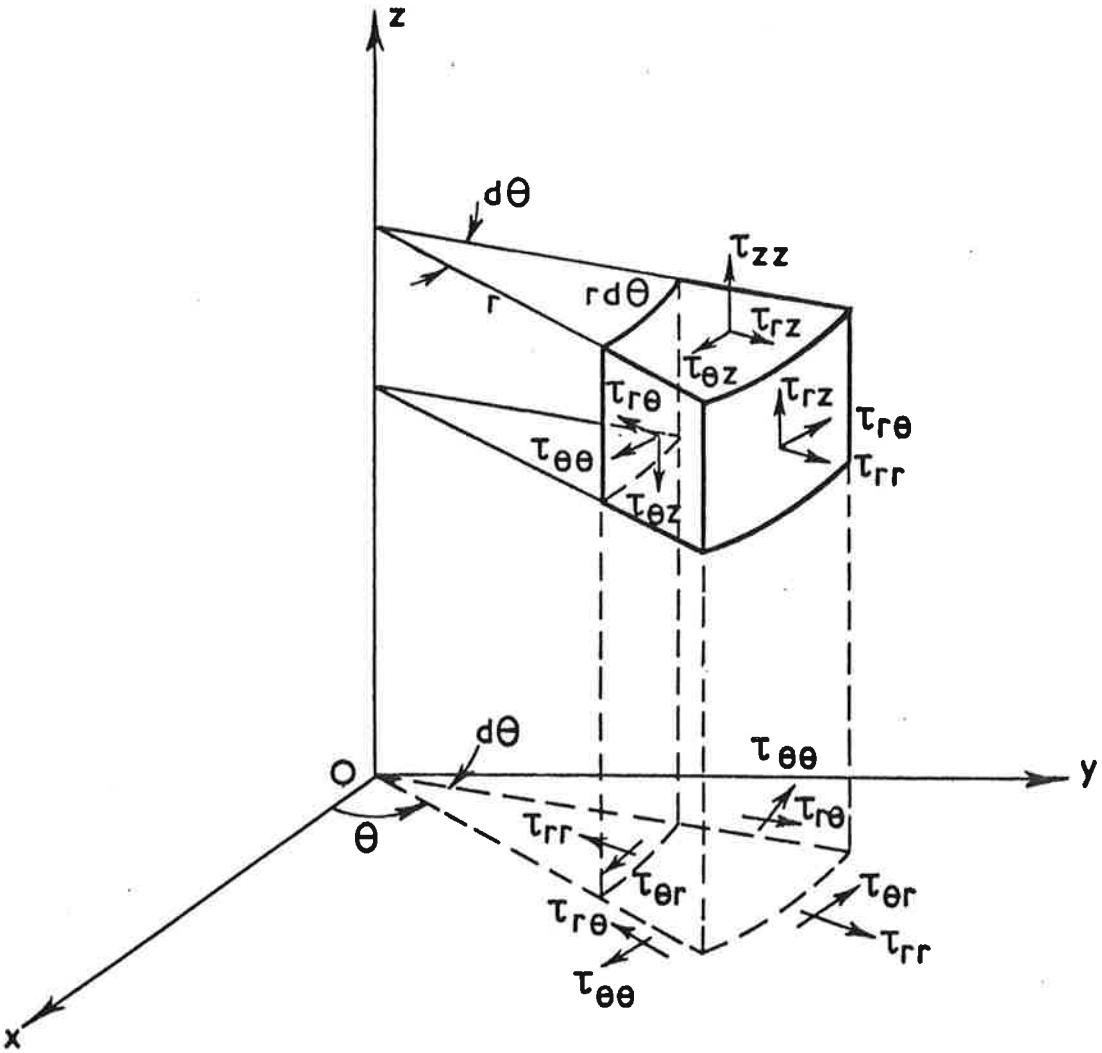

Figure 37. Element for cylindrical coil stressing.

These values are for the inside face of the wound section, where the shear stress is at a maximum.

If the magnetic pressure P_M is taken to be identical to the coil energy density, then to a first approximation

$$P_M = \frac{B^2}{2\mu_0} \quad J/m^3 \qquad (50)$$

where B is the coil flux density. Naturally the coil flux density is modified for the same ampere turns as the corner radius is changed. Figure 38 shows the central field normalized by the factor $\frac{\mu_0 I}{\pi a}$ for the transition from a square coil to a circular coil. The values range from $\frac{\pi}{2}$ (circular) to $2^{\frac{1}{2}}$ (square), and are the combination of field calculations for quadrant and straight line filaments. Although the value of flux density used in equation 50 should be that of the inner face of the coil, the central field value gives a reasonable guide to the exact value.

Roark gives expressions for the corner moment for the simple portal frame and rectangular tube under internal pressure[227]. Knowing the bending moment, the hoop stress can be easily obtained at the inner edge. Figure 39 shows the tube and portal frame, with and without radiused corners. For the radiused corner tube, the maximum bending moment is given by

$$M = Cw\,(2\gamma e)^2 \qquad (51)$$

where C varies from 0 for a circular coil to 1/12 for a square coil[131] and w is the loading. The hoop fibre stress needs to be modified since the neutral and centroidal axes no longer coincide, and is finally given by

$$\sigma_\theta = 24\left(\frac{\rho}{s}\right) C \left[1 + \left(\frac{s}{6r}\right)\left(\frac{1}{(1-\frac{s}{2r})} + 1\right)\right] P_M \qquad (52)$$

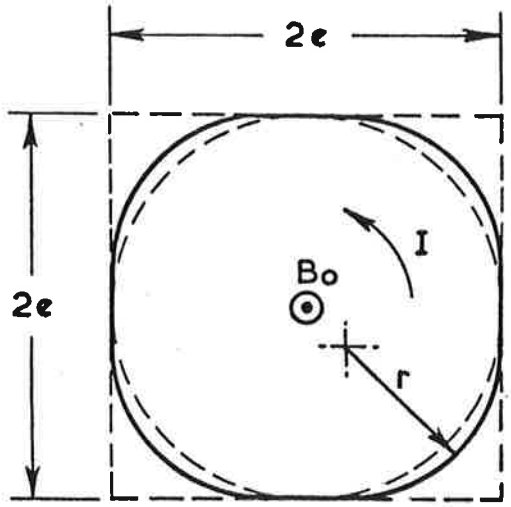

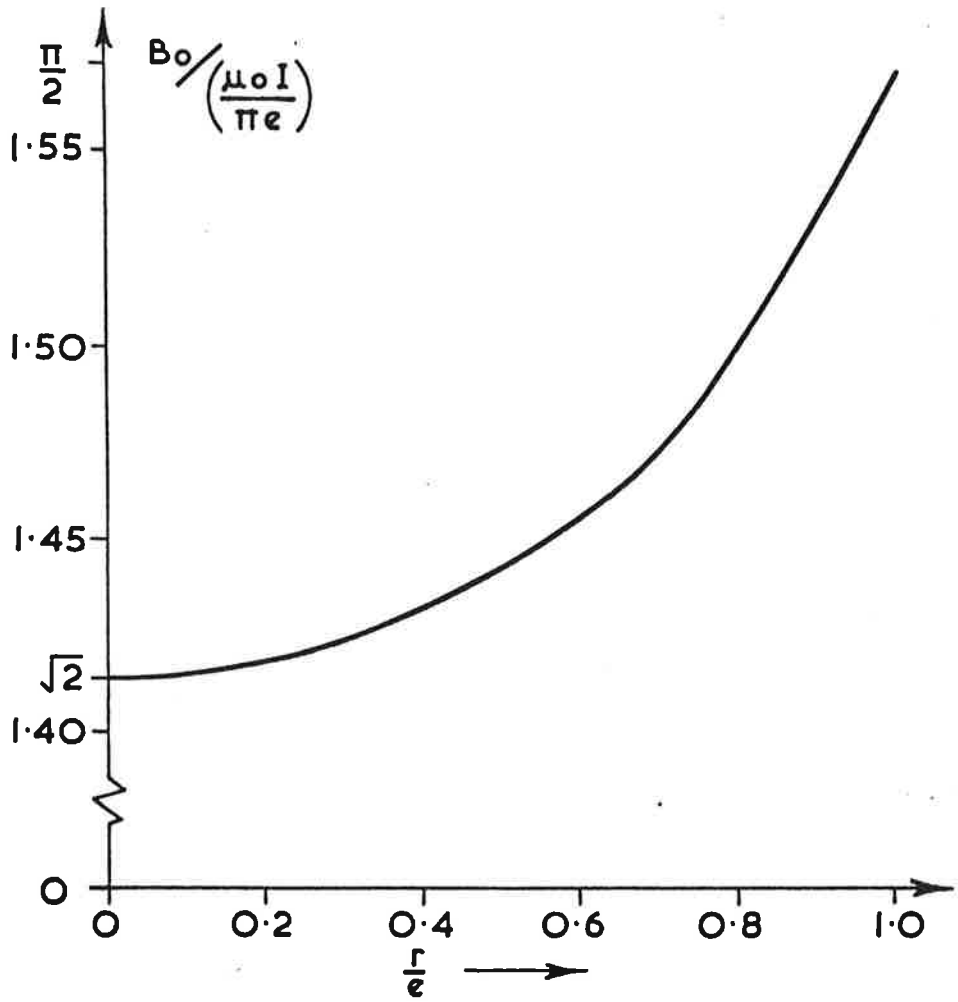

Figure38. Central field change for transition from square to circular coil.

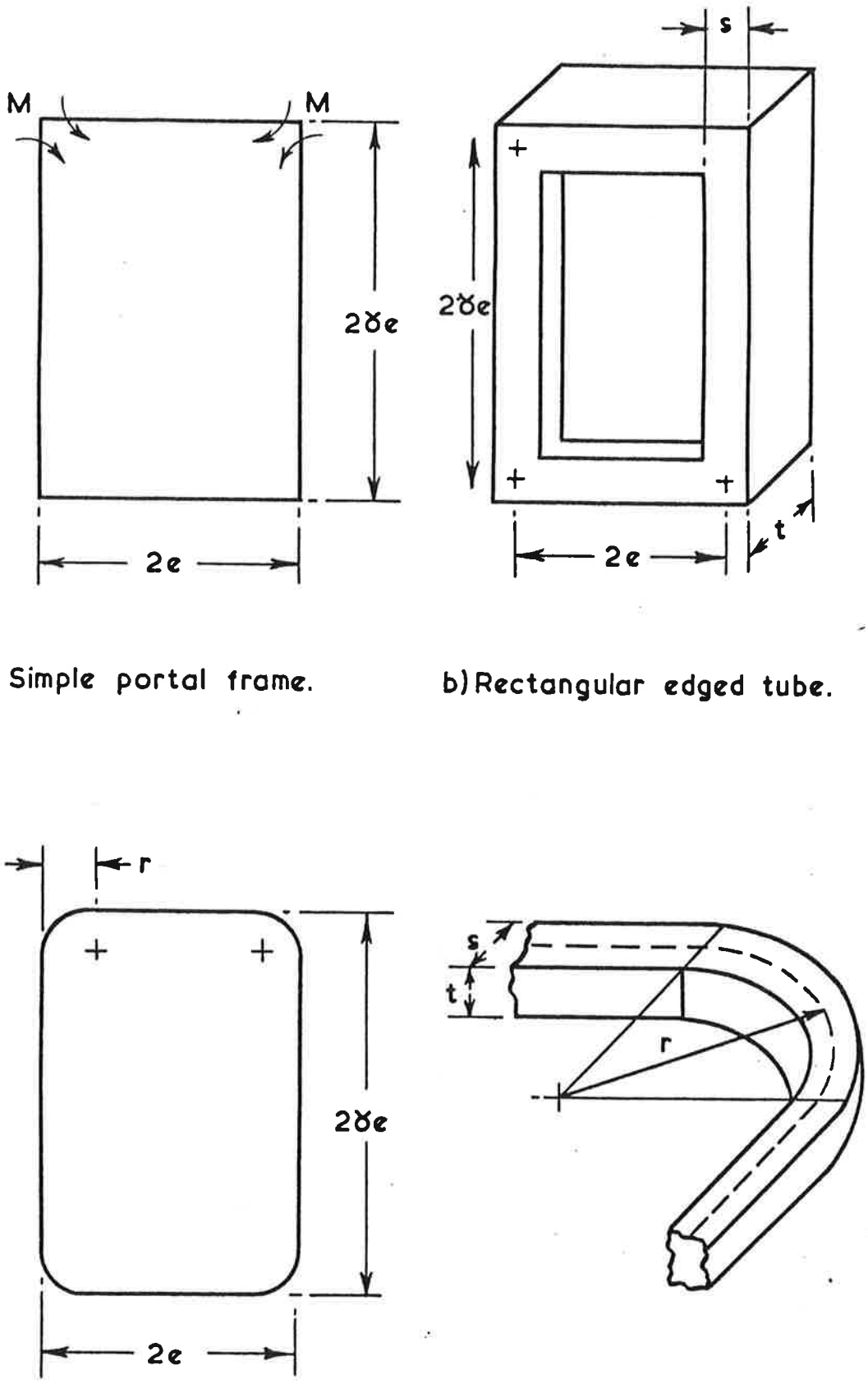

a) Simple portal frame.

b) Rectangular edged tube.

c) Radiused portal frame.

d) Corner section of tube.

Figure39. Tube equivalents to radiused coils.

Equations 48 and the first half of 49 still hold for the radial and shear stresses.

For a particular wound section (implying buildup and thickness) the radius can be found where the stress levels equal an equivalent circular coil of the same section. The circular equivalent coil can then be analysed using exact solutions including anisotropy. Alternatively, for a particular corner radius determined by factors other than stress levels, accurate computation of stress is provided by the circular equivalent. If this value is excessive a design iteration must be performed.

CHAPTER FOUR

LINEAR COMMUTATOR MOTOR

4. Linear Commutator Motor

4.1 Original Design Philosophy

The idea of using a dc machine with a superconducting field winding seems to have been first considered by Richards and Tinkham in 1972[81]. Their concept was to use current reversing switches controlled by the vehicle position to drive dc current into track loops as the vehicle passes. They also expressed concern that the dc linear motor practicability depended on the cost of the large number of switches required. About the same time Atherton proposed a similar scheme, of track coils that were supplied by either ac or dc through bidirectional switches controlled essentially by vehicle position[228]. It was felt at the time that this machine variant could avoid any of the expected problems of low speed starting of linear synchronous motors with limited frequency range inverters.

At Warwick University, the reasons for investigating linear commutator motors (LCM) were slightly different. For the 550 metre linear test track, initial designs for LSM had been based on an acceleration length of 250 metres in which a 250 kilogramme vehicle was accelerated at 1.3 gee to 80 metres per second. At this speed the drag power was 32 kW and the inertial power was 108kW, a ratio of 3.4 to 1. On the assumption that a suitable inverter could be acquired for the research programme, the track was first designed for a three block length operation with two blocks permanently connected at any one time, and the acceleration and deceleration blocks switched over as the vehicle entered the central measurement steady state speed section. On evaluating the additional power required to make up losses in the track winding, in addition to the power transferred to the vehicle, it was considered necessary to examine the effect of either providing larger conductor cross section in the main track feeder cable or to supply the track from the feeder at more frequent intervals. Since the track winding is at least two active lengths per wavelength longer than the feeder; a considerable saving could be made in power loss by only energising short lengths of track from the inverter through a feeder line

Figure 40 shows the fraction of power loss for a subdivided track winding with respect to a full length section of track; for the Wolfson design width to half wave-length ratio of 0.375, a 50 metre length has only 66% of the losses of a 250 metre length. Further subdivision only gains at the most another 8%. The track winding would then have 12 bidirectional three phase switches, which would provide a synchronous following of the vehicle, with traversed sections' power being disconnected to leapfrog to the next section. The inverter terminal rating would be reduced, and the individual sections of track would not experience such a long energised time, allowing more time for cooling between runs. If the vehicle magnets were connected to give the same polarity, the track would be wound for a 400mm pole pitch and the ratio of width to pole pitch would be 0.75. The 50 metre block length implied 71% of the 250 metre losses, with a limit of 64%, so the longer pole pitch would be the best choice.

As the concept of short block length continued, it became apparent that the limit was set essentially by the vehicle length, or even single track coils. The power could be ac or dc, provided commutation was possible, and the trackside semiconductors could replace the inverter or cycloconverter units. By phasing the track current relative to the vehicle field, levitation as well as propulsion could be achieved, which coincided with the rest of the Wolfson design of an integrated lift guide and propelled vehicle, using a tandem magnet array. Although the very short energised length LSM, with one coil per bidirectional switch would have to be controlled diferently from the multiple wavelength interconnection to an inverter fed tie line, the generic term of LCM was used to describe both types of machine[124,126]. A further subdivision was possible, depending on whether the armature winding was a distributed progressive or concentrated discrete coil winding (Figures 41 and 42).

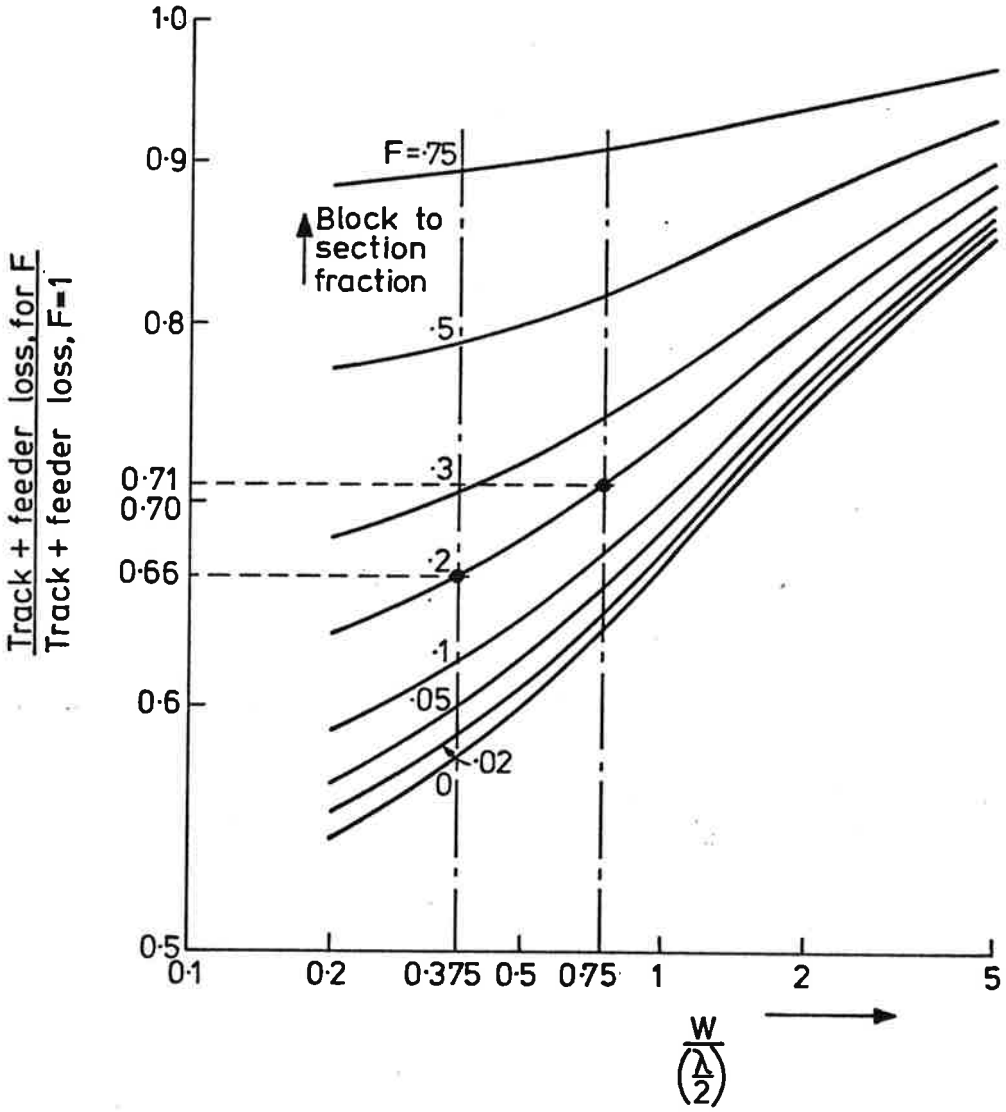

FIGURE 40. FRACTIONAL POWER LOSS IN BLOCK SECTIONED ARMATURE.

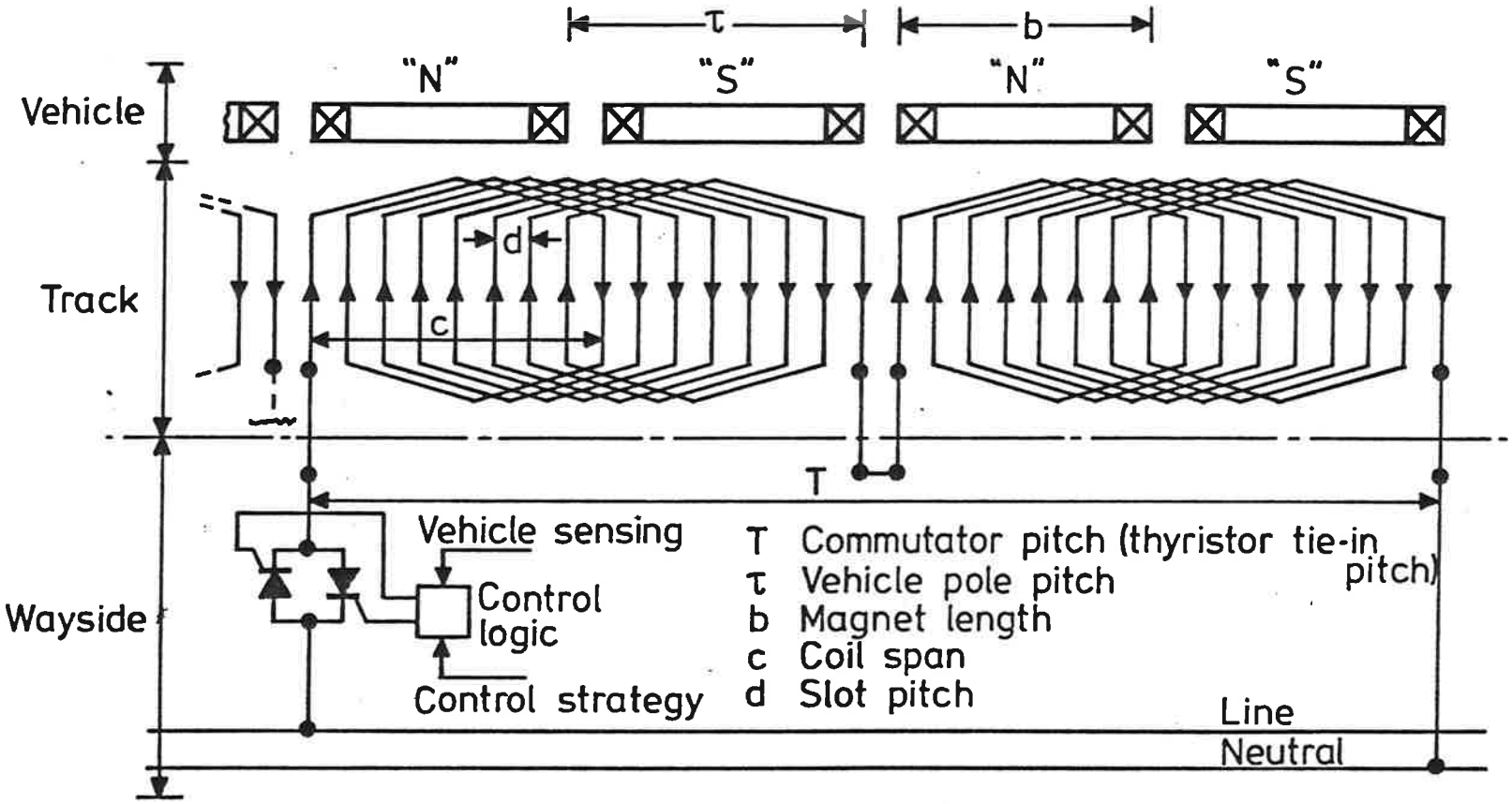

FIGURE 41. L.C.M. DISTRIBUTED PROGRESSIVE WINDING, SERIES CONNECTION OVER TWO POLE PAIRS.

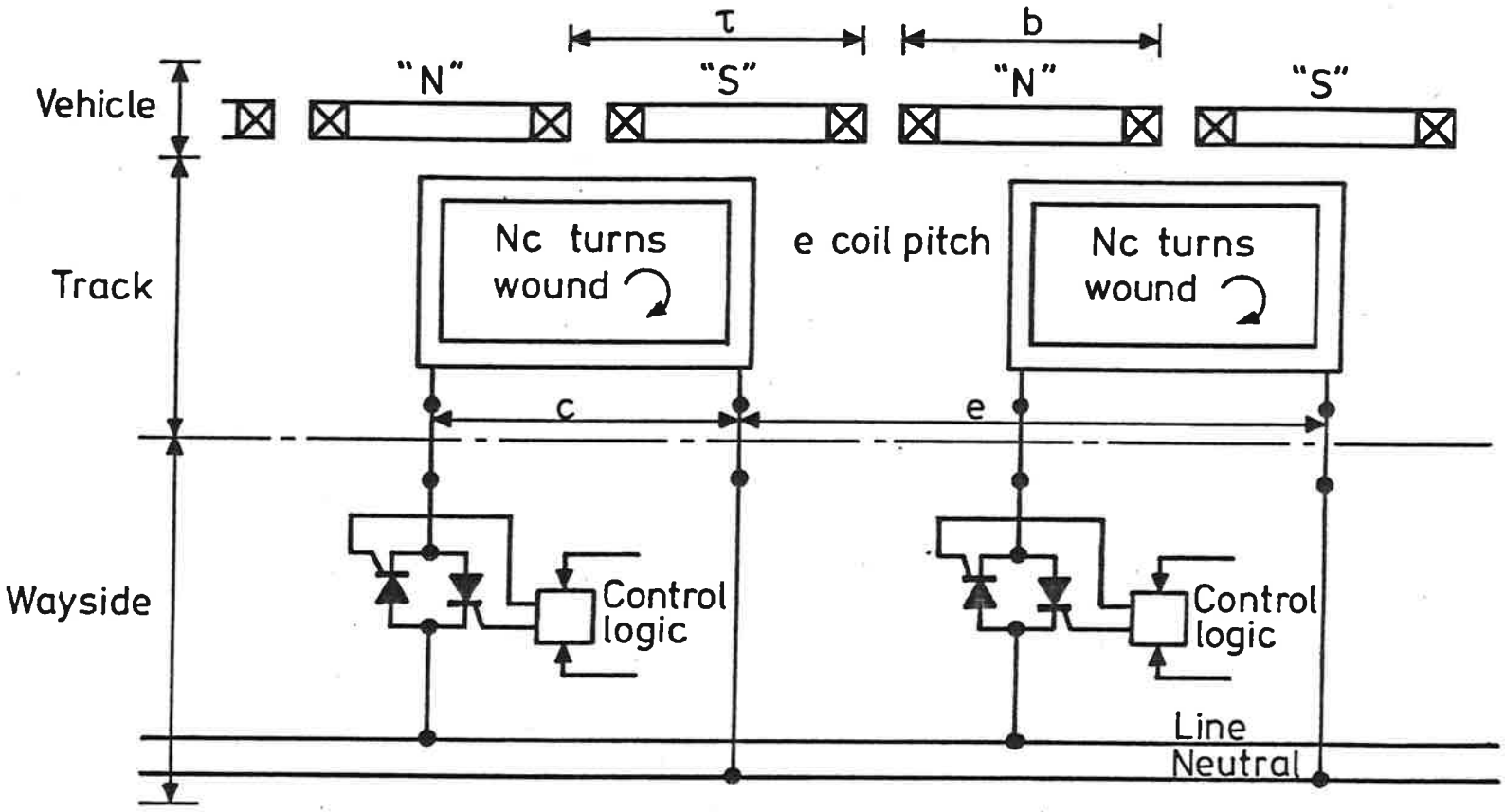

FIGURE 42. L.C.M. DISCRETE WINDING, PARALLEL CONNECTED OVER ONE POLE PAIR.

At the same time as the preliminary track designs were being established, the JNR DCLM was also publicized[205]. The DCLM used essentially the same philosophy as the switch-per-coil version of the LCM, but the field windings were iron cored normal copper conductors. The JNR work used a dc controlled rectifier feed with a "flip flop" inverter synchronised to propulsion requirements.

Dukowicz, Hoppie and Wang at General Motors had also considered an elementary form of dc propulsion motor, and had filed a US Patent[229]. The main claim was for a vehicle with a long length superconducting coil inclined to the horizontal, interacting with a horizontal array of switched coils. The vehicle coil inclination was meant to provide a change in mutual inductance along the direction of motion. The patent loosely describes alternatives with permanent or iron cored magnets, with more than one magnet per vehicle, and overlapping track coils. The practicality of such a system, which relies on the inclination of vehicle coils to provide thrust must be suspect, and would certainly not be easily incorporated into an economic system, because of the waste of vehicle space.

Warwick research continued with the conversion of a 0.5 metre drum used for LSM work, into a LCM model, using mains commutated thyristors to switch individual discrete windings as they passed under three blocks of ferrite magnets. The machine was also used with a specially designed superconducting magnet to examine coil impressed voltage and the possibility of excessive ac loss due to the harmonic content of the machine. With the detailed comparison of the economics of the short energised length LSM form of LCM completed[130], further study was curtailed because of lack of effort and the change in emphasis of the programme.

The original design philosophy of the LCM, as adopted at Warwick, has been taken up by both JNR and Transrapid. For the Miyazaki test track, the LSM armature winding is energised in block lengths of 29.4 metres, which is only slightly longer than the vehicle length. Transrapid will energise Weh's

design of iron cored LSM at very short lengths; for Emsland the stator will consist of two parallel kilometer blocks connected in series, and the inverter MVA rating is 1.39 times the vehicle required power. With a 6 kilometer feeder cable this rises to a 1.49 increase[230]. The need to provide block switching of the iron cored LSM stator arises because of the large track self inductance which results in a very low power factor. Weh has also suggested energising the track in subfractional vehicle lengths of one to two metres, and with four branches of power transistors (in parallel) and diodes (antiparallel) supplying each phase of the stator winding. Two or three of these four quadrant choppers supply a two or three phase winding, and the main feed carries only dc and the substation contains only a transformer and rectifier set.

4.2 Model LCM

Early in 1974 it was decided at Warwick to produce a working model which demonstrated the LCM concept with a concentrated winding arrangement, and one switch per coil, as shown in Figure 42. The model was based on the 0.5 metrte diameter drum that had been used to successfully demonstrate LSM operation. The coils were connected to the 50 Hz mains through slip rings and thyristors rated at 400V and 12A. The thyristor gating signals were provided by a mechanical commutator which gave a pulse as the appropriate coil side passed under one of three blocks of ferrite magnets. The magnets were a full wavelength pitched, and were therefore polarised in the same direction. Thyristor turn off was forced by the mains reversal. Although the drum machine was meant to be for demonstration purposes only, it successfully ran at up to 250 rpm with multiple coil and thyristor failures, indicating the redundancy in this type of machine. A variac controlled the input voltage to the thyristors, and the position at which they were turned on relative to the field magnets was fixed by the position of the brushgear on the commutator. The firing position could be varied by shifting the brushes, so that thrust in either direction could be obtained.

In connection with the Wolfson programme, a superconducting coil was constructed to test the concept of winding square coils with tight corner radii, but was sized to provide an alternative field arrangement for the drum machine. The machine, as shown in Figure 43 produced about twice the thrust with one superconducting magnet compared to three ferrite poles. The main characteristics of the magnet are given in Table VIII. The coil load line cut the critical current line at 90A, which was also the short sample current. A magnet quench through reaching critical field was therefore not anticipated. Cooldown lasted typically six hours from ambient, and the coil appeared to behave good naturedly. Only slight training was observed from the first quench at 42A to repetitive quenches during the first and subsequent cooldowns of 47A.

When the coil was energised over the running machine, the mains voltage waveform effectively commutated by the track windings was observed as a small value impressed voltage on the coil terminals. The radiation shield, cryostat base and coil support attenuated the reaction field to such a level that there appeared to be no significant change in the helium boil off rate with the armature energised, even though the impressed voltage could be observed. This confirmed calculations for the worst case of a machine on the Wolfson test track which had full inverter frequency and a stalled vehicle at low gap. The calculations[231] based on Freeman's multilayer region analysis[232] had indicated that the reaction field would be sufficiently attenuated by the intervening conducting layers, so that the superconductor would be effectively shielded.

The full superconducting machine was demonstrated publicly at the 1975 Intermag Conference in London, and represented the first realization of a practical superconducting commutator machine.

Figure 43 Superconducting Model LCM

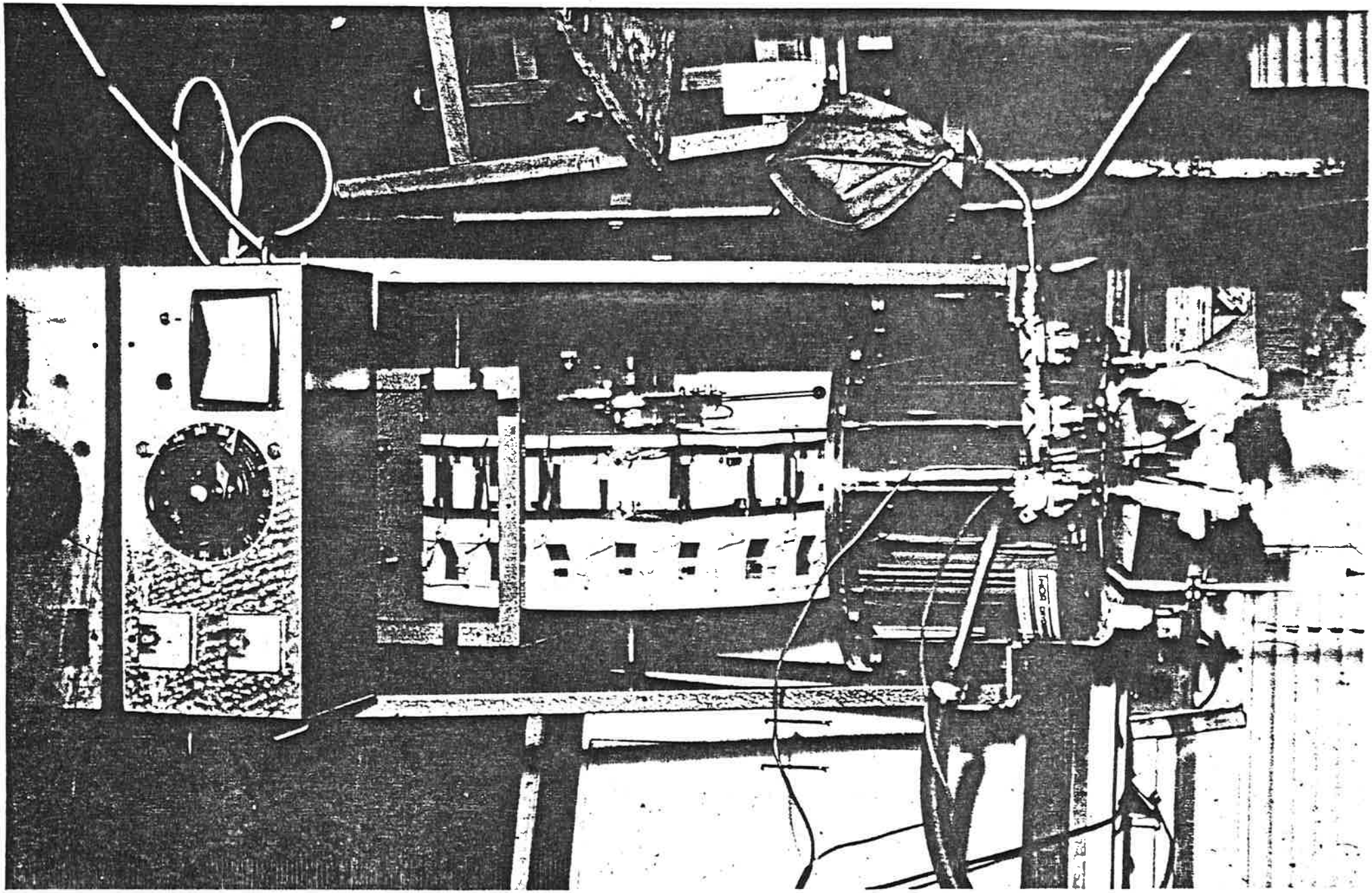

TABLE VIII Characteristics of LCM Superconducting Coil

Conductor

Type	Multifilamentary core wire
Material	Nb-Ti IMI Niomax FM A61/33
Filament diameter	0.028 mm
Wire diameter	0.33mm
Copper/superconductor ratio	1.35:1

Coil

Shape	Square
Meanturn side	115mm
Cross section	15 x 15mm
No turns	1050
No layers	28
Corner radius	10mm
Excitation mode	Persistent current
Short sample current	90A
Quench current	50A
Operating current	35A
Excitation	37 kAT
Overall current density	160 A/mm^2
Winding resistance at 20°C	157 Ω
Inductance	132mH
Stored energy	80 J

Field

Central	10.43 mT/A
Peak	30.4 mT/A
80mm below centre	3.4 mT/A

4.3 Comparison with LSM[130]

Where the very short length LSM is considered, a separate economic assessment needs to be made. If the armature system is accessed too frequently, the track installed cost of the semiconductor or vacuum switches may well exceed the cost of additional track losses associated with greater block lengths. It is by no means immediately apparent where the trade off lies, especially if other factors such as armature power loss and conductor mass can vary, as can interest changes on capital, power cost etc. Also machine design may dictate radical changes in wavelength, and no feel can be given to the effect that this might have on interrelated parameters. Some kind of economic optimisation is required after preliminary machine optimisations have been performed, which can indicate the sensitivity of change in particular parameters on the overall transport system cost. In this way a system optimisation will be achieved, on an iterative basis, by modifying parameters to effect a minimum overall cost, including infrastructure capital repayment, power and running costs.

In searching for a baseline design to compare a short energised LSM with, the CIGGT economic study[107] was finally chosen[130]. The route was based on the Canadian corridor between Toronto and Montreal via Ottawa, approximately 594km. Trip times of about 75 minutes would be possible for vehicles cruising at 504km/h, averaging with stops 475 km/h. The Canadian vehicle has passenger capacity of 100, so with a 60% load factor and 144 trips per day per direction the specified load capacity of the line would be 6.3 10^6 passengers per year. The average number of vehicles per hour was six.

So that an alternative comparison could be made, the MIT Magneplane was reoptimised for 504km/h and minimum terminal rating duty. Thornton had outlined the design of the Magneplane LSM for 360km/h synchronous speed, governed by the top frequency limit on the cycloconverter control. The thrust at this speed was 45 kN developing 4.5 MW of power, of which 3MW was

aerodynamic drag[91]. Since the magnetic lift force had saturated, drag power would remain constant at higher speeds, and aerodynamic drag would scale up with velocity ratio cubed. The projected drag was 60kN implying 8.4MW would be required for thrust power. Further optimisation of the current angle required gave an operating point of 113° and terminal rating of 10.1 MVA. Figure 44 shows the operating characteristics for the reworked design with base E_T and I of 3.63kV and 558A. The design works at a high power factor because of the large number of ampere turns per coil (1.25 MAT) and low MIT calculated track inductance. At the original speed of 360km/h Thornton had chosen the design operational point for total power factor correction, which although an improvement over the low current angle initially chosen, could still be bettered by minimum terminal rating operation. High efficiency results from ample allowance in conductor cross section. Table IX gives details of the reworked MIT designs at 360 and 504km/h.

The system costs can be broken down into three parts. Fixed costs are associated with the track conductor and inverter initial installed costs, which are subject to loan repayment amortization. Running costs are dominated by the power required for vehicle propulsion. It is assumed for the purpose of this analysis that maintenance costs will remain relatively unaltered whatever choice is made for the track parameters. A cost equation can be established which lumps together these costs and is expressed as a cost per unit track length, per year. In its most basic form the equation is

$$C = \frac{amk}{100} A \left(1 + \frac{2w}{\lambda}\right)\sigma C_c + \left(\frac{P_B}{G} + \frac{am\rho}{A} \cdot \left(1 + \frac{2w}{\lambda}\right) I_c^2\right)\left(\frac{C_I k}{200} + 8.76\, C_p \frac{\bar{n}}{\bar{v}} G\right) \quad (53)$$

where

C	Annual cost \$ per year-metre	C_I	Inverter cost, \$ per kVA
G	Excited length, metres	C_p	Power cost, \$ per kWh
a	No of parallel paths per phase	C_c	cable cost, \$ per kg
m	No of phases	A	cross section of conductor, m^2
$\bar{n}$	Average vehicle frequency per hour	ρ	Resistivity, ohm-metre
$\bar{v}$	Average speed, km/h	σ	Density, kg/m^3
I_c	Conductor current (Phase current ÷ a)	k	Repayment factor, %
w	Armature width, metres	P_B	Real power developed, W
λ	Wavelength, metres		

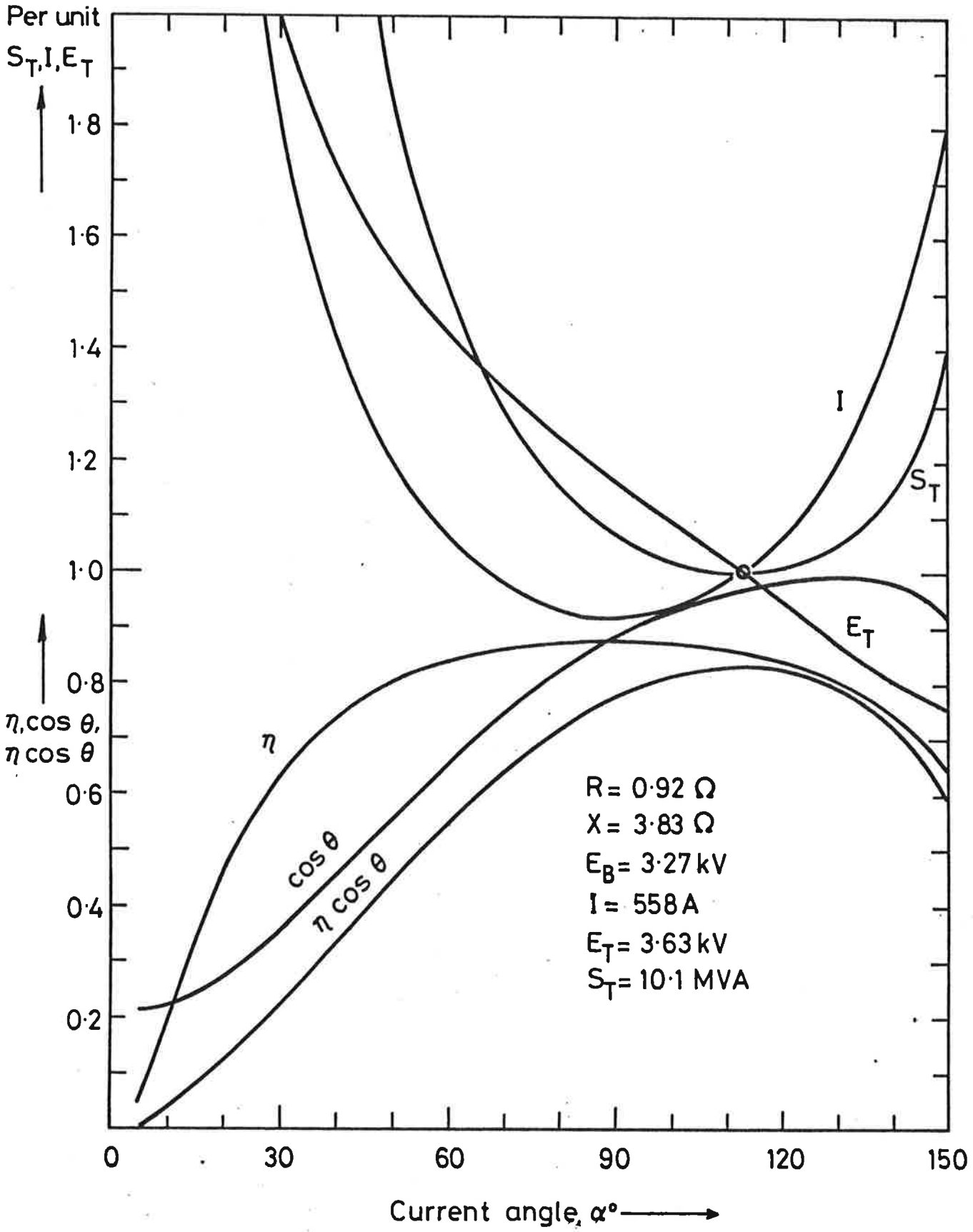

FIGURE 44 PERFORMANCE CHARACTERISTICS OF MIT-LSM

Table IX Magneplane Parameters

Common Factors	
Vehicle weight, tonnes	44.8
Length x width x height, m	50 x 3.8 x 4.35
No Passengers	140
Levitation height, m	0.25
No phases	5
Wavelength, m	2.75
Conductor spacing, m	0.275
Stator width, m	2
No Magnets	16
Magnet strength, MAT	1.25
Magnet size major, minor id x od	3.3 x 1.5, 2.4 x 0.6
Magnet pitch m	2.75

Speed Influenced Factors*		
Cruise speed, km/h	360	504
Frequency, Hz	36	50.4
Nominal thrust, kN	45	60
Phase current, A	359	558
Back emf, kV	2.31	3.27
Terminal emf, kV	2.55	3.63
Terminal Apparent Power MVA	4.58	10.12
Current Angle °	107.3	112.9
Efficiency	0.87	0.86
Power Factor	0.99	0.97
Apparent Efficiency	0.865	0.83

*Recalculated for minimum terminal MVA

An easier form of equation 53 is found by substitution of the expressions for the power loss and mender mass per unit track length, P_A and M_A, given by equations 41 and 42. The annual unit length track cost becomes

$$C = \frac{k}{100} C_c M_A + \left(\frac{P_B}{G} + P_A\right)\left(\frac{C_I k}{200} + 8.76\, C_p \frac{\bar{n}}{\bar{v}} G\right) \qquad (54)$$

The cost per passenger kilometer is proportional to $\frac{C}{\bar{n}}$ x vehicle capacity.

M_A and P_B and ultimately the phase current can be replaced by the parameters of thrust and back emf, which are essentially fixed for the design speed. Differentiating 53 with respect to A and G produces values of minimum annual unit cost for a particular choice of wavelength, inverter, cable and power cost. For the range of parameters, families of cost curves can be generated. Figure 45 shows cost C for a fixed cable cost of 8.52 $/kg, an inverter cost of 25 $/kVA and a wavelength of 1.14 metres (i.e. the CIGGT optimum wavelength). The power cost C_p is shown varying from 1 to 4 ¢ per kWh,and the minimum points for each cost layer are projected down to the optimum G and A axes. Figure 46 represents four such projections for fixed wavelength and cable cost, but various inverter cost as well as power cost within the carpet plot. If the optimisation is performed for a range of differing wavelengths, an even greater variation in optimum G and A results. Figure 47 displays the locii of G and A optima for different wavelengths. Surprisingly, when the minimum costs associated with the optimum G and A values are calculated, the cost is a slowly rising near linear relationship with wavelength (Figure 48). As inverter cost increases, the gradient of the minimum cost steepens, but not dramatically. For low inverter cost, the gradient is such that a four fold increase in wavelength only increases the cost by approximately 10%. It can be said,therefore, that since cost increases slowly in a monotonic relationship with wavelength, absolute choice of a non-optimum wavelength may not necessarily produce a significant impact on the overall economics of the system. This conclusion is especially important for the integrated system of levitation and propulsion, since other factors strongly influence the choice of pole pitch. Lateral stiffness and lift to drag ratio -

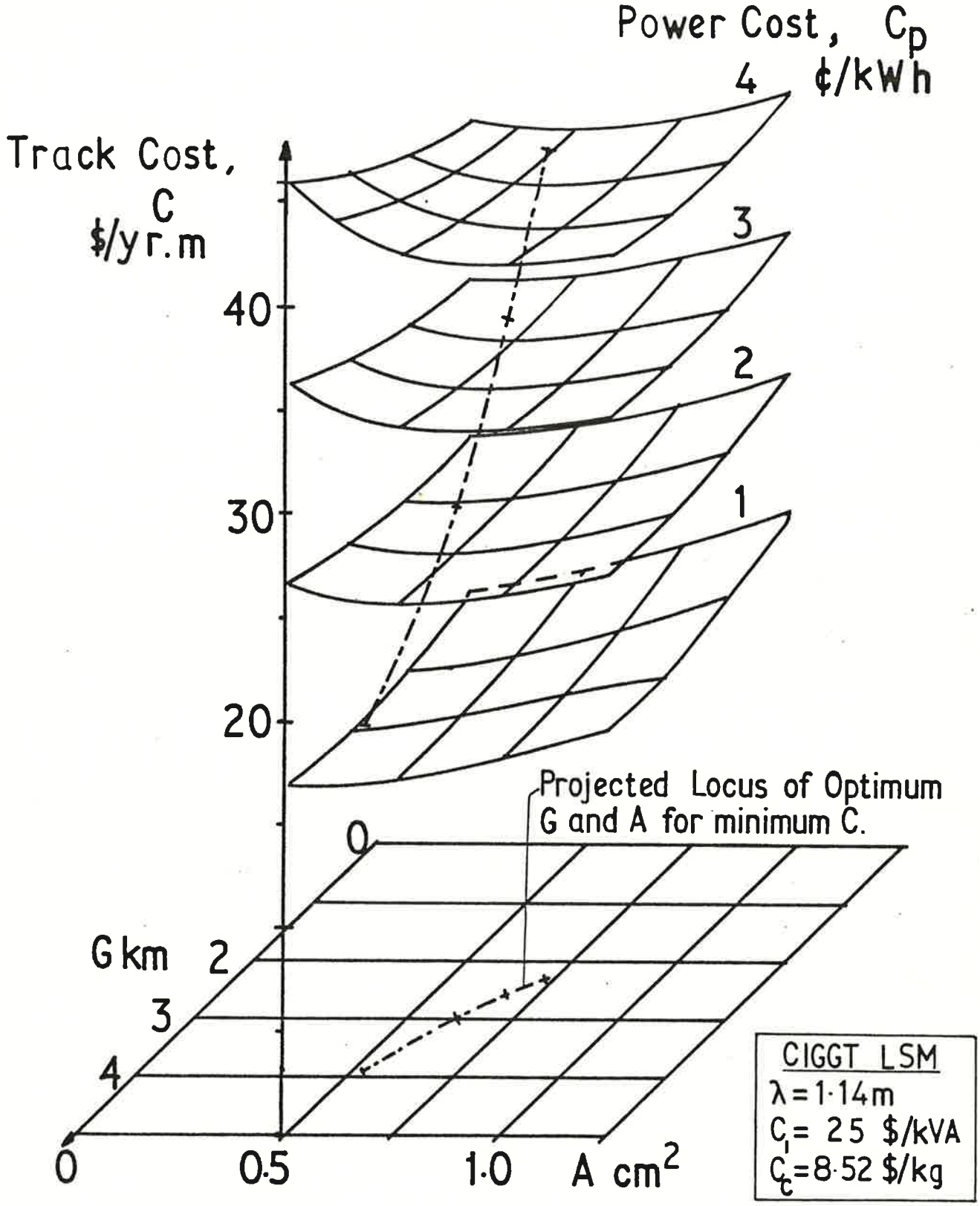

Figure 45. Annual unit track armature cost, C.

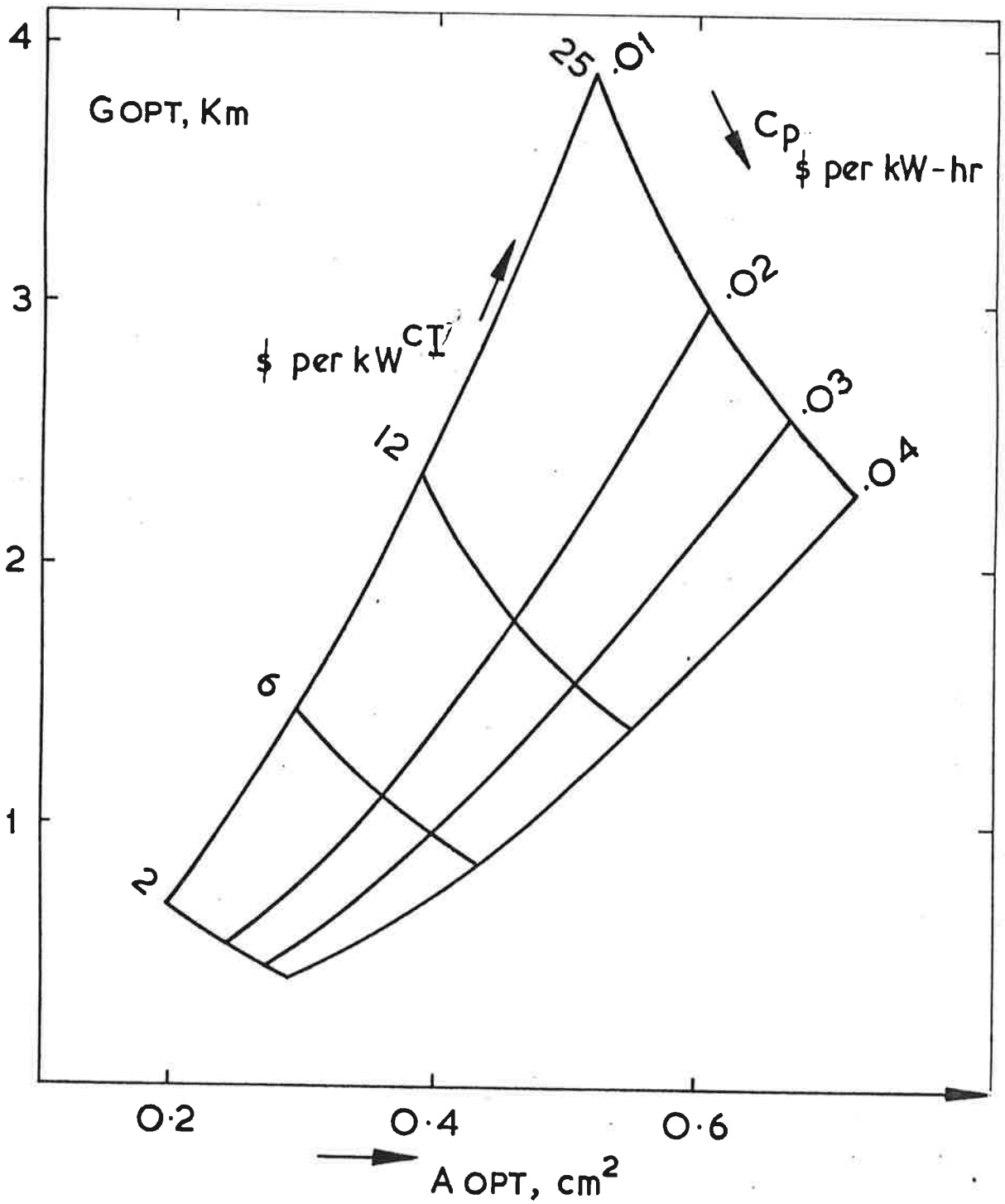

FIG. 46. OPTIMISATION FOR G, A.

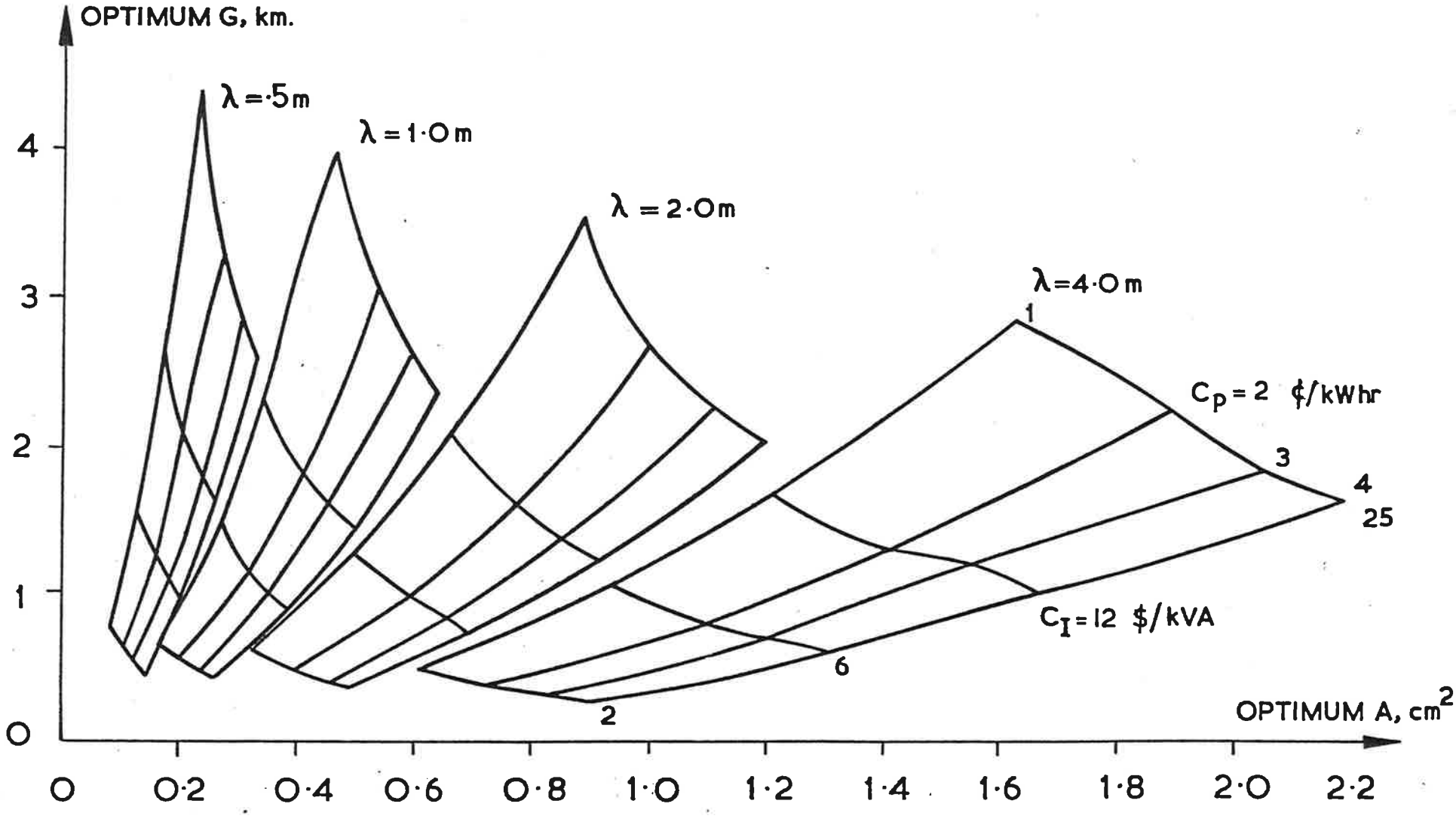

Figure 47. Loci of optimum G, A, for different λ.

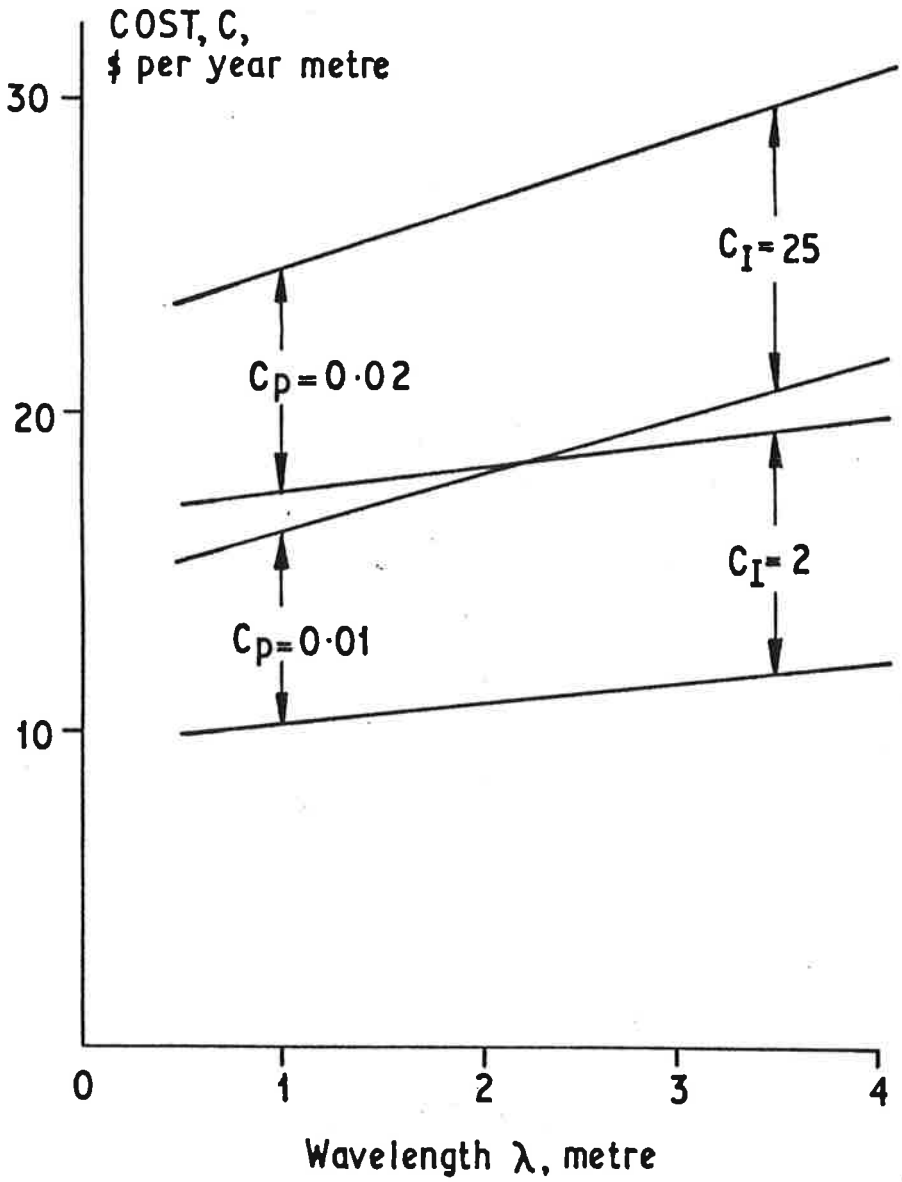

Figure 48. Costs as a function of wavelength.

are all enhanced by relatively long pole pitches, and for the Wolfson revenue vehicle design a 3 metre wavelength was chosen. Optimum G and A were found to be 300 metres and $50mm^2$[130], and represents a tradeoff in inverter cost reduction achieved by reduction of track losses and block switching an inverter into many sections.

The LCM Wolfson revenue vehicle was loosely based on a CIGGT type structure, and had similar passenger capacity, and drag characteristics. Table X gives the final choice of parameter values used in the comparison, the machine variants and their resultant optimum cross section, energised length and ultimate journey cost. Although the LCM requires essentially the same propulsive power as the CIGGT vehicle, the reduced block length allows a more efficient power transfer, resulting in lower inverter power handling requirement[129]. Of significance is the result that a LCM propulsion is not necessarily a lot more expensive than an inverter or cycloconverter fed linear synchronous machine. The JNR Miyazaki and the Emsland test facilities both confirm this principle of economic advantage derived from block switching into a frequency converter feed line at frequent intervals.

Table X Optimisation Parameters

Cost Equation Parameters

Amortization, k	15%/annum
Track Conductor cost, C_c	8.25 \$/Kg
Unit Power Cost, C_p	2 ¢ /kWH
Vehicle Frequency, $\bar{n}$	6 per hour
Load Factor	60%
Average speed $\bar{v}$	475 km/h
Cruise speed, v	504 km/h
Passenger Throughput	360 passengers/hour

Machine Parameters

	MIT	CIGGT	Warwick
Machine Type	LSM	LSM	LCM
Levitation Height, mm	250	220	240
Wavelength	2.75	1.14	3.0
Conductors/pole	5	6	6
Cruise Power, P_B, MW	8.4	5.6	5.6
No passengers/vehicle	84	60	60
Track cross section, mm^2	100	60	50
Excited length, G, m	5000	3000	300
Conductor Mass, kg/m	3.3	3.5	1.9
Journey Cost, ¢ /pass.km	1	0.8	0.6

CHAPTER FIVE

MACHINE ECONOMICS AND SYSTEM COMPARISONS

5. Machine Economics and System Comparisons

5.1 The Need for System Comparisons

Future new transport systems will require massive capital expenditure to establish the infrastructure needed for high speed operation. On top of this, the vehicle cost must be added, as well as the running and operating costs. Previous sections have examined system performance and optimization techniques which give the designer and planner a basic structure for overall system economic analysis, for ACLSM. Usually however, the problem is not just to provide an optimum answer for one particular configuration, but to establish the criteria that can be used for comparisons of systems completely different operating or technical bases. Since the decision on whether to proceed or abandon the advanced research and development programmes will often be made at government level, the choice of specific parameters to represent essentially competing systems must be taken with particular care, to avoid confusion and inaccurate judgement.

The major magnetic levitation research and development projects employ linear motor or air fan propulsion for cruise speeds up to 500 km/h. Chapter 2 has given the background details of the status of the various systems, all of which have either reached, or are rapidly approaching, full sized revenue vehicle conceptual design, with a firm understanding of the engineering principles involved, confirmed by high speed rotary or linear testing. Usually one of the main parameters used in comparing levitation and guidance systems is the power to weight ratio, measured in kW/tonne. For the overall system, lift to drag ratio represents another speed dependent variation of power to weight, and specific energy intensity (MJ per passenger-km) indicates the total power consumption. A typical specific energy intensity diagram for various transport modes is shown as Figure 49, using alternative units of Wh per passenger-km. Maglev appears to be competitive with car and rail travel, even though the speeds are much higher, and is considerably cheaper than commercial aircraft[233,234].

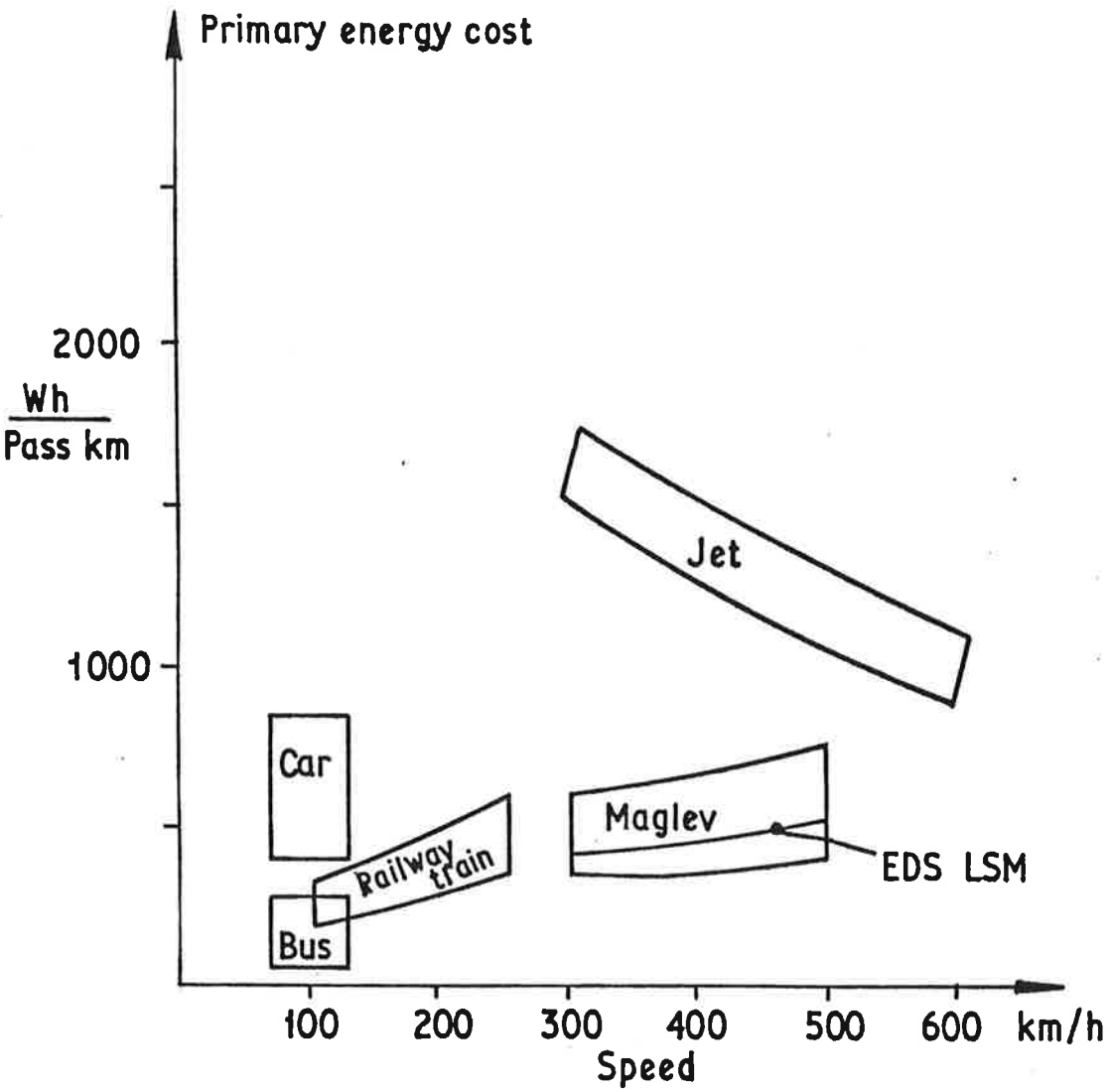

Figure 49. Specific primary energy cost of transport modes.

Of more importance than a rigorous application of specific parameters in system comparisons, is the need to completely identify the energy make up, preferably by evaluating complex power levels reflected through the system to the load presented to the utility. Parameter variation and sensitivity to change must also be included in a reasoned comparison. Finally, wherever possible the systems must be compared at similar benchmarks of speed, passenger density, scheduling and routing.

5.2 German Maglev Revenue Passenger Vehicles

The analysis and design details of proposed German Maglev revenue vehicles are given in the 1977 Statusseminar[36], and the basic characteristics are repeated in Table XI. There are two EMS design options, and one EDS German system, with Philco Ford and CIGGT EDS vehicles included in the table. The vehicles are made up from two mirror image sections to allow bidirectional running, with the EDS design speed being 500 km/h, EMS 400km/h. Two propulsion schemes are considered for the EMS vehicle, one being a double sided LIM, and the other, an iron cored LSM in a long stator configuration, supplying lift as well as thrust to ease the on board power requirement. Both the systems designs of EMS and EDS were prepared for a BMFT "System Comparison" to allow a decision to be made on the preferred option to be taken up and pursued to a near full size operational vehicle. Leonhard produced a superficial preliminary system comparison of the three alternatives of Table XI and concluded that none of the systems was sufficiently well developed to allow a clear choice to be made[132]. This comparison showed the power requirements at the substation, but only included the real power for the main magnetic and aerodynamic drag. Although this represents all the losses for the EDS for a given motor efficiency, no mention was made of, for example, the EMS cooling momentum drag, the short stator dc feed line loss, and the long stator track iron and distribution loss, all of which appear downline from the substation. Furthermore, since the speeds of operation were also different the

TABLE XI Characteristics of Conceptual Maglev Revenue Vehicles

System	PM-EDS	EMS		EMS	PHILCO FORD EDS		CIGGT EDS
Propulsion	LSM	shortstator LIM		long stator ICLSM	Ducted Fan		LSM
Variation		high η	low η				
Speed, km/h	500	400		400	483		483
Mass, tonnes	135	170		165	37.3	50.7	28.8
Length, m	56	64		64	33.67	42.9	36.5
No Sections	2	2		2	1		1
No Pasengers	200	240		240	80	140	100
Payload, tonnes	20	24		24	7.2	13.2	9.3
Height, m	4.2	4.2		4.0	3.454		3.20
Width, m	3.5	4.2		4.2	2.94	3.454	3.20
Aerodynamic Coefficient, m^2	3.94	4.75		4.75	1.80	2.20	2.42
Substation Spacing, km	15	12		12	-		5
Specific Energy Intensity MJ/pass-km	4.45	6.51*	11.2*	5.1*	3.63	2.75	3.72

*At 500 km/h

aerodynamic drag power would introduce a further discrepancy; an increase in speed from 400 to 500 km/h results in a doubling of the aerodynamic drag power. Leonhard acknowledged the difficulty in performing a meaningful comparison, and suggested that because of the long term nature of the R&D required, premature decisions in abandoning one system in favour of another were, in fact, unjustified.

The exact power requirements of the different systems can be calculated; including the power factor and motor efficiency allows the substation complex power to be completely specified. When the speed is extrapolated to 500 km/h for the EMS vehicles an additional double sided motor is required for the short stator vehicle, and the weight is increased by 20% to 205 tonnes. The long stator design at 500 km/h requires an increase in gross weight of 10%, to 180 tonnes. Operation of the EDS vehicle at 400 km/h needs no modification to the vehicle, and the LSM can still perform at a near optimum point.

In trying to establish the terminal conditions at the substation for the EMS vehicles, the choice of power factor and efficiency is made difficult because of lack of experimental or even design figures for multimegawatt high speed motors. Winkle suggests calculated efficiencies of 0.6 and 0.78, with associated power factors of 0.5 and 0.65 respectively as the first and second stage of development[235], and the following calculations are based on using these sets of values. Results from the LIMRV tests seem to imply that these figures are representative, although it must be stressed that the EMS LIM requirement is several times the LIMRV power.

The distribution systems for the three options of EDS, and EMS with short or long stator, are shown in Figures 50-52. The EDS system allows leapfrog connections to be made between the track sections and the wayside inverters, with tie reclosures into both directions (not shown). Short stator EMS power is picked up at 4kV and fed via an inverter to the LIM, and through controlled rectifiers to provide on board supply for services and lift and guidance systems. The long stator motor uses a linear

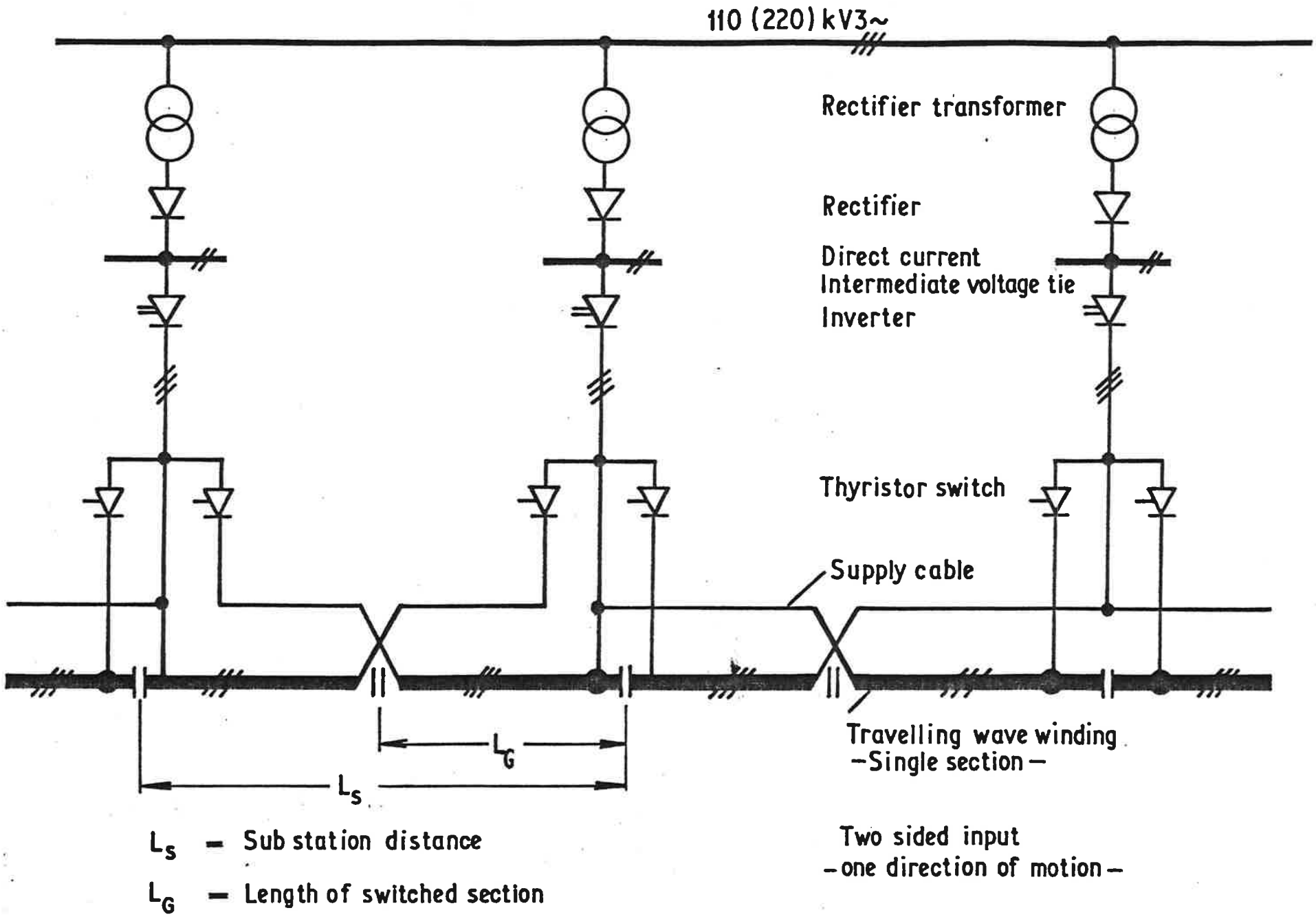

Fig.50. Distribution diagram for the EDS long stator motor propulsion.

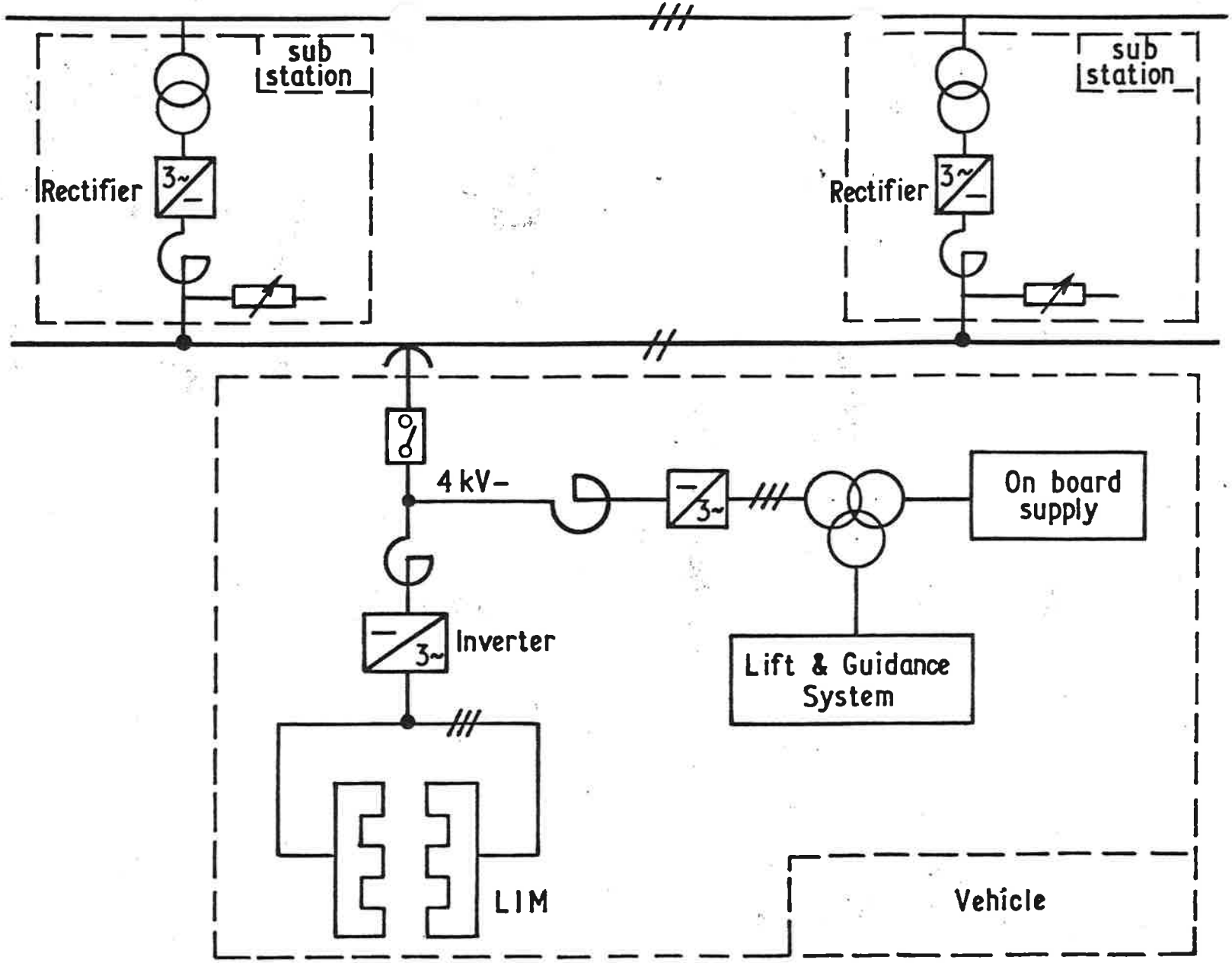

Fig.51. Distribution diagram for the EMS short stator motor propulsion.

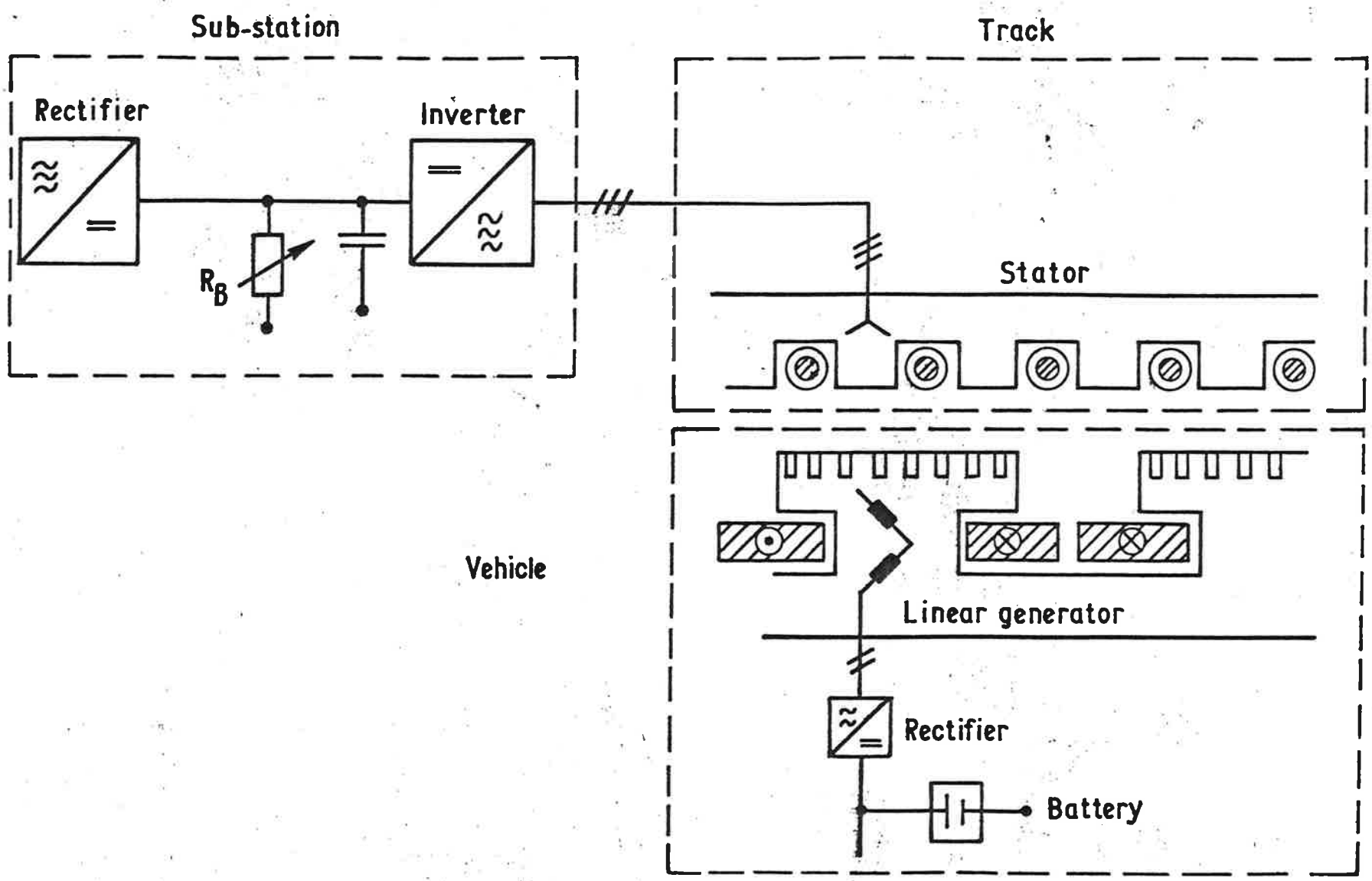

Fig.52. Distribution diagram for the EMS long stator motor propulsion.

generator formed by switching in pole face windings to produce sufficient power for the on board systems above a certain speed. Batteries provide the low speed power.

There are seven main components to the active power requirement for maglev vehicles. Aerodynamic drag is usually a predominant factor in any high speed system, and is proportional to the aerodynamic coefficient, which represents the frontal and surface skin drag, and the velocity squared[236]. The magnetic drag for the systems are also speed dependent. For EDS, once the lift and guidance forces have reached a saturation speed, then drag force is inversely proportional to speed, so that drag power is essentially speed independent. For EMS, an approximate relationship is that lift and guidance power scales as $(\text{velocity})^{(3/2)}$. The EMS Maglev vehicles require entrained air for cooling of the levitation and guidance magnets, as well as the linear machine conductors and the on board power conditioning. The on board systems drag power will scale with the vehicle weight, and represents picked up power to drive the vehicle services such as air conditioning, battery backup charging etcetera. Track winding (EDS) and distribution losses represent the remaining steady state drag values.

Extra power capability is needed to accelerate the vehicle against headwinds, gradients and other inertial forces. Both systems are claimed to be capable of providing propulsion capacity for 3.5% gradients at cruise speed, but the more lenient figure of 0.013 gee was chosen for the comparison. Figure 53 shows the total breakdown of active power requirements for the EDS and EMS systems, at two alternative cruise speeds of 400 and 500 km/h[133,134]. The two options of LIM propelled EMS vehicles are included for comparison purposes to Weh's long stator LSM design. The steady state or cruise power for EDS is the sum of blocks 1, 2 and 5, which are the only system losses. The EMS losses are given in blocks 1 to 5. It should be

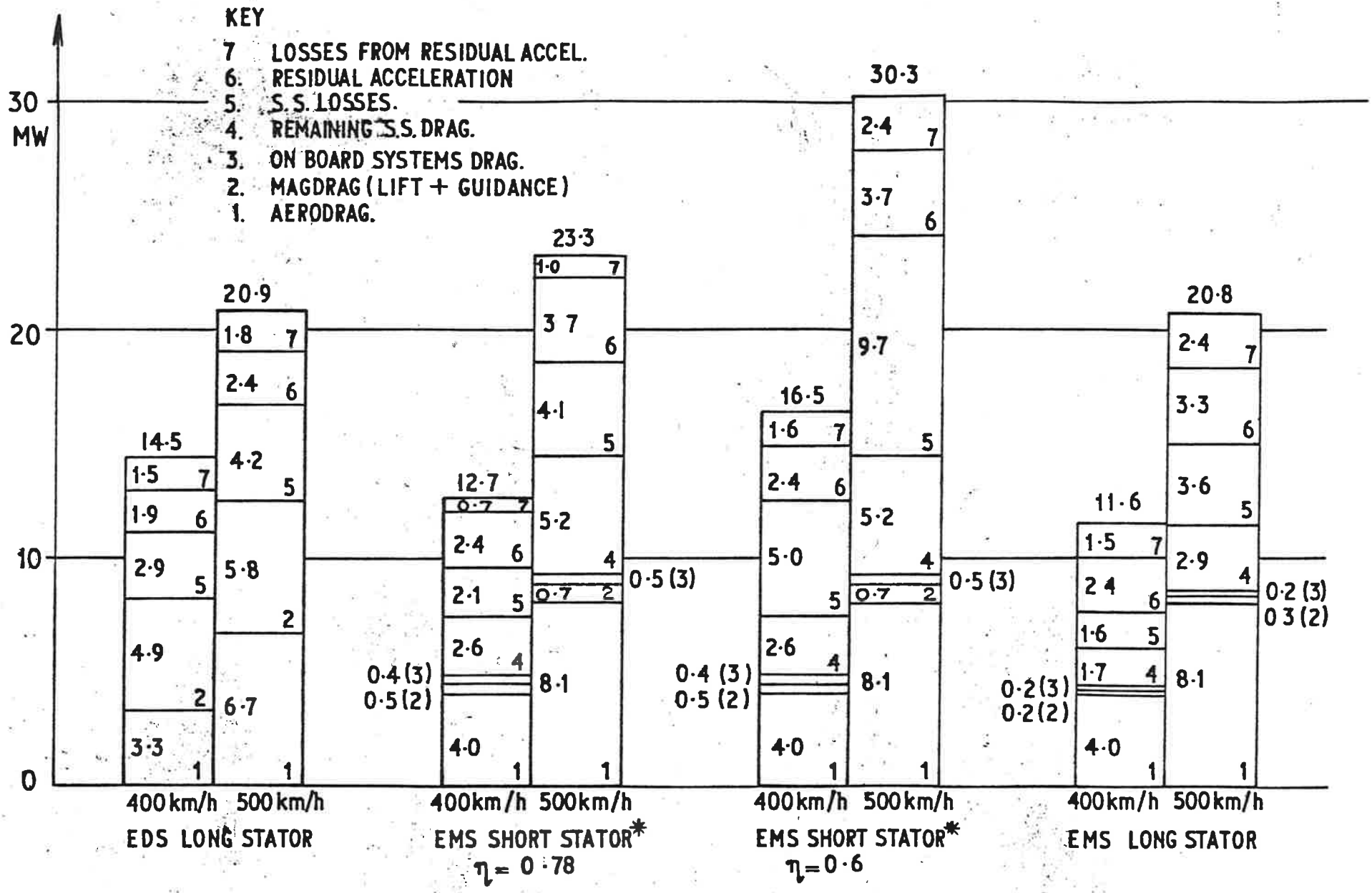

Fig. 53 Total active power of systems (MW) *NOTE. D.C. DISTRIBUTION & PICKUP LOSS NOT INCLUDED.

noted that the figures used for the EMS long stator should be treated with some scepticism, if only for the reason that detailed overall figures on machine design for the IVA and Emsland vehicles are not readily available. Figure 54 is an alternative presentation of the active power requirements for the four operating regimes of 400 and 500 km/h, steady state or acceleration. The 100% base is the EDS 16.7MW consumption at 500 km/h, steady state. It is apparent that, in terms of real power consumed, the long stator EMS and the EDS are both roughly equivalent when loaded at 500 km/h. The low efficiency LIM short stator EMS uses roughly 45% and the high efficiency LIM EMS 11% more active power. If an estimate is made for the DC line loss for the LIM, before current pickup, of 15%, then the modified EMS/LIM figures are 70 and 31% respectively.

The values here could not have been deduced from the suspension lift-to-drag ratios, or specific powers. For example, the EDS 500 km/h magnetic lift to drag of 32 (equivalent to 36 kW/tonne) is modified by aerodynamic drag so that cruise lift to drag becomes only 15 (92 kW/tonne). Similarly, the EMS short stator magnetic specific power of 3 kW/tonne at 400 km/h (equivalent to a magnetic lift to drag ratio of 370) is modified by the addition of aerodynamic and cooling drag to a steady state value of 44 kW/tonne (a lift to drag ratio of 25). The choice of a suspension subsystem with high magnetic lift to drag ratio does not ensure an overall high ratio because of the aerodynamic and other system losses.

The change in efficiency and power factor of the three systems is indicated in Table XII. The apparent efficiency (power factor - efficiency product) is fixed at either 0.51 or 0.3 for the high and low efficiency versions of the LIM, as mentioned previously. The EDS system loses 7% in going from unloaded 400 km/h to loaded 500 km/h operation. A similar transition for the EMS long stator motor results in a 21% loss representing a conservative estimate, as it ignores non linearities in the iron cored system. The short stator motor values were held constant as the design called for a doubling

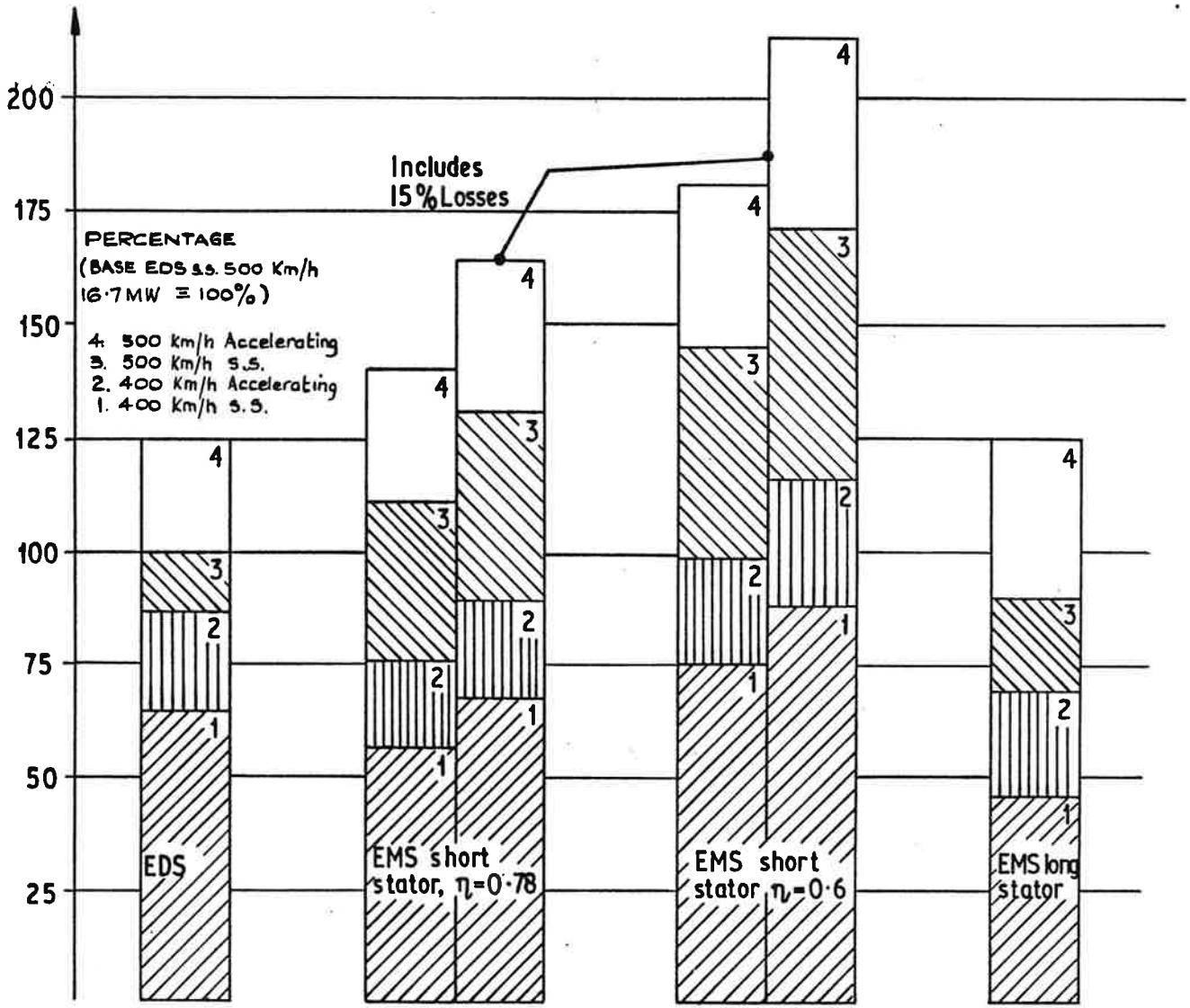

FIG.54. Relative system active power requirements at 500 and 400 KM/H.

TABLE XII Apparent Efficiency of the German Vehicles

	steady state	loaded	steady state	loaded
EDS	0.67	0.62	0.66	0.60
EMS, long stator	0.57	0.46	0.44	0.36
EMS, short stator, high efficiency		0.51		
EMS, short stator, low efficiency		0.30		

up of the motors to give sufficient thrust at the higher speed; each motor remained at much the same output, but would be operating at a different slip.

Using the values in Table XII it is possible to directly obtain the complex or apparent power required at the substation. The reactive power flow in the machine-power network is stored in the leakage and airgap fields, and as such does no useful work. However, the reactive power represents an energy demand that has to be catered for both in plant rating and running cost. An iron cored structure such as a LIM or the EMS long stator motor must have a much lower power factor than a LSM of the same mechanical power output, since air gap magnetization is provided by superconductors requiring no input reactive power, and the armature leakage inductance is small since the track winding is air cored. These points are born out by Figure 55, where complex substation power demand is an ordinate value against the active power for each of the four operating regimes. The success of the electrodynamic system in requiring only small amounts of reactive power to provide propulsion throughout the speed and loading variation is immediately apparent. The size of the ordinate, i.e. the complex power, therefore demonstrates the relative merits of the overall systems, at the substation. Despite the rough equivalence of active power used, the EMS long stator requires 38% more than the EDS base at 500 km/h, and the high efficiency short stator 51% more. Including a line loss the LIM value rises to about 78%. If the lower efficiency short stator EMS is considered, then the figures become increases of 156% and 202% on the EDS base. Figure 56 shows the complex power for the systems, on a percentage base.

From this data, a realistic power requirement comparison can be made between the three German Maglev vehicles operating under similar conditions. The comparisons cannot be strictly rigorous, since the EMS and EDS vehicles are primarily designed for different baseline operation. However, the spread of the system total complex power in relation to the actual transferred

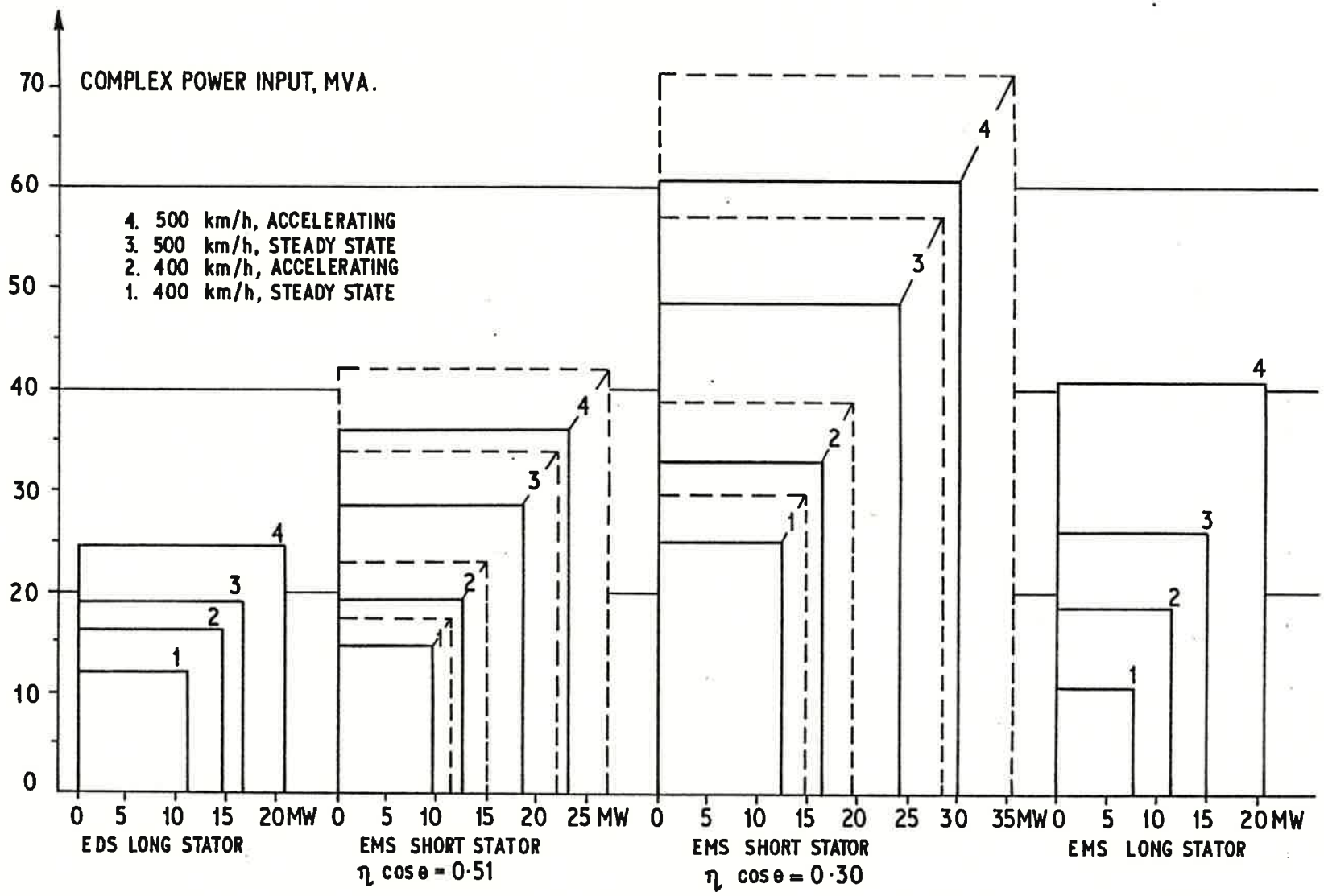

Fig. 55. Total complex and active power of systems. Note:- Short stator: Broken lines indicate an included 15 % distribution loss.

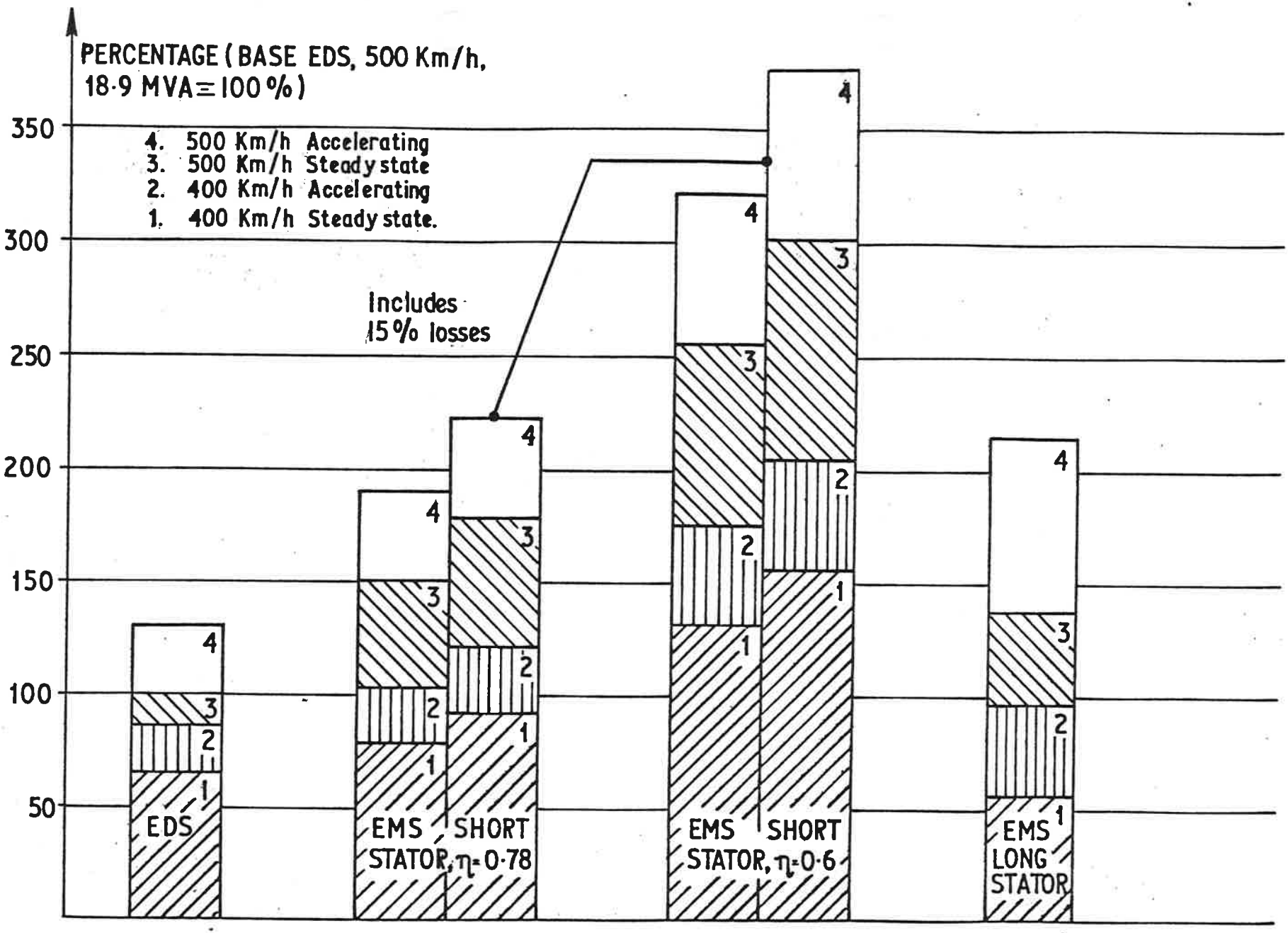

Fig. 56. Relative system total complex power requirements at 500 and 400 Km/h.

mechanical power requirement (Figure 55) is indicative of the type of system performance that might be expected for identical service conditions. Several factors emerge from the analysis.

The EDS has good system performance at both 500 and 400 km/h in terms of energy conversion and power consumption, and has scope for increases in power factor and efficiency, depending on the economic costs of power and capital equipment.

The short stator induction machines for the EMS are quite unsuitable for high speed (500 km/h) operation, and are probably also unsuited to 400 km/h operation, primarily because of their high reactive power consumption and hence excessive overall power requirement. For example at 500 km/h the high and low efficiency LIM's respectively required 1.8 and 3 times as much complex power as an EDS-LSM, and at 400 km/h, 1.4 and 2.4 times as much.

The long stator motor EMS appears to need marginally less power than the EDS at 400 km/h (90%) but when loaded, or at the higher speed of 500 km/h, this slight advantage is lost. Another consideration is that this machine concept has only been tested at relatively modest speeds, and so high speed operating characteristics must be regarded as tentative. Results from the Emsland vehicle trials will establish 400 km/h running of the iron cored LSM, and confirm theoretical calculations. To get the supply power factor to a reasonable level, the 1 kilometre track sections, connected in series are tied through a supply cable to the inverter. Inverter spacing is 6 kilometres[230].

Generally, it can be said that using specific power, lift to drag ratio, or specific energy intensity to assess system performance only indicates the active power supplied to make up thrust and losses (if included) in the system. Low power factors in the LIM systems mean trackside and transmission components as well as utility energy supply costing must be in terms of total complex power used by a system. The MVA as well as the MW requirements of a system must be obtained in relation to a common guideway

route together with similar baseline specifications before reasonable comparisons can be made.

5.3 Maglev Vehicle Weight Breakdown

Another area for comparison of vehicle data is that of weight breakdown, and for this study the two additional single section EDS systems are included with the German vehicle data presented in Figure 57[135]. The two EDS vehicles characteristics have been listed in Table XI previously, and are the Philco-Ford[86] and Canadian[109,110] conceptual vehicle designs.
Two options are included for Philco-Ford, the baseline 80 passenger vehicle, and their 140 passenger variant. In relative terms, the Philco-Ford and CIGGT designs make available a fifth to a third of their all up weight for payload, whereas all the German vehicles have roughly a 14% allowance. Figure 58 shows the six vehicles' weight breakdown in absolute terms. The overall weight per seat of the German EDS vehicle compared to the CIGGT and Philco-Ford 140 seat vehicles is approximately double. This is largely because of the weight penalty of the heavy duo-rail compatible wheelsets and their emergency integrated guidance system employed, opposed to the lightweight aircraft-type wheels of the other EDS designs. The EMS figures for weight-per-seat demonstrate the large amounts of power conditioning and mechanical hardware in the subsystems penalizing payload capacity.

5.4 Specific Energy Intensity

The specific energy intensity (ψ) of a transport system evaluates the amount of prime energy required per passenger, per kilometre of travel. Within the calculation, the substation converter efficiency, generation and transmission efficiency and load factor for the vehicles are included. In obtaining a value for ψ for non-electrical systems the heating value of the fuel and the journey stage length need to be known. The values of specific energy intensity (including the effects of power factor)for the six vehicle variants considered are shown in Table XI.

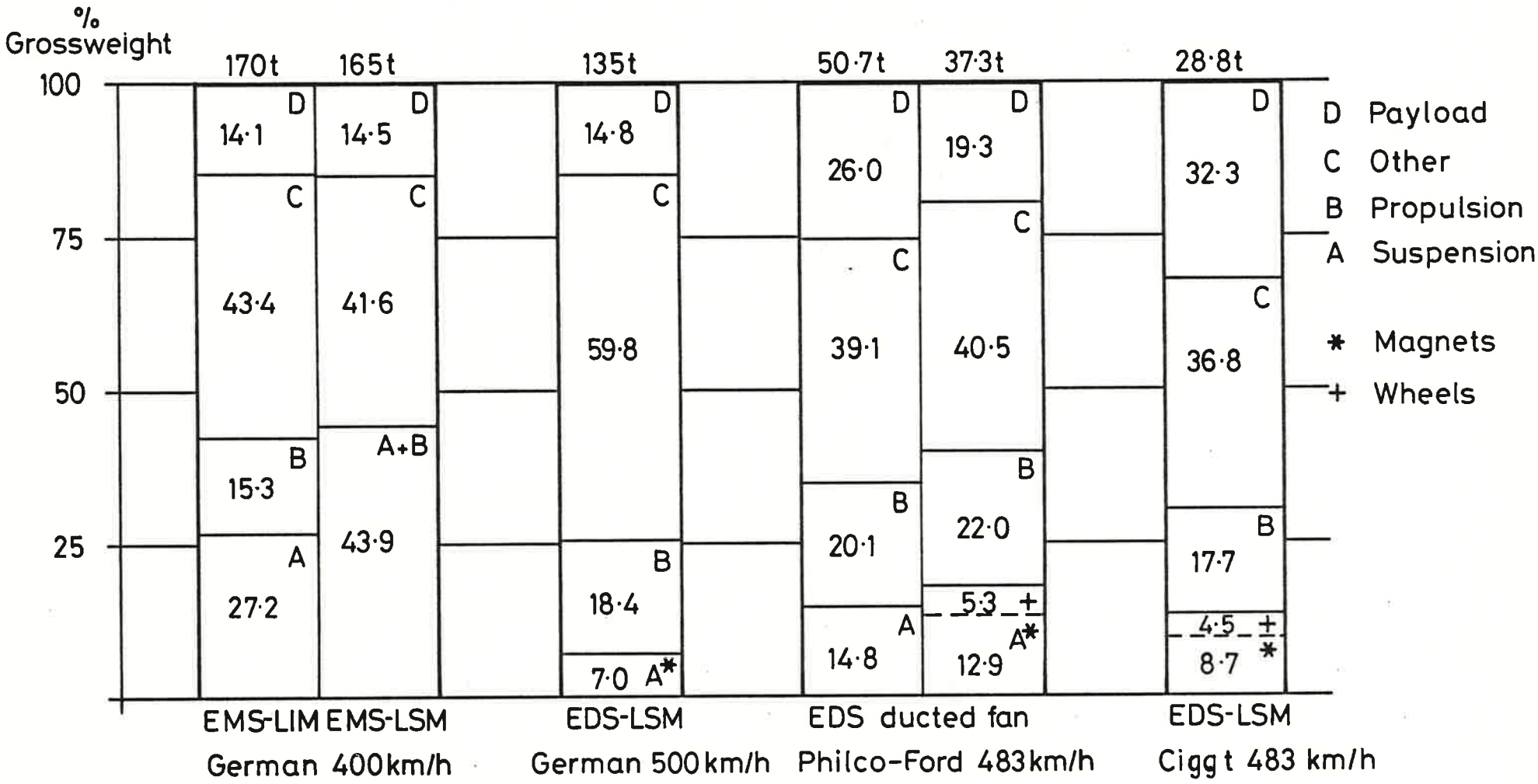

FIGURE 57. SUBSYSTEM WEIGHT BREAKDOWN (% GROSS)

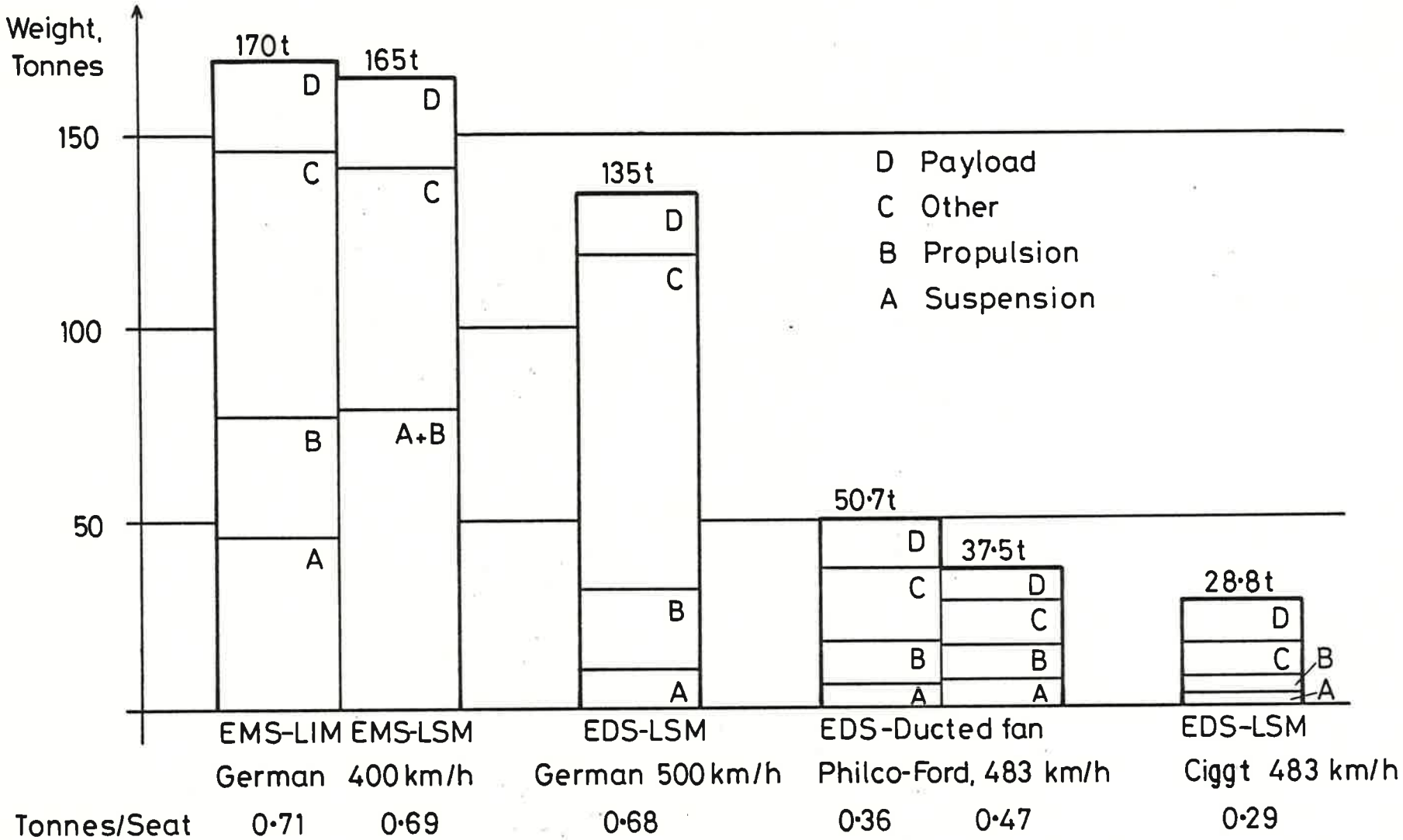

FIGURE 58 SUBSYSTEM WEIGHT BREAKDOWN

The Philco-Ford values are low because of the low aerodynamic coefficients chosen, together with the high magnetic lift to drag ratio obtained with a 25.4mm thick aluminium levitation and guidance conductor. In comparing the CIGGT value of 3.72 MJ per passenger-kilometre with the German EDS value of 4.45, the large vehicle weight of the latter has completely offset the advantage obtained by increasing the vehicle length, as shown by the Philco-Ford difference between short and long vehicles (3.63 and 2.75). Aerodynamic drag per seat decreases with increases in vehicle length, and this effectively means that ϕ will drop with longer vehicles.

Although specific energy intensity is an important factor to consider in making transport comparisons, as has been shown in the sections of the chapter, it is insufficient in completely defining all system parameters adequately, and represents just one part of a total system description.

CHAPTER SIX

FLUX PUMPING AND CRYOGENICALLY COOLED MACHINES

6. Flux Pumping and Cryogenically Cooled Machines

6.1 Pulsed and AC Operation of Coils

Large field value coils tend to use superconductors in the conductor material because of the advantages to be had in the lightweight construction, absence of iron, low power requirement, and the high current density in the conductor section. The majority of applications have been concerned with dc fields produced with very little superimposed ac component. Coil charge and discharge rates are such that only low additional losses occur, and can be easily handled by the refrigeration system at the beginning and end of the coil duty cycle. For maglev systems the ac loss problem stems from air gap harmonics generated by the LSM - the worst case being when the machine stalls and the vehicle sees a full frequency fundamental track mmf before an inverter trip. The other major source is from vehicle transitory motion and track discontinuities influencing the constant flux condition of the coil, and producing a ripple current on the main dc current. The ac loss has been evaluated by several researchers(237-240), for this common condition, and loss calculations have been confirmed by experiment.

Work on ac cables running at 50 Hz have used superconductors which are exposed to self-fields generated by the transport current. The field levels are only a few tenths of a Tesla(119). The need to develop superconducting coils which can successfully operate at substantial field rates of change has been due to programmes on Superconducting Magnetic Energy Storage (SMES)(241), and also on Fusion Reactors, especially the large Coil Programme (LCP) and other Tokamak research sponsored by the US DOE(242,243). It is to be expected that the large scale application of Nb_3Sn or V_3Ga rather than NbTi superconductor material, with their higher $T_c(H)$ values, will promise a higher stability against thermal disturbances caused by excessive eddy current or other ac loss. Since diffusion fabrication of Nb_3Sn in filaments of diameter markedly less than one micron is feasible, as compared to the NbTi size of between one and five microns,

large field amplitudes at industrial frequencies may well be possible, and work to this end is underway[244].

If the pulsed operation of superconductors is not feasible for high rates of change of field, then a realistic state of the art alternative solution is to use normal conducting metals such as copper or aluminium and benefit from their reduction of resistivity at low temperatures. A conductivity gain of roughly an order of magnitude is possible from room temperature down to LN_2 temperatures, and this may increase to four orders of magnitude at LHe temperatures. Nitrogen cooled pulsed copper coils have already been used as substitutes for superconducting coils at Warwick in Maglev test applications[136,245]. Their low weight in free open bath cooling allowed more sensitive measurements of force and torque, compared to a cryostat housed superconducting coil. Schauer has discussed the tradeoffs involved in comparing the competitive advantages of cryomagnets (cryogenically cooled magnets) with superconducting coils. The indication is that for only moderate fields in the range 3-4 Tesla, at pulse durations of 5 seconds or shorter, and at temperatures of about 10K, the cryomagnet is a cost effective and technically reliable solution[246].

6.2 Application to HSGGT

In a paper by Melville[247], the principle of providing thrust for a Maglev vehicle by reaction of the levitation and guidance magnets to sidepieces set at an angle within the main guideway reaction rails was described. Unfortunately, Melville failed to realise that there was no nett thrust force generated, since for a forward motion, thrust was balanced by an equal and opposite drag force in the second half of the cycle. The concept of a variable reluctance track was considered further at Warwick, where it was seen to fall naturally into a class of machines requiring variable frequency operation of the vehicle magnet currents to achieve superconducting LRM effect with a passive track structure[248].

Wipf elaborated on the variable reluctance track concept and also used variable frequency operation of vehicle coils[249]. The track structure chosen however would be difficult to construct: the choice is a sinusoidal elevation with amplitude of 300mm and period of 6 metres. The coil frequency would be 16.7 Hz for the design speed of 360 km/h. Coil current forcing was derived from a three phase superconducting generator on board which was driven either by a gas turbine or perhaps a LH_2 based turbine. The problem of ac losses was hardly mentioned.

6.3 Flux Pumping Motors (FPM)

6.3.1 Components

The foregoing sections suggest that it may be possible to design a realistic propulsion unit using variable frequency operation of superconductors or cryomagnets, although previous attempts have not produced feasible systems. It is likely that the operating regimes open to such units would be passive track propulsion of duorail or equivalent vehicles, rather than full magnetically levitated vehicles, because of the additional complexity of on board systems compared to an EDS-LSM vehicle.

The coil array construction is based on a three phase, three layer concentric winding arrangement (Figure 59). The three layers provide better volume utilization than a two layer winding and the coils can all be preformed into pancake windings, potted and then assembled into a fabricated array. Coil cross bracing would be eased because the mechanical structure will be very rigid.

The cryostat outer case will probably be a fibre reinforced plastic, perhaps with a eddy current shield on the top face to attenuate field projections into the passenger compartment. The use of plastic cryostats for pulsed coils is already proved[243], and total eddy current loss has a marked reduction. Coil energisation would follow one of four options, depending on the power rates required, and the heat losses that were acceptable. Track structure would be flat and embody ferromagnetic blocks at regular intervals

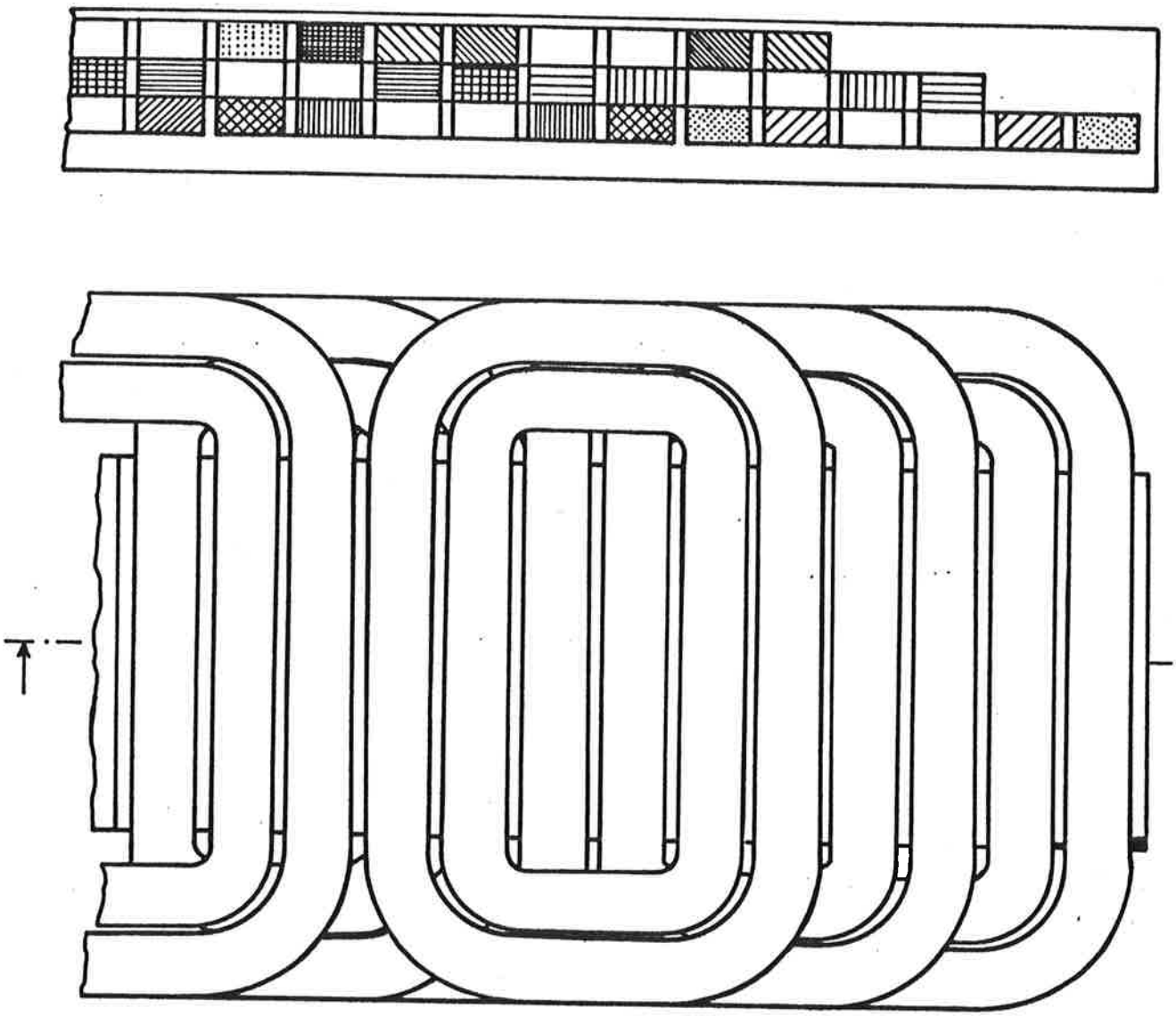

Three phase, three layer winding.

Figure 59. FLUX PUMPING MOTOR COIL ARRAY.

to provide saliency, although it would be possible to reconfigure the scheme to allow some of the normal attractive force to produce significant lift. As with the Rohr application of ROMAG[158], the track structure could incorporate a cage winding or sheet to produce even more thrust with the machine acting essentially as a superconducting linear induction motor. Using superconductors for airgap magnetization means that the overall power factor will be high, even at large clearances, so the normal problem of low apparent efficiency suffered by conventional LIM and LRM would be avoided. Rotating superconducting induction machines have been proposed[250], with a LN_2 primary stator winding and a superconducting rotating secondary. However, the superconductor matrix takes the secondary slip frequencies during start up, until the hysteretic and eddy current losses are sufficiently small to allow the whole cage to be cooled down to the superconductor transition temperature, at relatively low slips. At this point the machine locks into synchronism as the superconductor current oscillates with the cage's transient acceleration and deceleration resulting from load changes.

Some of the advantages of this type of motor result from it being energised from one side. The track could be simple to construct, and if a cage winding or sheet reaction rail was used, there would be no need to synchronise the existing frequency to the vehicle speed. The choice of prime energy for coil power would depend on the application. For low to medium speed operation a dc pickup would be most suitable, with an on board chopper and pulse inverter to supply the coils with a variable amplitude and frequency current source. At higher speeds where current pickup becomes physically awkward and economically unattractive, a gas or hydrogen turbine would almost certainly be chosen, to drive a rotating, perhaps superconducting alternator or dc generator with an inverter following.

6.3.2 Methods of Coil Energisation

Figure 60 shows four methods for controlling the energy flow into the superconducting (or cryogenically cooled) coil array. The first two methods supply the coils with sinusoidal controlled current from either a current source inverter or an alternator set driven by a prime mover or motor fed from picked up power. The second two methods energise the coils sequentially by either thermal or semiconductor switching.

The first method is probably the most simple, and involves feeding the separate coil phases with alternating currents. The coils within the array are internally connected to form the phase spreads, and a remote star connection within the cryostat obviates the need for another current lead.

The second method involves the use of a representative phase pitched additional flux pumping coil. The coil is fed with ac as before, but is closely coupled to the first pole pitch of the coil array. By correct choice of coil span and relative cross sectional ampere turns, the whole array will essentially be linked to the single flux pumping coil, since the phase overlap will "pass on" the flux variations. Although this option requires an additional coil to the first, only two current leads are required, for the flux pumping coil, and there are no interconnections to be made between coils in the cryostat. Flux pumps are a proven technology, and can be highly efficient in energy transfer(251).

The third and fourth schemes are similar in that individual coils are sequentially energised through switches to produce a moving mmf from the vehicle. The function of the inverter is shifted to within the cryostat, and the power feed into the cryostat is dc. The thermally switched flux pump (TSFP) method provides each coil with its own integral thermal switch which is powered up from a source outside the cryostat. The return to a superconducting state after the switch heater is de-energized is accomplished rapidly because of the low thermal inertia of the switch. Homer et al have used this method to produce recovery times as fast as two milliseconds, and have run their switches at about 20Hz to obtain high power densities(252).

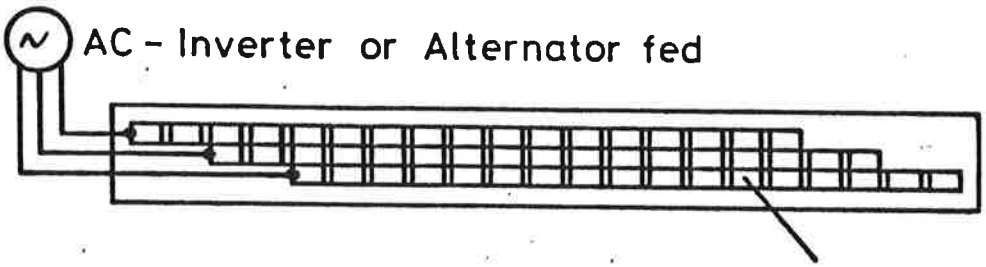

(a) Series Connected Coils

3 layer winding

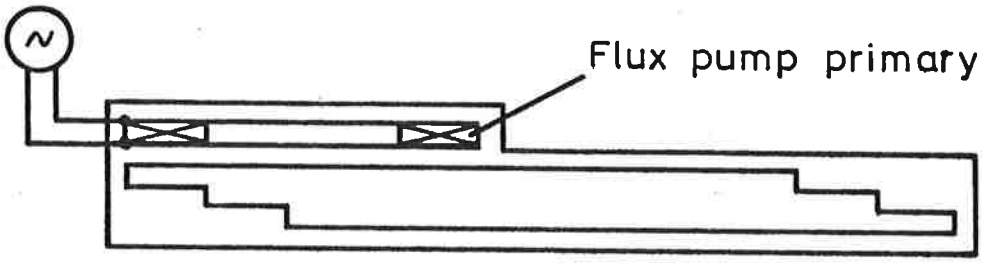

(b) Representative Phase Flux Pump

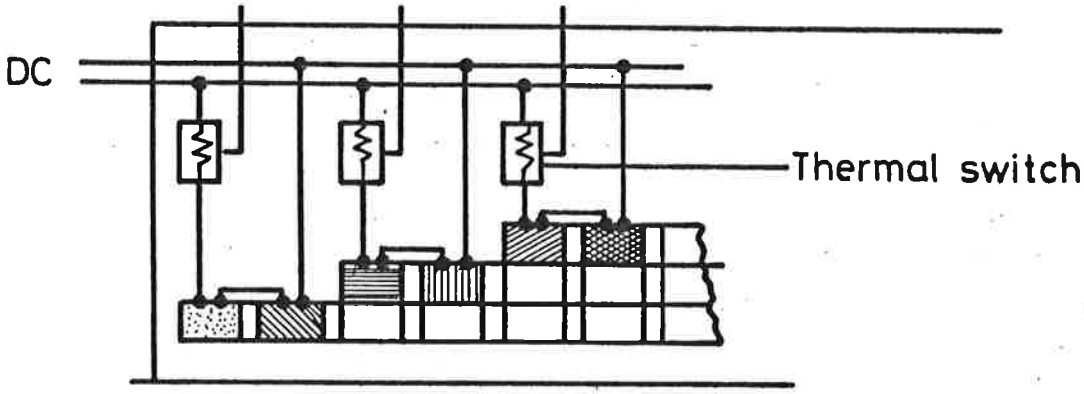

(c) Thermally Switched Flux Pump

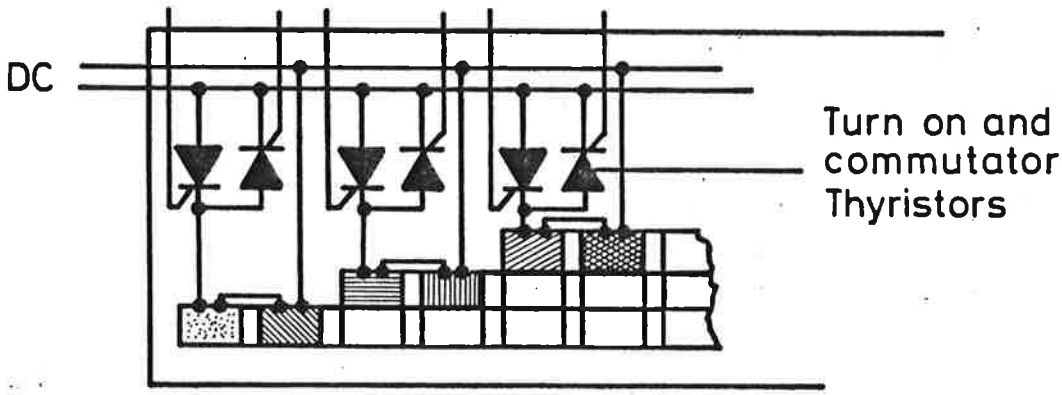

(d) Semiconductor Switched Flux Pump

FIGURE 60. METHODS OF COIL ENERGISATION.

The semiconductor switched flux pump (SSFP) produces the same effect as the TSFP, but uses either thyristors or transistors to produce the switching action. If thyristors are used, a commutation thyristor will have to be added to produce turn off of the first thyristor. A free wheel diode will not be required because the coil energy will be inductively dumped into the other coils on turn off. The advantage of the thyristor SSFP is that both the switching and commutation thyristors are only given a pulse of energy to turn on and the heat input to the cryogen down the gate leads will be a lot less than the equivalent TSFP heater leads, which are continuously energised when the switch is open. If a transistor switch is used, a continuous base drive is required, but no additional commutation component is necessary. The tradeoffs between thyristor and transistor SSFP and TSFP are difficult to qualify further at this stage. A compromise situation might be to allow the transistor switch to dissipate its base power at a LN_2 shield temperature, and run coil array current leads between LHe and LN_2 levels. The use of active semiconductors at any cryogenic temperature is not widespread, although Alsthom have used freon forced-cooled thyristors in a lightweight chopper circuit for a railway traction application.

The final choice for the best method of energising the coil array will no doubt be dependent on the exact application. If superconducting LIM are proved to be feasible with the expected advances in materials and wire fabrication, then other non-transport applications will develop, in much the same way as have applications of iron cored LIM. The high fields available will allow significant increases in the throughput of processes which use conventional LIM, and open up areas which were previously impractical. Typical examples of LIM application are scrap metal sorting, molten metal stirring, and even liquid metal pumping in foundaries or fast reactors. Liquid metal pumping shows particular advantages because the main pump component is external to the liquid metal, avoids contamination, and can be easily maintained.

6.4 Superconducting Homopolar Linear Synchronous Motors

Various forms of linear homopolar motors were considered during early Maglev development, the most common arrangement being a superconducting coil on the vehicle interacting with a track conductor system that was energised through vehicle brushgear to produce a fixed force angle[126]. There is however, no reason why the Aberdeen Transverse Flux Homopolar Machine (Figure 12), for example, cannot be constructed with the dc flux being sourced from a superconducting racetrack winding. Airgap magnetization could be provided with relatively small amounts of input power making up refrigeration losses. The transverse flux armature coils could still be fixed in laminations carrying the ac flux, so the overall machine would mix superconducting and normally conducting coils. Such combinations using a superconductor to effectively provide a dc bias on the magnetic circuit are presently being tested on a prototype super-transductor or fault limiting device, constructed by Parsons Peebles Power Transformers Ltd and IRD[253].

For large thrusts, the HLSM would effectively span the vehicle width. To provide the iron core at reasonable cross section would produce a very heavy structure. Figure 61 shows an alternative arrangement where the two armature lamination packets are each energised by separate racetrack superconducting windings, and the top flux transfer is assisted by the addition of a superconducting screen. The screen effectively compresses the flux and aids the lateral flux linkage. The added advantage is that the passenger compartment is totally screened from extraneous background fields. Whether figure of eight armature windings link both armatures or separate windings are used will depend on the available lateral space for a particular thrust requirement.

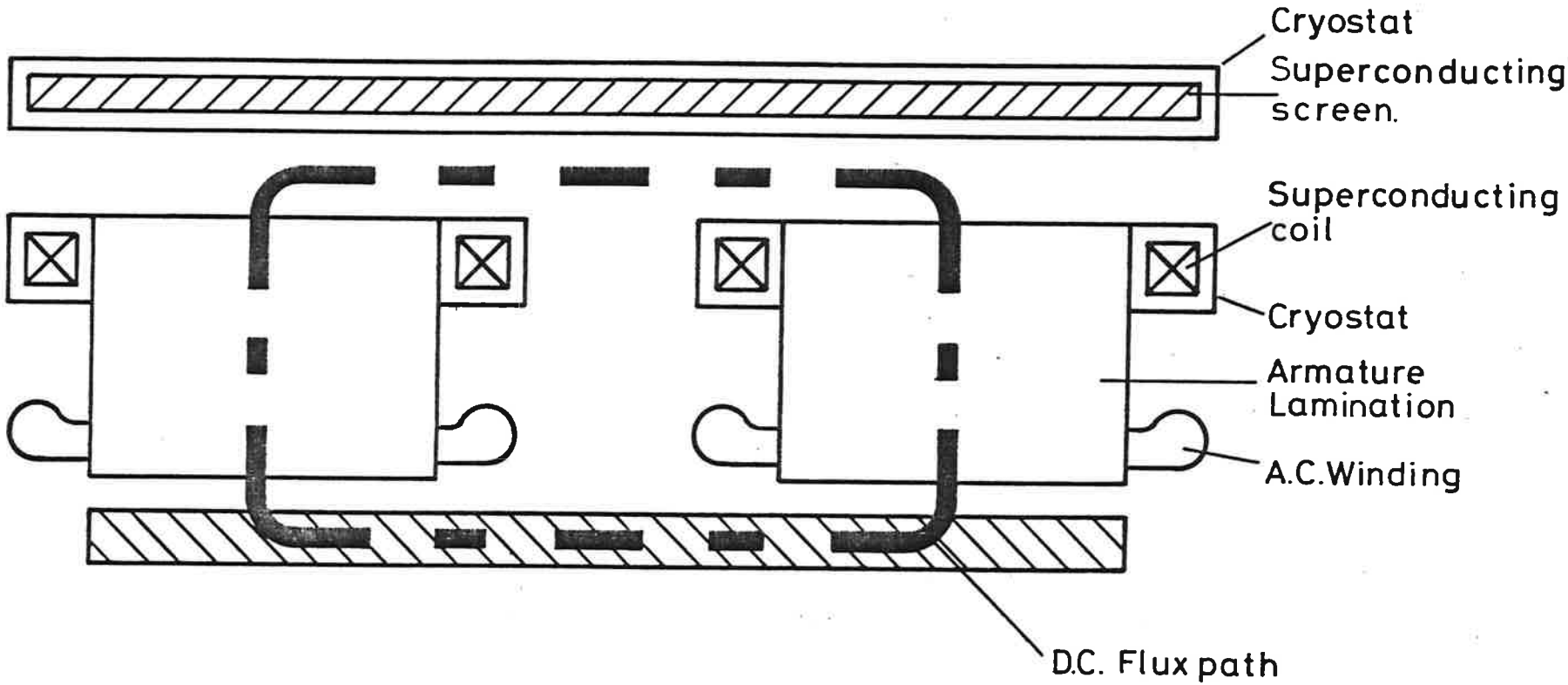

FIGURE 61. SUPERCONDUCTING HOMOPOLAR LINEAR SYNCHRONOUS MOTOR

CHAPTER SEVEN

HYBRID APPLICATIONS OF ACLSM

7. Hybrid Applications of ACLSM

7.1 Introduction

Railways throughout the world are beginning to rely more heavily on advances in technology to increase their effectiveness as a transport mode compared to the airplane and motorcar. In doing so the emphasis is usually placed on achieving higher average speeds to generate a commercial gain of reduced trip time, with the conflicting constraint of increase of cost usually providing the limiting factor. Technological change in railway practice is usually gradual, but it is possible to improve on existing systms. Aerodynamic drag and energy usage can be reduced by body shape and under body flow styling, and improved suspension design allows increased average speed and hence increases in load factor. Further automation will reduce manpower,but this has a natural bottom limit.

Although some of these effects can be achieved by slight extensions to common practice, others represent distinct changes in philosophy for railway administrations. In particular, the trend has developed to produce fixed formatation articulated-rake trains with integral power for operation in the 200-300 km/h range. Included in this trend has been the development of tilting axis trains such as APT, and the ASEA and FIAT versions. The growing interest in the development of novel techniques of propulsion, guidance and suspension for the very high speeds of 300-500 km/h has not in general been pursued with great vigour by any country's indigenous railway authority (except in Japan). In fact some of the new suspension philosophies have been regarded as rival systems to steel wheel on rail, rather than being accepted as part of an overall transportation solution.

In all the proposed configurations, the method of traction chosen will heavily influence the other sub-systems' design. For example, to meet the tractive power requirement at 400 or 500 km/h either a wheeled trainset with the best of conventional traction motors, or an attractive, magnetically levitated vehicle with linear induction motor drive, would face severe

problems in finding adequate remaining space for payload.

Previous sections have demonstrated maglev characteristics; a development under way in Germany is attempting to qualify the practical limits to conventional railroad. Following on from roller rig tests at up to 500 km/h German Federal Railways(GFR) and Fried.Krupp GmbH are to test a three car 220 tonne 60 metre long vehicle with 12 driven axles[254]. The power rating will be approximately 12 MW and a top speed of 400 km/h is planned on a converted freight line 23 kilometres long between Rheine and Freren, in North Rhine Westphalia. If the tests are satisfactory, GFR's research department at Minden will determine and develop a suitable configuration for an overall system and its components that could enter revenue service. One aim is to develop the system to 300 km/h, at which point air has no advantage over rail in journey time, for a 500-600 kilometre trip.

Although these tests will not be completed until 1984, it is unlikely that a very high speed system incorporating driven axles will be acceptable in terms of noise generation and track maintenance costs. A possible solution is to provide traction by using a linear machine, and the most suitable system in terms of power transfer is a LSM. The following sections examine the possiblity of using an ACLSM as a propulsion device for conventionally railed vehicles.

7.2 Advanced Passenger Train with ACLSM

7.2.1 APT Origin

In the early 1960's British Rail set up a research team to attempt to establish the cause of instability in running freight waggons at high speeds. Above a typical running speed of 80 km/h four wheel waggons tended to derail. At the usual running speed of 70 km/h traffic routing problems would arise when trying to integrate freight and passenger traffic on the same line. Any improvement in freight speed would therefore affect the whole system throughput potential. As a result of the subsequent research a new series of freight bogies allowed freight waggons to run at 50% higher speeds.

The results of the freight analysis and general suspension and vehicle dynamics expertise acquired by British Rail was applied to a proposal to build the Advanced Passenger Train, to similarly extend the useful speed range of trains with no drop in ride quality. This experience was also responsible for BR to be chosen as consultants on vehicle dynamics to the LIMRV programme. The LIMRV ran at up to 400 km/h without flange contact, using the double taper wheel profile chosen by BR for APT.

The concept of providing a tilting suspension on the passenger compartments to allow faster running through curves was chosen as being more cost effective than realignments at greater curve radii and increased cant angles, because British passenger density is generally low. Active control of the tilt using hydraulic jacks was necessary because the simpler passive-damped pendular system could not give sufficient response through tortuous routes, and required an excessively narrow body profile.

Articulation of the train was favoured, since to reduce the track damage rate a lower unsprung mass is required in the wheel sets, which are also subject to a minimum axle loading to sustain ride quality. Articulation of a lightweight train with a low wheel count meets these criteria, and adjacent carriages share common bogies. In general rake length is determined purely by availability of maintenance facilities, and for the London-Glasgow route the rake length can be up to six trailer cars.

Power for traction in the early APT-E (experimental units) was based on British Leyland prototype gas turbines. SNCF also adopted gas turbines for the TGV prototypes. Leyland Truck stopped development of the power units and BR were forced to adopt an electrical power supply, using pantograph equipment. The power car is rated at 3MW. Original plans for 2+12 configuration (two power cars + 12 trailer cars) with the power cars in the middle of the train were dropped in favour of a 1 + 10 make up, with the power car leading. As well as the operational advantage of not having a bisected train, the aerodynamic loading in side gust gives the greatest

moment on the leading car, so a weight increase is of benefit.

The three APT-E units are planned to enter service in late 1981 on the west coast London-Glasgow route. Provided government approval is forthcoming, a 60 train fleet of electric APT-S (S= Service) could fully serve the west coast route in 1985. Although they represent the state of the art in conventional railway practice, their top speed is unlikely to exceed 250 km/h, simply because the maintenance costs will become excessive. Track damage will result from increased power car weight and increased unsprung mass on the axles. Although diesel powered versions of reduced length (say six or seven cars) are planned, they would represent a retrograde step in BR's modernisation and electrification proposals.

7.2.2 Problem Areas in High Speed Running

Whenever a problem area arises in the engineering of a complex system, it is directly reflected in a cost penaltty. For a railway system the cost areas are well defined as initial first cost (infrastructure), running cost and maintenance cost. The engineering problems are generally caused by the breakdown of the wheel-rail interface, track damage, ride quality deterioration, and power collection discontinuity.

The wheel rail interface is naturally the most critical area in railway design. Surface contact is limited to the highly stressed area through which the traction power must be transmitted. Adhesion on the driving wheels must be carefully controlled to ensure that wheel slip does not occur during acceleration and that wheel lock does not occur during deceleration. The APT has to brake from 250 km/h to keep within existing signalling distances, at 0.14 gee peak. The hydrokinetic brakes saturate at low speeds, when friction braking takes over. Friction braking needs the provision of wheel slip detection equipment to prevent wheel flats developing under slippery conditions. When the wheels slide rather than purely roll, spalling occurs on the rolling surface from overheating; slip detection has the auxiliary function of monitoring this type of failure.

The acceleration rates on the train are also limited by environmental conditions, the state of the wheel sets' surface, and track profile. By having to generate tractive effort through an essentially slippy surface, power train losses are considerable. Consistent acceleration and deceleration rates cannot be achieved by design factors only.

In general the driven wheel sets are located near or under the power car, whose high axle load allows a higher degree of transmitted tractive effort for a particular track surface condition. There is therefore a requirement for a high axle load for good traction which is in conflict with the desire to produce a lightweight trainset to minimise power demand. The axle load itself results in track damage which has only recently been understood. Track damage is caused by the dynamic loading of the unsprung mass becoming large compared to the static load, and the effect is especially accentuated at joints and crossings. The forces additional to the static loading are known as the P1 and P2 forces, so called because they occur first and second in a force-time history of a rail joint. P1 occurs a $\frac{1}{4}$ - $\frac{1}{2}$ millisecond after meeting a discontinuity and may have an impulse peak up to six times the static load. P2 is a broader response several milliseconds later, at roughly four times the static load. The P1 force is due to a high frequency (500 - 2 kHz) bounce on the Hertzian contact stiffness between wheel and rail, and the P2 force is due to a lower frequency (20 - 100 Hz) bounce of the wheel set on the track foundation stiffness. It is the P2 force which causes the major damage to ballast and leads to track top deterioration as the ballast migrates, but this also sets up a spiral of increasing P1 too.

Vehicle design philosophy is to limit the forces generated to be no greater than a Deltic travelling at 166 km/h. Since the P2 force is largely a function of the axle unsprung mass, it has been found that for any increase in vehicle speeds, the unsprung mass has to be reduced in roughly a velocity squared ratio. APT uses a cardan shaft from the motor driven braked gearbox to a second gearbox on the bogie. The shaft is necessary to take up all the

body movements, especially the tilting motion. The second gearbox on the bogie drives the wheel set through a Quill drive which keeps the unsprung wheel set mass and the primary sprung bogie masses to a minimum. The total unsprung mass is 1.5 tonnes, which is acceptable for 250km/h duty, compared to HST's 2.2 tonnes for 200 km/h and the Deltic's 3.25 tonnes at 160 km/h. A proposed resilient wheel was found to be unsatisfactory because it lacked torsional stiffness. Any required increase in speed is limited therefore by having to reduce the driven wheelset's unsprung mass.

Power collection is likely to remain by pantograph. It is generally accepted that pantograph systems have an upper speed limit although its value is not clearly defined. SNCF have run successfully at up to 280 km/h, and the design speed for the TGV-Electric train sets is 6.3MW power pick up at 270 km/h. The Japanese have run at 256km/h on a timetable service but have considered three phase rigid conductor rail for very high speed current collection. The main problem is that the catenary requires maintenance and repair, as does the brush material on the pantograph head. The original APT 2 + 12 design called for two power cars collecting a total of 6MW for a 270 km/h balance speed.

Figure 62 shows the power and thrust requirements of the 2 + 12 APT with 600 passengers running at constant speed on level track. The 6MW requirement at 270km/h increases to 7.8MW at 300 km/h and 17MW at 400 km/h. The promise of transmitting this level of power, even through a servo controlled pantograph, is daunting and really requires a completely different approach.

7.2.3 ACLSM Extension of APT Capability

The ACLSM for APT propulsion would use the high field superconducting magnet systems similar to EDS Maglev. In the hybrid vehicle the suspension and guidance would for the most part, be provided by the steel wheel on steel rail, but the propulsion and major braking functions would be taken over by the ACLSM. The immediate advantage in choosing an ACLSM over say a LIM or HLSM with iron cored passive secondaries is that power can be transmitted

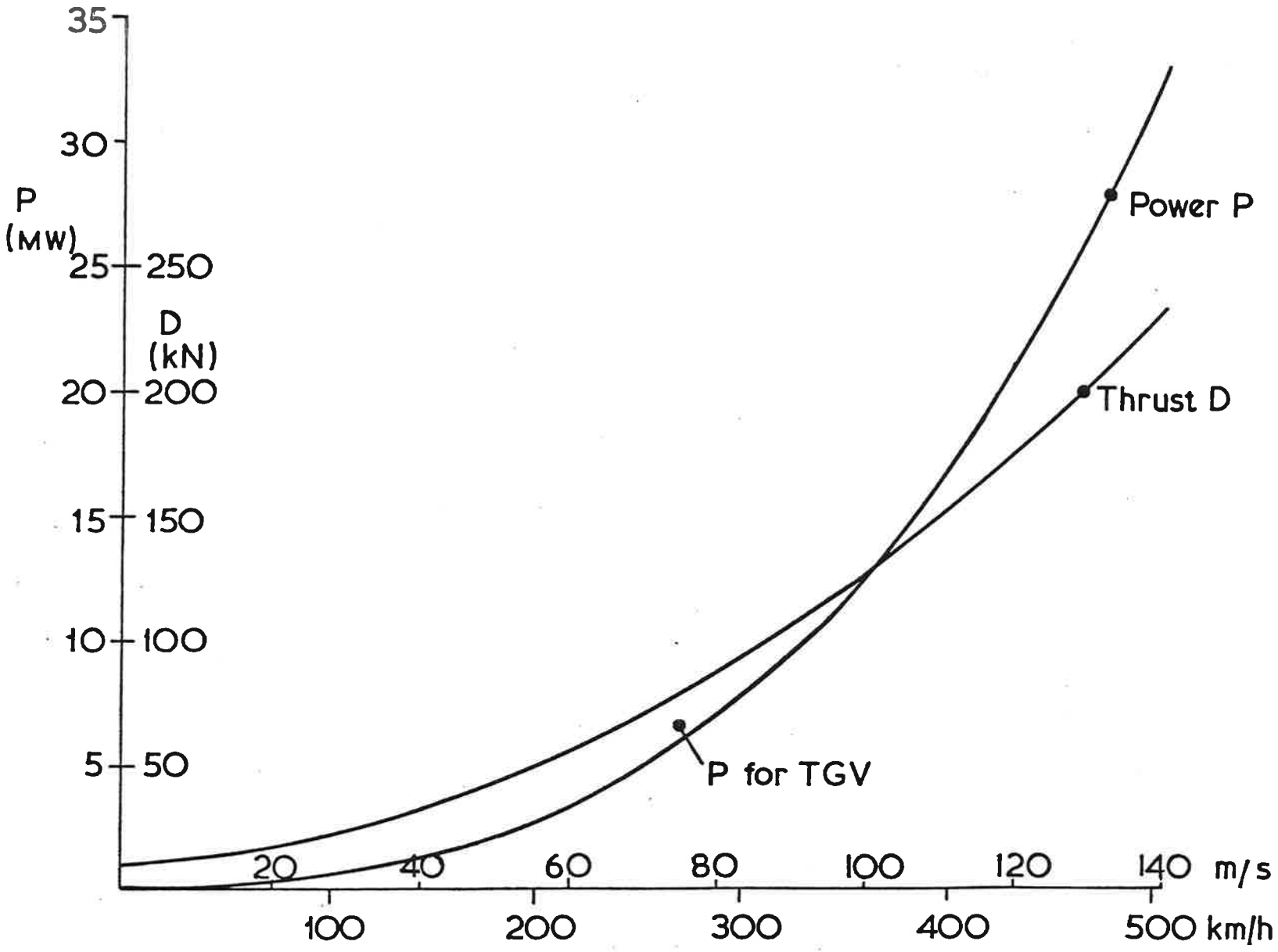

Figure 62. Power requirements for APT.

through the machine airgap to the vehicle for traction, without requiring massive on board generation, or very high power current collection. The pantograph and catenary equipment is immediately superfluous. Braking and acceleration is accomplished through the airgap field without the need to power the wheel sets, avoiding the problems of wheel slip and speed matching. In addition the axle weight in the bogie unsprung mass is allowed more freedom for a lighter structure design that could run at much higher speeds.

The magnet system would consist of a multiple array fixed to the train subframe, and would be housed in isochoric cryostats. Persistent current mode operation (with no current leads or external power supply) would be used, and a working day's duty could be achieved before servicing of the cryostat to depressurize and refill was necessary. A totally closed helium cycle is obligatory to conserve a natural resource, and the servicing facility at the terminii must have LHe liquefaction and power supplies to re-energise the magnets.

The track winding would be an air cored winding made up of conventional stranded insulated cable laid in a meander configuration either at track surface level or mounted on a slight plinth in the slab track. Figure 63 shows a suggested end view arrangement of plinth armature and cryostat, with an electromagnetic "airgap" clearance of 255mm, and mechanical clearance of 100m. The plinth might be required to minimise the eddy current drag in the rails from the magnet's motion and the armature winding mmf. An exact analysis of this effect has not been performed since it was found that non magnetic rails were only marginally more expensive than the high quality steel used in conventional rails[120]. The armature conductor would be grouted into the track surface to allow not only good force transmission with minimal strain, but also to provide protection from damage and the environment.

The cryostat assembly would form a magnet pad housed in a mounting arrangement that could be easily and automatically decoupled from the train's subframe. This modular approach means that at termini the magnet pads can be rapidly

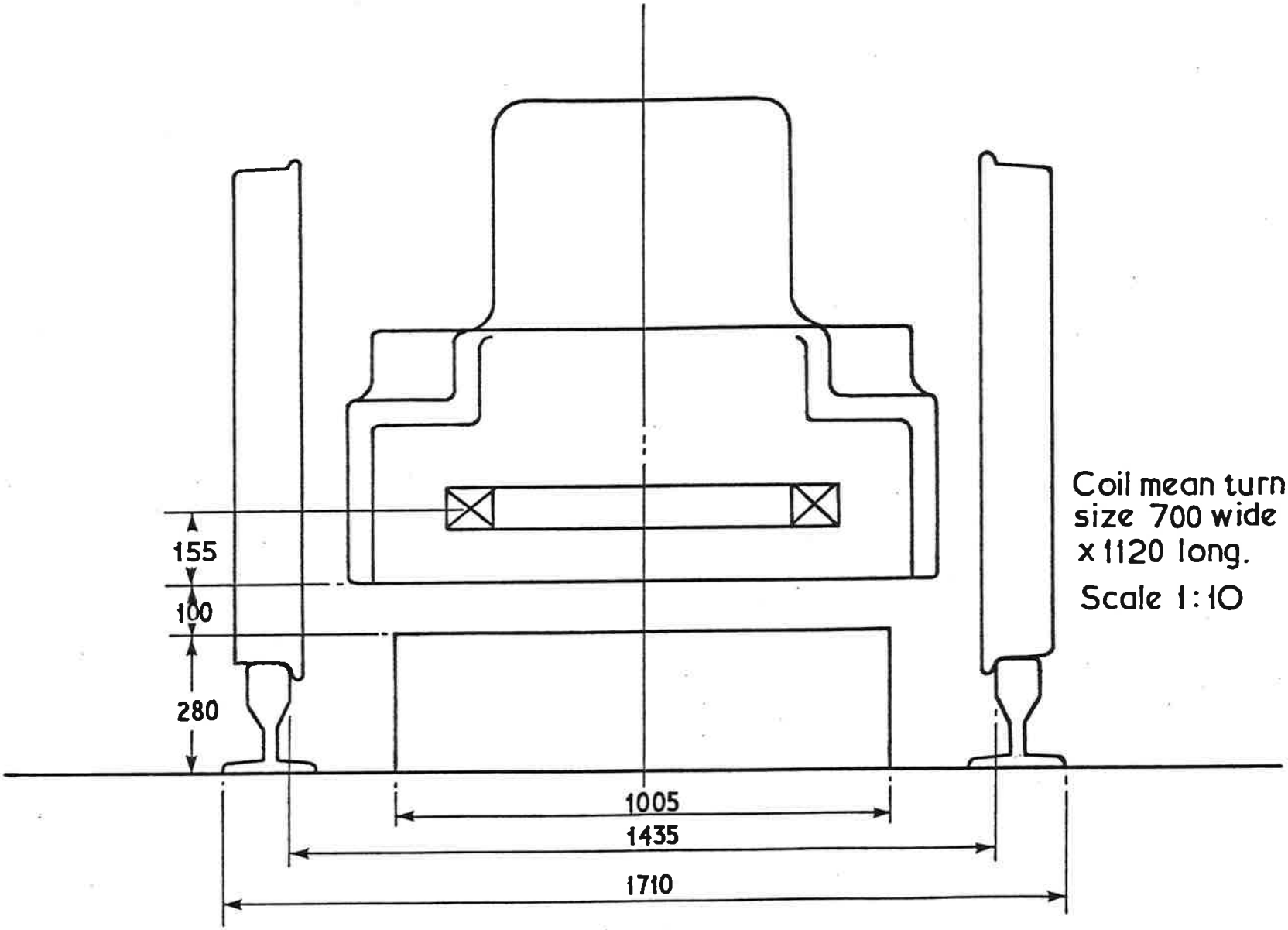

Figure 63. Cryostat End View.

demounted and then taken to a servicing facility where helium transfer through flexible tubing to a liquefier can occur, and connection to a flux pump module will allow magnet recharging and discharging if required. It is quite conceivable that a one to two hour turnaround could be achieved, that would also fit into a daytime operating schedule. If a buffer supply of ready charged cryostats was available, turnaround could be even shorter. An alternative scenario is to provide track incorporated mirror cryostats at the servicing facility, over which the train is positioned. The mirror cryostats would contain flux pumps which would reenergise the coils automaticlly. On train umbilicals would connect to service ports for LHe transfer. The latter scheme might be preferred by the operator who can afford to effectively spread his servicing operation along many train lengths, rather than concentrating the specialized operations at a service centre and requiring only relatively simple mechanical operations (such as remounting the serviced cryostats to the vehicle body) to be performed at the train.

Conceptually, ACLSM propulsion would not require major technological development, although higher temperature superconductors would ease the temperature rise limitation in isochoric operation. It is possible to design in a system which could make cryogenics operationally easy to handle. A cryostat design such as Figure 64 (Siemens' AVF) would be suitable for conversion to an isochoric duty and ten such units with 30 coils would provide the 90kN required to drive an APT at 300 km/h, with a current sheet track density of about 8kA/m. Using the Emsland design coils and cryostats[119] only 3 double sized cryostats (each with six coils) would be required since the active length is greater at 800mm compared to 700mm and the pole pitch at 1 metre is shorter. Two of the double sized cryostats would fit under the existing power car, whose wheelset pitch is 13 metres.

ACLSM adoption would impact all three of the cost criteria. Lower first cost would result since the track bound armature serves as the distribution, pickup and one side of the propulsion motor. Its design is governed more by

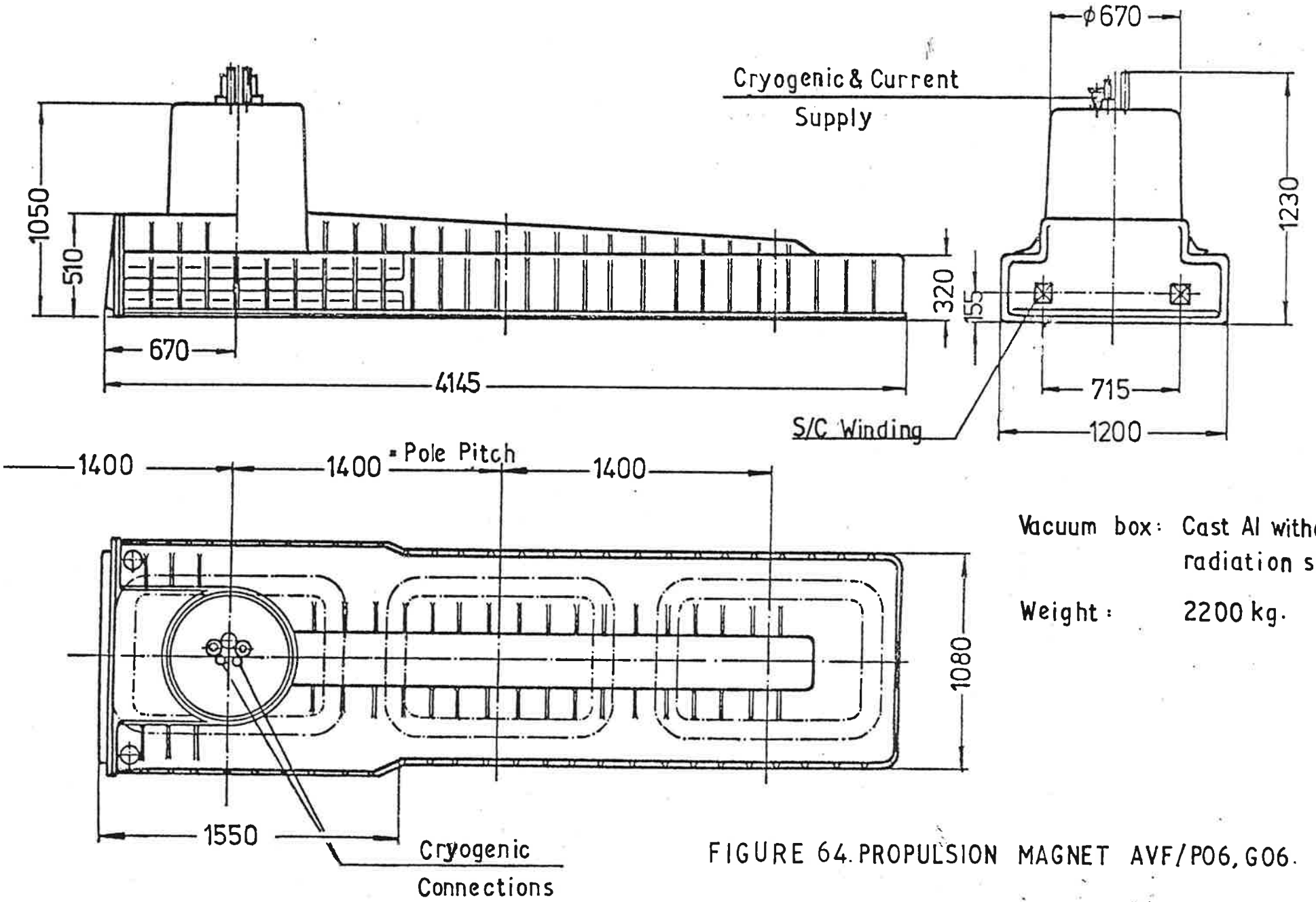

Vacuum box: Cast Al without radiation shield

Weight: 2200 kg.

FIGURE 64. PROPULSION MAGNET AVF/P06, G06.

tradeoff of repayment factor of conductor cost against power cost through the track resistance. Because there is no iron in the track the inductance is very low, and voltage drop in the magnetically unlinked feeding section of the winding must also be similarly low. Because there is no catenary, there are no overhead tensioning devices, and no trackside masts. Load equalisation between sections is unnecessary since the multiphase system is inherently balanced. This would be particularly important for high speeds since loosely tied areas will experience phase imbalance on existing 25kV ac supplies at 132kV feeders.

The armature winding has the option of either being fabricated off site into a "conductor mat" which only requires a minimum of fixing at the installation, or can be automatically track wound into precast blocks which have preformed slots in their surface. The former scheme has the advantage that the conductors are factory formed and installation damage risk is minimised since relatively simple fixing rather than fitting is required. A combined scheme of laying formed and braced conductor into a slip casting machine might provide an alternative method of installation.

Because of the preforming processes involved, track armature lay time will be comparable to catenary stringing time. Lightning protection should be unnecessary, since substantial insulation will be provided by a conventional jacket insulation, and will be aided by epoxy cement grout. The amount of armature material will depend on power density required from the machine. Typically it is in the range of 5-30 kilogramme/metre. The steel rail is roughly 60 kilogramme/metre. Train turbulent windage will allow slightly higher than normal current densities to be used.

The overall machine efficiency and power factor will be high, even though the design limits are set by the economics involved rather than any particular engineering difficulties. Since the main airgap flux is sourced from the vehicle magnets, the magnetization is not reflected into the power supply as a low power factor. For multiple vehicle operation, it may be possible to

operate some of the machines at leading power factors to reduce the overall reactive power consumption and compensate for the line inductance. It is more likely that this effect would not feed through the system since each vehicle will be controlled by one inverter, or a split inverter. Regeneration through the inverters before the main utility connection is made would trade off some of the acceleration and braking loads in the system.

Vehicle cost may be reduced through lightweight construction. APT has attempted to do this by using aluminium extrusions in the body shell design of the passenger sections. The Siemens cryostat weighs approximately 2 tonnes, and would be less for an isochoric design. This can be compared to the main APT incoming transformer weighing 5.3 tonne (53 kW losses), in a 69 tonne power car. The existing power car has very few longitudinal features and is inherently less stiff than a lightly loaded trailer car, so aluminium loses its advantage. Steel was chosen as the main structural material, with the heavy items in the central portion of the car, depressing the natural frequency of the body. With the absence of the majority of the power car equipment, a similar constructional technique could be used to decrease the axle load, and there should be sufficient room to accommodate passengers in the main power car. Naturally, with the absence of driven wheels, the unsprung mass of the power car is reduced too, the wheels being designed for pure rolling.

Maintenance cost will be reduced at the trackside because there is a simple slab track with enclosed conductors. The need for reballasting and catenary adjustment with restringing will have disappeared. Rail damage will be minimal because axle loads of the power car and unsprung mass of wheel sets are all reduced. Provided that armature hot spots do not occur to break down the insulation the track should be essentially maintenance free.

Vehicle maintenance is dominated by the need to reprofile wheel treads. The major causes of the wheel damage are, apart from the unsprung mass

bounce, flats and localised heating producing creep caused by wheel slip. With tractive effort and braking being derived from the motor air gap power transfer, wheel damage and deterioration should be reduced dramatically. Running cost means basically power consumption of the trainset. With the total vehicle construction being lightweight, the inertial power required to accelerate is reduced. Although the steady state power consumption follows a cubic relationship with speed (Figure 62), constant headway limits imposed by signalling means that power requirements will increase as velocity squared. With the omission of the pantograph, the APT has an immediate reduction in the drag force experienced of 8%. Similarly a continued study of underbody flow could possibly reduce aerodynamic drag by as much as 10%.

By being able to provide a magnet pad for any of the trailer cars, it would be possible to match train length to passenger demand more closely. Since synchronous operation is assured, the operation of the system can be either platoon following or exclusive block, depending on the strategy chosen. Inverter control is already required and this could be incorporated into an overall computer control of all vehicle scheduling, with exact knowledge of vehicle position. Further control of the inverters could provide motion control, for example heave and surge motion control. If vehicle overturning is considered to be a problem, then an attractive normal force can be achieved by altering the machine current angle operation.

Since the armature can be built to match local conditions, additional cross section or armature conductor density may be included where extra acceleration is required, for example near stations and at slow grades. This will affect infrastructure first cost as well as running cost. For example the Paris-Lyon route is built for maximum gradients of 3.5%, which means only 1.3% of the 427km is made up of bridges. This compares with 30% on the FS Direttissima, and 33% on JNR's Tokaido Section. A reasonable ACLSM design could easily accommodate up to 15% grade climeability at rated

cruise speed by additional track conductor, without penalizing payload. The ACLSM has scope for improving the overall vehicle performance and has the opportunity for lowering both first cost as well as maintenance and running costs compared to conventional traction drives. Dual running of conventional and ACLSM vehicles is possible since neither scheme requires removal of the alternative facilities. No new infrastructure is required. Freight services would remain unaffected, and might even benefit from LSM drive.

The appearance of an ACLSM propelled APT would not be radically different from the existing vehicle. Because of the higher speed operation, shorter higher loaded vehicles at reduced headways might be expected. Figure 65 gives an impression of a high performance four car vehicle, with removeable cryostat assemblies mounted under the body in between the wheel sets. The vehicle is bidirectional, and passengers are accommodated throughout the front and tail cars, except for small areas containing on board services such as heating and ventilation plant.

7.3 Urban Vehicles with ACLSM

The concept of the ACLSM propelling wheeled vehicles can be extended down in the speed range. Whereas EDS with ACLSM were not considered for urban and low speed operation, the ACLSM on its own can be reconfigured to suit lower speeds. Linear motors have not generally been considered suitable for urban vehicles since the more advanced UMTA projects never really materialised. However with UTDC's, ICTS, the situation may rapidly turnaround, despite their choice of LIM for propulsion. Nondahl at General Electric has studied the alternatives of SLIM and HLSM as propulsive units for design vehicles running at 112 to 400 km/h, requiring 200-3735kW[215]. The track structures are essentially passive, but not necessarily inexpensive. For example the 200 kW SLIM design uses 32 kg/m back iron, and 63kg/m in the 3735 kW design. On top of this the SLIM naturally has aluminium secondary material and there is a current pick up

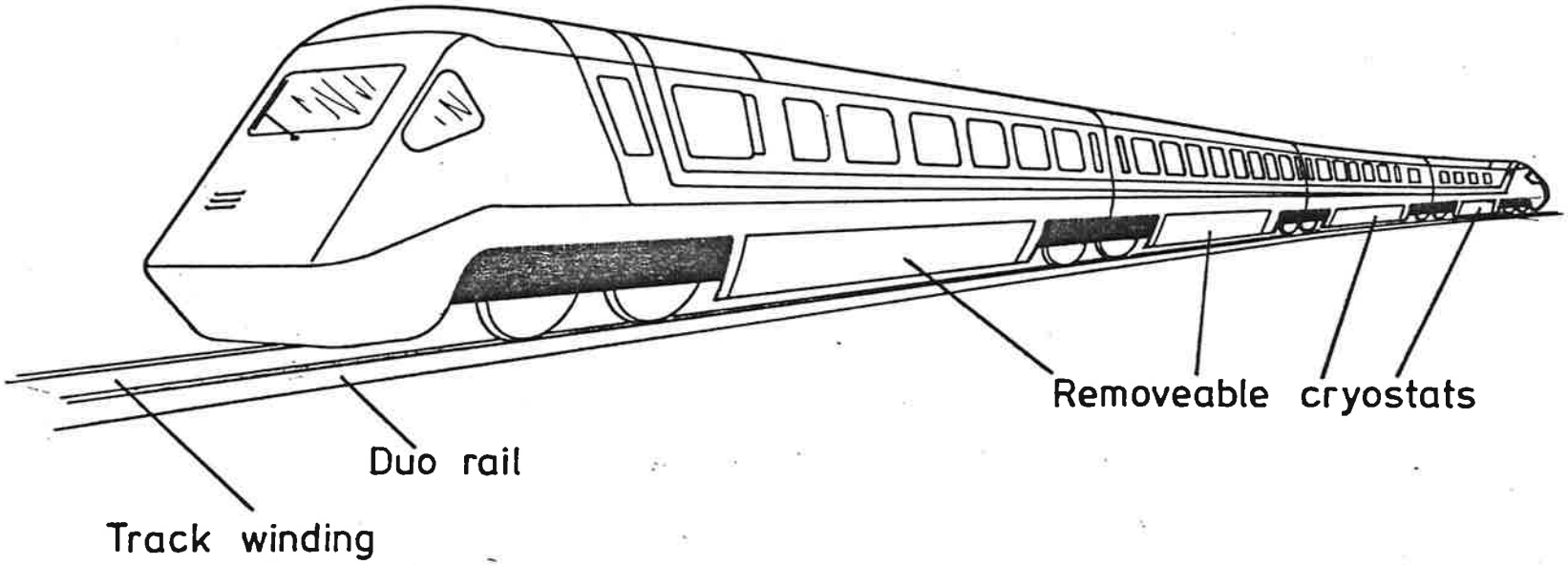

FIGURE 65. APT WITH TRACK WINDING AND REMOVEABLE CRYOSTATS.

system required.

The pressure to reduce the cost of urban rail vehicles has been demonstrated by the Railbus, which consists of two Leyland single-deck bus bodies joined back to back and mounted on a rail underframe supported by high speed freight wagon bogies[255]. The vehicles are powered by a 150kW diesel for a maximum speed of 120 km/h, with 64 passengers. Vehicle cost for production versions will be about £130k, roughly a third of the price of an equivalent conventional rail vehicle.

Slemon has designed out a LSM vehicle rated at 240kW for urban service at 72 km/h, with an air cored winding, inverters at 200 metres, and a rare earth magnet field assembly weighing about 1 tonne[213]. Although the machine has good overall performance, the economics are unlikely to be acceptable. Operationally, because the magnets cannot be deenergised, maintenance problems will arise in dealing with magnetic debris picked up from the track.

With the continued pressure on cryogenic development from MHD, Fusion, rotating machinery, as well as Maglev the development of reliable and cost effective superconductors will allow an urban vehicle to be equipped with lightweight cryostats. The advantages of the previous section will still apply for simple, low maintenance track, and easily controlled vehicles.

For a typical urban vehicle a thrust of about 12kN is required. This value could be derived from a 3 metre long cryostat assembly with three coils. There would be no particular problems in operation or maintenance if the isochoric magnet pad concept was again applied, since the only part of the vehicle supplying thrust would be easily removeable.

Other field arrangements may prove as suitable. For example, air or iron cored magnets with normal conductors could be used. Power would be generated either on board or picked up through a third rail. To get sufficient ampere turns on the vehicle a cryoresistive coil is likely to be the best option, but at lower ampere turns track and coil windings would need to be iron cored with small mechanical clearances to allow an efficient magnetic circuit to be made.

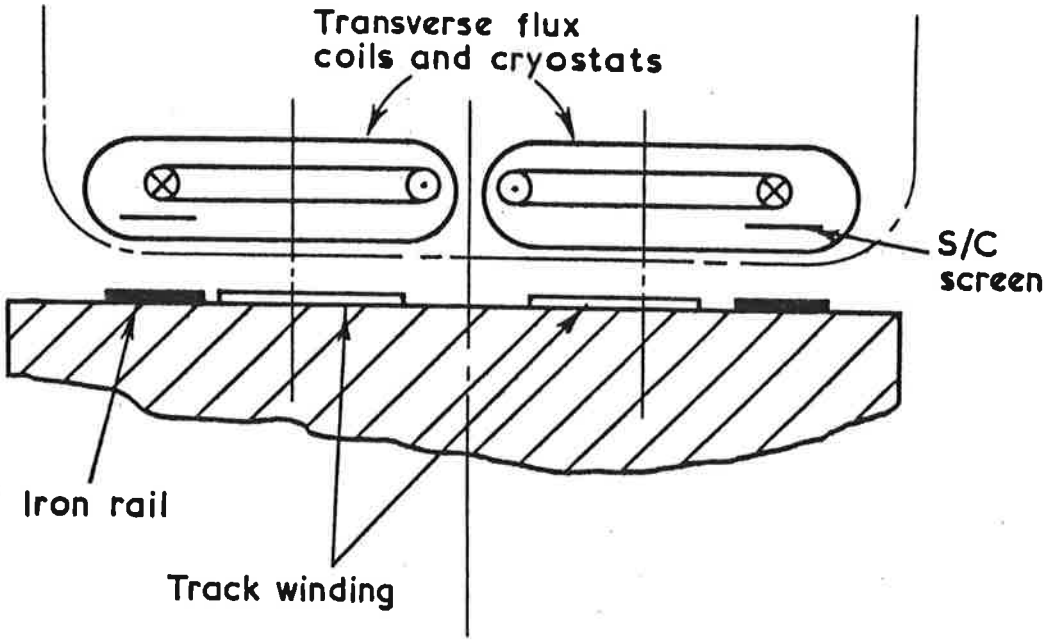

a) Mixed – μ suspension and transverse flux (dual motor) linear synchronous propulsion.

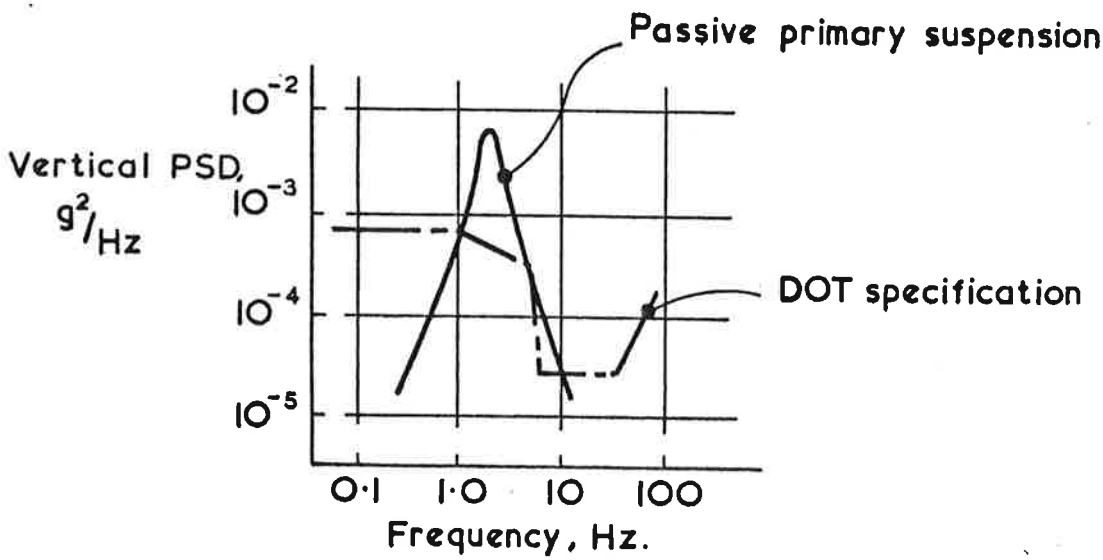

b) Typical ride quality results expected for mixed μ suspension and passive primary damping.

Figure 66. Mixed μ suspension and transverse flux linear synchronous motor propulsion.

A form of EDS which might take the place of EMS suspensions at low speed for urban applications, is the mixed μ system[256]. The system involves the use of superconducting screening material between a solenoid and a ferromagnetic rail. Russell suggests a saddle shaped coil formed around an iron rail with a pinch wheel drive on a vertical plate. A more reasonable approach is shown in Figure 66 where a flat track transverse flux motor interacts with a flat iron rail. The superconducting screen is in the same cryostat as the coil and allows lateral stability by edge effect. The transverse motor arrangement is adopted to provide heave roll and surge damping as well as thrust and normal force trim. The PSD expected is shown. To move the ride quality spectra to within the DOT standard, active ride control is necessary, achieved by the LSM. If lateral damping is required then active secondary suspension could be used. A lateral screen working in 'mixed μ' but incorporating a persistent current type heater to locally quench it might be an alternative form of lateral active damper, although the heat leak rate is likely to preclude its prolonged action.

The urban vehicle with a passive on board magnet array that was energised at the beginning of the working day, and reacts with a simple controllable air cored track winding running at low power dissipation (and hence high efficiency) is indeed feasible. Its infrastructure is cheap and the track material content is small considering the power that is transferred. Vehicle cost will be low since a lightweight structure with no power conversion equipment on board is all that is required.

CHAPTER EIGHT

CONCLUSIONS

8. Conclusions

The most important areas of interest concerning air cored linear machines, their design, development and application to guided ground transportation have been presented. ACLM began as the favoured propulsion unit option for the electrodynamic system of magnetic levitation. The machine characteristics can be represented by an equivalent circuit model with which design performance can be calculated, and the way in which the circuit components are evaluated and optimised is discussed. An analysis of the field to stator flux linkage allows harmonics to be minimised by phase spreading or short pitching the stator winding. Rectangular vehicle coil stresses were modelled by matching the corner body forces to those of a circular coil with a similar field profile and cross section.

For high acceleration loading, the track power dissipated for long section lengths can become excessive. The linear commutator motor was conceived in two main variants to combat this problem. In its most elementary form each track wavelength is energised through a bidirectional chopper from a dc bus. The substation requires only a transformer rectifier set, and the utility is effectively buffered from low power factors. A less sophisticated form uses the LSM geometry with the inverter either at much more frequent intervals or more frequent tie reclosures per inverter, to produce short block lengths of energised track. An economic analysis of the LCM in relation to several LSM designs shows that for low inverter unit cost and short block lengths, a LCM is still an attractive option to LSM for revenue duty, despite the added track complexity. A superconducting model LCM was successfully built and tested. Both the Miyazaki and Emsland high speeed linear test facilities have adopted short block length switching to remote converters as the most economic solution with the minimum of overall losses.

A systems comparison of EMS and several EDS full sized designs highlighted the need to perform comparisons on similar baselines of speed, passenger density scheduling and routing, rather than just specifying lift to drag

ratio, specific energy intensity or machine efficiency. In particular the SLIM was shown to be inadequate for 500 km/h operation of German EMS vehicles, and not very efficient in energy conversion at 400 km/h. The Siemens EDS vehicle was also shown to be heavily penalized by its duo-rail compatible low speed suspension system, compared to other EDS designs which used aerospace type vehicle construction, and light weight suspensions.

Several different variations are proposed for a new type of ACLM which uses on board flux pumping either by direct drive from an on board alternator or inverter, or by thermal or semiconductor switching of currents into superconducting or cryogenically cooled coils. The flux pumping motor (FPM) requires a passive track structure with either saliency for reluctance operation, or a sheet secondary for induction motoring. A superconducting HLSM design is also considered.

Finally, the application of ACLSM to propulsion of advanced duo rail vehicles is proposed. The gains in speed envelope, reduced track damage and lower installed and maintenance cost are examined. As a short term development, conversion of an APT type vehicle with removeable cryostats and coils which operate isochorically would show immediate advantages in reduced operational expense to conventional versions. Extension of the technique to low speed urban vehicle design is also possible, with a simple low maintenance track structure.

In general, development of ACLM has proceeded agains a background of increasing world recession, which has limited the need for growth in high speed guided ground transportation expected in the late 1960's. However, the last few years have shown that the basic concepts and design criteria are justified, and can be made to work at the very high speeds of 500km/h. Although EDS no longer has the impetus of major development in the main industrialised countries, with the exception of Japan, ACLM can be used for other forms of contact guided vehicles, with a less complicated infrastructure required. It is apparent that it is this need that ACLM must satisfy,

otherwise the associated research and development will suffer the same fate as Bachelet's electromagnetic experiments at the turn of the century.

CHAPTER NINE

REFERENCES

References

1. S S Wheeler, C S Bradley, "Improvements in Electic Transportation Systems" UK Patent 4,751:1891, 18 April 1891.

2. "Tangential Traction", Electrician, vol.52, 29 January 1904, p.561-2.

3. H H Wilson, "Electrification of Railways", Trans. Liverpool Engineering Society, vol.26, 1905, p.181-234.

4. A Zehden, "Improvements in Electromagnetic Traction or Driving Apparatus for Railways, Lifts, Machine Tools and Other Apparatus", UK Patent 12,581:1902, 2 June 1902.

5. id., "New Improvements in Electric Traction Apparatus", US Patent 88,145, 4 June 1902.

6. The Electric Carrier Co., "Electric Induction Transport System for Mails", Engineering, vol.96, 10 October 1913, p.501.

7. "Electric Carrier Railways for Rapid Transfer of Mail and Express", Engineering News, vol.70, No.14, 2 October 1913, p.637-9.

8. E Bachlet, "Electromagnetic Levitating and Transmitting Apparatus", UK Patent 9,573:1911, 19 April 1911, also "Levitating Transmitting Apparatus" US Patent 1,020,943, 19 March 1912.

9. "Foucault and Eddy Currents Put to Service", "The Engineer" vol.114, 18 October, 1912, p.414, 420-1.

10. H Kemper, "Schwebende Aufhangung durch elektromagnetische Krafte:eine Moglichkeit fur eine grundsatzlich neue Fortbewegungsart", ETZ-A, Vol.59, No.15, 14 April 1938, p.391-5.

11. id "Elektrisch angetetriebene Eisenbahnfahrzeuge mit elektromagnetischer Schwebefuhrung", ibid, vol.74, No.1, January 1953, p.11-14.

12. "A Wound-Rotor Motor 1400 Feet Long", Westinghouse Engineer, vol.6, September 1946, p.160-1.

13. M F Jones, "Launching Aircraft Electrically", Aviation, vol.45, No.10, October 1946, p.62-5.

14. "An Electrical Runway", The Engineer, vol.182, 25 October 1946, p.379-80.

15. J M Shaw, H J H Sketch, J M Logie, "The Theory, Design Construction and Testing of an Electric Launcher", RAE Report No.AERO 2523, EL1484, July 1954.

16. I G Black, R F Gillie, C J Longley, T H Thomas, "Advanced Urban Transport", Warwick University/Lanchester Polytechnic Urban Transport Research Group Working Paper No.21, December 1973.

17. D L Hearn, N H Van Dorn, "Modern Transportation Systems", Automotive Engineering Congress, Detroit, 25 February - 1 March 1974, SAE Preprint No.740225.

18. G P Kalman, "Linear Motors to Power DOT's High Speed Research Vehicles", Ralway Gazette International, vol.130, No.10, October 1974, p.378-83.

19. J H Dannan, R N Day, G P Kalman, "A Linear Induction Motor Propulsion System for High Speed Ground Vehicles", Proc.IEEE, vol.61, No.5, May 1973, p.621-30.

20. M Guarino, "Development of the Linear Induction Motor in the United States, Past, Present, and Future," BMFT Statusseminar, 1978.

21. R W Crosby, R J Ravera, "The Transportation Advanced Research Projects Program - An Overview", Proc.Joint Automatic Control Conference, San Francisco, 22-24 June 1977, IEEE Publ.No. 77 CH 1220-3 CS, p.472-80.

22. T G Fellows, "High Speed Surface Transport", Railway Engineering Journal, vol.3, No.2, March 1974, p.1-20.

23. A Garnault, "Technical and Economical Results of the Use of Air Cushion in Guided Ground Transportation", International Automotive Engineering Congress, Detroit, 8-12 January 1973, SAE Paper No.730161.

24. Societe de l'Aerotrain, Publicity Material on Aerotrain Suburbain, "Cergy-Defense" and Aerotrain Tridim.

25. J Bertin, J Berthelot, "Aerotrain Tridim for Urban Transportation, a System Designed to Spare Initial Costs and Energy", Proc.International Hovering Craft, Hydrofoil and Advanced Transit Systems Conference, Brighton, 13-16 May 1974, p.307-15.

26. R G Hoch, M Berthelot, "Use of the Bertin Aerotrain for the Investigation of Flight Effects on Aircraft Engine Exhaust Noise", Third AIAA Conference, Palo Alto, July 1976, Paper No.76-534, also J. of Sound and Vibration, vol.52, No.2, 22 September, 1977, p.153-72.

27. H Yamashita, "Progress of Research and Development on Repulsive Levitation Railway in JNR", Quarterly Reports of the Railway Technical Research Institute, vol.19, No.3, September 1978, p.99-105.

28. R A Nelson,P W Shuldiner, M Miller, R L Winestone, P J Barbato, "Northeast Corridor Transportation Project Report", Office of High Speed Ground Transportation, April 1970, NTIS PB 190929.

29. W D Osmer, "Air Versus High Speed Rail Operating Costs for Intercity Passenger Travel", Boeing Transportation and Logistics Service Report, August 1979.

30. W Herbst, "Weight and Performance Characteristics of Magnetically Suspended High Speed Trains as Compared to Aircraft", 34th Annual Conference of the Society of Allied Weight Engineers, Seattle, 5-8 May 1975, Paper No.SAWE 1059.

31. OECD, "The Future of European Passenger Transport", Brussels, 1973.

32. Birlinghovener Kreis, "Komponenten fur Neue Technologien in Verkehr und Transport" BMFT Project NT91, Final Report, 1971.

33. BMFT, "Spurgebundener Schnellverkehr mit beruhrungsfreier Fahrtechnik, "Third Statusseminar, Berlin, 18-24 March 1974, BMFT-FBT 74-38 to 40 December 1974, (Also NTIS, N75-33941/65T)

34. G Winkle, "Forschungs-und Entwicklungsstand der elektromagnetischen Schwebetechnik in der Bundesrepublik Deutschland", ETZ-A, vol.96, No.9, September 1975, p.367-73.

35. A Lichtenberg, "Elektrodynamisches Schweben im Fernverkehr der Zukunft", ibid, p.378-83.

36. BMFT, "Spurgefuhrter Fernverkehr, Magnetbahnwicklung", Sixth Statusseminar, Konstanz, 1977.

37. D Rogg, H Schulz, "Systemtscheidung bei der Magnetschwebetechnik," Eisenbahntechnische Rundschau (ETR), vol.27, No.11, November 1978, p.721-8.

38. "Ministry Takes Over Maglev Projects" Railway Gazette Interntional, vol.134, No.10, October 1978, p.726.

39. HSB Studiengesellschaft mbH, "HSB-Studie uber ein Schnellverkehrssystem", Munich, 1971.

40. C Albrecht, G Bohn, "Neue spurgefuhrte Transportmittel",(Part I) Physikalische Blatter, vol,32, No.7, July 1976, p.309-26.

41. E Gottzein, K-H Brock, E Schneider, J Pfefferl, "Control Aspects of a Tracked Magnetic Levitation High Speed Test Vehicle", Automatica, Vol.13, No.3, 1977, p.205-23.

42. E Gottzein, W Cramer, "Critical Evaluation of Multivariable Control Techniques Based on Maglev Vehicle Design" Pro.Fourth IFAC International Symposium on Multivariable Technological Systems, Fredericton, July 1977.

43. E Gottzein, R Meisinger, L Miller, "The Magnetic Wheel in the Suspension of High Speed Ground Transportation Vehicles", IEEE Trans. on Vehicular Technology, vol. VT-29, No.1, February 1980, p.17-22.

44. HSB Studiengesellschaft mbH, "Trassierung einer Strecke Hannover-Kassel fur ein neuartiges Schnellbahnsystem (EMS-Technik) und Vergleich mit einer Rad-Schiene-Trassierung" Sixth BMFT Statusseminar, Konstanz, 1977, Section W.

45. P A A Koerv, "Control Systems for Operating the Long Stator Maglev Vehicle TR05", IEEE Trans. on Vehicular Technology, vol. VT-29, No.1, February 1980, p.23-34.

46. P Hartman, H Schulz, "Versuchs-und Demonstrationsanlage Magnetbahn zur Internationalen Verkehrsansstellung 1979 (IVA'79) in Hamburg, "Elektrische Bahnen, vol.77, No.5, May 1979, p.117-22.

47. D J Frenzel, H P Neubar, "Versuchsanlage Magnetbahn im Emsland", ibid, p.122-6.

48. Konsortium Magnetbahn Transrapid, "Im Jahr 1835 war es Nurnberg-Furth. Heute ist es Lathen-Dorpen. Das Emsland macht Bahngeschichte,", September 1978, MBB UR

49. Krauss-Maffei, "Transurban TAKT-System", Publicity Material, May 1973, BK5733.

50. H Weh, Linear Synchronous Motor Development for Urban and Rapid Transit Systems", IEEE Trans. on Magnetics, vol. MAG-15, No.6, November 1979, p.1422-7.

51. H Weh, M Shalaby, "Magnetic Levitation with Controlled Permanentic Excitation", IEEE Trans. on Magnetics, Vol. MAG-13, No.5, September 1977, p.1409-11.

52. H Weh, H Mosebach, H May, "Design and Technology of the Iron Core Linear Synchronous Motor for Advanced Ground Transportation", International Conference on Electrical Machines, Brussels, 1978, p. L4/5-1-10.

53. H Weh, H May, "Permanent Magnetic Excitation of Rotating and Linear Synchronous Machines", Journal of Magnetism and Magnetic Materials, vol.9, No.3, October-November 1978, p.173-8.

54. H May, M Shalaby, "Berechnung von geregelten Permanent-Magneten fur Tragen, Fuhren und Antriebsaufgaben", ETZ-A, vol.100, No.2, February 1979, p.63-7.

55. Transrapid-EMS, "Gessellschaft fur elektromagnetische Schnellverkehrssysteme", Publicity Material, December 1975.

56. BMFT, "Technology of an Iron Cored Long Stator Motor", Sixth Statusseminar, Konstanz, 1977, Section H.

57. H Weh, "Investigation into EMS Long Stator Technology", ibid Section G.

58. id., "Synchroner Langstatorantrieb mit geregelten, anziehend wirkenden Normalkraften, "ETZ-A, vol.96, No.9, September 1975, p.409-13.

59. H Weh, H Mosebach, W Deleroi, "Mechanical Suspended Vehicle with an Active Guideway", Proc.Second International Conference on Hovering Craft, Hydrofoil and Advanced Transit Systems, Amsterdam, May 1976, p.101-9.

60. A Lang, "Propulsion Systems for Magnetically Suspended Vehicles", International Conference on Electrical Machines, Brussels, 1978, p.L3/3-1-10.

61. Y Kyotani, "The Current State of Development of Noncontacting Suspension and Propulsion Systems in Japan", Japanese National Railways, 1977.

62. A Hayashi, "HSST:A Viable Alternative for Rapid Airport-City Centre Transportation", ICAO Bulletin, January 1978, p.21-4.

63. S Nakamura, A Hayashi, "Development of HSST System, "Japan Airlines, May 1979.

64. S Nakamura, "Development of High Speed Surface Transport System (HSST), "IEEE Trans. on Magnetics, vol. MAG-15, No.6, November 1979, p.1428-33.

65. J Ideguchi,Private Communication, 7 May 1980

66. S Nakamura, Y Takeuchi, M Takahasi, "Experimental Results of the Single Sided Linear Induction Motor", IEEE Trans. on Magnetics, vol. MAG-15, No.6, November 1979, p.1434-6.

67. Y Hika, Y Takeuchi, "Detail and Experimental Results of Ferromagnetic Leviation System of Japan Air Lines HSST-01/-02 Vehicles", IEEE Trans.on Vehicular Technology, vol.VT-29, No.1, February 1980, p.35-41.

68. S Yamamura, "Magnetic Levitation Technology of Tracked Vehicles - Present Status and Prospects", IEEE Trans. on Magnetics, Vol. MAG-12, No.6, November 1976, p.874-8.

69. B V Jayawant, P K Sinha, A R Wheeler, R J Whorlow, J Willsher "Development of a 1 Ton Magnetically Suspended Vehicle Using Controlled DC Electromagnets", Proc.IEE, Vol.123, No.9, September 1976, p.941-8.

70. D Linder, "Design and Testing of Low Speed Magnetically Suspended Vehicles", Second Conferences on Advances in Magnetic Materials and their Applications, London 1 - 3 September 1976, IEE Conference Publication No.142, p.96-9.

71. D J Dobbs, D Linder, D S Armstrong, R M Goodal, R J A Bevan, M G Pollard, R W Barwick, R A Williams, "Magnetically Levitated and Wheeled Minitram Comparison Study" BR Technical Report TR EDYN 5, January 1976.

72. "New Maglev Link Opens Door to World Sales", Electrical Review, vol.208, No.10, 13 March 1981, p.21,23.

73. R D Freuchte, R H Nelson, T A Radomski "Power Conditioning Systems for a Magnetically Leviated Test Vehicle" IEEE Power Electronics Specialists Conference, Palo Alto, June 1977, p.275-85; see also IEEE Trans. on Vehicular Technology, vol. VT-29, No.1, February 1980, p.50-60.

74. D A Young "Soviets Drawn to Magnetic Train", Industrial Research/Development, vol.20, No.12, December 1978, p.52.

75. IZV. VUZ Elektromekahnka, No.8, August 1977.

76. J R Powell, "The Magnetic Road: A New Form of Transport", IEEE-ASME Railroad Conference, Atlanta, 25-26 April 1963, Paper No 63-RR-4.

77. J R Powell, G R Danby "High Speed Transport by Magnetically Suspended Trains", Winter Annual Meeting, New York,27 November - 1 December 1966, Paper No ASME 66-WA/RR-5.

78. Id, "Magnetically Suspended Trains for Very High Speed Transport" Trans. 4th IECEC, Washington, 22-26 September, 1969, p.953-63.

79. Id, "The Linear Synchronous Motor and High Speed Ground Transport", Proc.6th IECEC, Boston, 3-6 August 1971, p.118-31.

80. C A Guderjahn, S L Wipf, H J Fink, R W Boom, K E MacKenzie, D Williams, T Downey "Magnetic Suspension and Guidance for High Speed Rockets by Superconducting Magnets", J Applied Physics, vol.40, No.5, April 1969, p.2133-40.

81. C A Guderjahn, S L Wipf, "Magnetic Suspension and Guidance for High Speed Trains by Means of Superconducting Magnets and Eddy Currents", Proc.1969 Cryogenic Engineering Conference, California, Advances in Cryogenic Engineering, vol.15, p.117-23.

82. P L Richards, M Tinkham "Magnetic Suspension and Propulsion Systms for High Speed Transportation" J Applied Physics, vol.43, No.6, June 1972, p.2680-91.

83. H T Coffey, F Chilton, L O Hoppie, "Magnetic Levitation of High Speed Ground Vehicles", Proc.Applied Superconductivity Conference, Annapolis. May 1972, IEEE Publication No 72 CHO 632-5 TABSC, p.62-75.

84. H T Coffey "SRI Magnetic Suspension Studies for High Speed Vehicles," Proc.1973 Croyogenic Engineering Conference, Atlanta, Advances in Cryogenic Engineering, Vol.19, p.137-53.

85. J R Reitz, R H Borcherts, L C Davis, T K Hunt, D F Wilkie, "Preliminary Design Studies of Magnetic Suspensions for High Speed Ground Transportation" Final Report to DOT, Report No FRA-RT-73-27, PB 223-237. March 1973.

86. J R Reitz, R H Borcherts, "US Department of Transportation Program in Magnetic Suspension (Repulsion Concept)", IEEE Trans. on Magnetics, Vol. MAG-11, No.2, March 1975, p.615-8.

87. Ford Motor Co. "Conceptual Design and Analysis of the Tracked Magnetically Levitated Vehicle Technology Program (TMLV)- Repulsion Scheme; Vol. I & II, "Final Report to DOT, February 1975, Report No FRA-OR&D-75-21 & 21A.

88. R D Thornton, H H Kolm, "Transportation System Employing an Electromagnetically Suspended, Guided and Propelled Vehicle", US Patent 3,768,417, 30 October 1973.

89. H H Kolm, R D Thornton, "The Magneplane:Guided Electromagnetic Flight", Proc.Applied Superconductivity Conference, Annapolis, May 1972, IEEE Publication No 72 CHO 632-5 TABSC, p.76-85.

90. R D Thornton, "Design Principles for Magnetic Levitation", Proc.IEEE, Vol.61, No.5, May 1973, p.586-97.

91. Id, "The Magneplane Linear Synchronous Motor Propulsion System", Conference on Linear Electric Machines, London, October 1974, IEE Conference Publication No. 120, p.230-5.

92. Y Iwasa, M O Hoenig, H H Kolm, "Design of a Full Scale Magneplane Vehicle" IEEE Trans. on Magnetics, Vol. Mag-10, No.3, September 1974, p.402-5.

93. Y Iwasa, W S Brown, C B Wallace "An Operational 1/25 Scale Magneplane System with Superconducting Coils" IEEE Trans on Magnetics, Vol. MAG-11, No.5, September 1975, p.1490-2.

94. C H Tang, W J Harrold, R S Chu "A Review of the Magneplane Project" IEEE Trans on Magnetics, Vol. MAG-11, No.2, March 1975, p.623-6.

95. C H Tang "Evaluation of Guideway Edge Effects" Presented by H H Kolm at Intermag Conference, London, 14-17 April 1975.

96. K Oshima, Y Kyotani "High Speed Transportation Levitated by Superconducting Magnet" Proc. 1973 Cryogenic Engineering Conference, Atlanta, Advances in Cryogenic Engineering, Vol.19, p.127-136.

97. Y Usami, J Fujie, S Fujiwara, "Studies on Linear Motor in the Institute of JNR" Conference on Linear Electric Machines, London, October 1974, IEE Conference Publication No,120, p.131-6.

98. Y Kyotani, Development of Superconducting Levitated Trains in Japan", Cryogenics, Vol.15, No.7, July 1975, p.372-6.

99. N Maki, H Okuda, T Tatsumi, J Fujie, T Iwahana, "A Combined System of Propulsion and Guidance by Linear Synchronous Motors", Tenth Annual Meeting of IEEE IAS, IEEE Conference Record 1975, IEEE Publication No 75 CHO 999-3IA, p.956-961.

100. H Ogiwara, N Takano, "Development of Superconducting Magnets for a Magnetically Suspended High Speed Train in Toshiba", Proc.Fifth International Cryogenic Engineering Conference, Kyoto, May 1974, p.94-6.

101. H Yamashita, "Progress of Research and Development on Repulsive Levitation Railway in JNR, "Quarterly Reports of Railway Technical Research Institute, Vol.19, No.3, September 1978, p.99-105.

102. "Special Issue on Levitation Railway",Railway Technical Research Institute Quarterly Reports, Vol.17, No.4, December 1976, p.145-181, and Vol.21, No.1, March 1980, p.1-56.

103. T Ohtsuka, Y Kyotani "Superconducting Maglev Tests" IEEE Trans. on Magnetics, Vol. MAG-15, No.6, November 1979, p.1416-21.

104. Id, "Recent Progress in Superconducting Magnetic Levitation Tests in Japan" Proc.IAS Annual Meeting, Cincinnati, 28 September-30ctober 1980, p.238-43.

105. Canadian Maglev Group "Study of Magnetic Levitation and Linear Synchronous Motor Propulsion" Annual Report for 1972, Phase I Contract Report to TDA, December 1972.

106. Id, "Analysis of Superconducting Magnetic Levitation and Linear Synchronous Motor Propulsion for High Speed Guided Ground Transportation" Annual Report for 1973, Phase II, Contract Interim Report to TDA, March 1974.

107. Id "Superconducting Magnetic Levitation and Linear Synchronous Motor Propulsion for High Speed Guided Ground Transportation" Phase II Contract Report to TDA, CIGGT Report No 75-5, March 1975.

108. Id, "Superconducting Linear Synchronous Motor Propulsion and Magnetic Levitation for High Speed Guided Ground Transportation", Phase III Contract Interim Report to TDA (Transport Canada), CIGGT Report No 76-7, March 1976.

109. Id, "Electrodynamic Suspension and Linear Synchronous Motor Propulsion for High Speed Guided Ground Transportation", Phase III Contract Report to Transport Canada Research and Development Centre, CIGGT Report No 77-13, September 1977. (Summary published separately as "The Canadian High Speed Magnetically Levitated Vehicle System, CIGGT Report No 77-12 September 1977, Verbatim Canadian Electrical Engineering Journal, vol.3, No.2, April 1978, p.3-26.

110. W F Hayes, "High Speed Electrodynamic Maglev Guided Ground Transportation System Conceptual Design Study", Final Report to Transport Canada Research and Development Centre, NRC Report No LTR-CS-176, September 1977.

111. Id, Private communication, 23 March 1979.

112. S A Haines "Going with Gauss, Maglev on Track", Science Dimension, Vol.12, No.6, June 1980, p.10-14.

113. C Albrecht, W Elsel, H Franksen, C P Parsch, K Wilhelm "Superconducting Levitated Systems :First Results with the Experimental Facility at Erlangen", Proc.Fifth International Cryogenic Engineering Conference, Kyoto, May 1974, IPC Science & Technology Press, p.28-34.

114. J Miericke, L Urankar, "Theory of Electrodynamic Levitation with a Continuous Sheet" Applied Physcs, Vol.2, 1973 p.202-211, ibid, vol.3, 1974, p.67-76.

115. P Klocker, C P Parsch, "ROSY, a Rotating Test Rig for Air Cored Linear Synchronous Motors", Siemens Review, Vol.65, No.10, October 1978, p.435-9.

116. J P Gibson, S Lingaya, "Control System for Air Cored Linear Synchronous Motors", ibid, p.439-43.

117. B Boning, W Leonhard "Propulsion Control of a Track Powered Linear Synchronous Motor for a Magnetically Levitated Vehicle on the Basis of Power Measurement in the Invertor Station", Proc.International Conference on Electrical Machines, Brussels, September 1978, p.L5/1-1-9.

118. J P Gibson, C P Parsch, "The Air Cored Linear Synchronous Motor as a Drive for Magnetically Levitated Vehicles", IAS Annual Meeting, Toronto, 1-5 October 1978.

119. G Bogner, "Applied Superconductivity Activities at Siemens", IEEE Trans on Magnetics, Vol. MAG.15, No.1, January 1979, p.824-7.

120. C P Parsch, Private Communication, 20 February 1980.

121. I A Alston, J M Clark, J T Hayden "Magnetic Suspension and Guidance of High Speed Vehicles" Final Report to Science Research Council, Cranfield CTS, Report 2, December 1972.

122. R G Rhodes, A R Eastham,M P Allen, B Mellen, "Magnetic Suspension of High Speed Trains" Report to Science Research Council, October 1972.

123. I A Alston "Superconducting Magnet Suspensions in High Speed Ground Transport" Cranfield CTS Report 5, August 1973, also TRRL Supplementary Report SR 28UC.

124. E Abel, A E Corbett, B E Mulhall, R G Rhodes, "Levitation and Propulsion of Guided Vehicles Using Superconducting Magnets" Conference on Linear Electric Machines, London, 21-23 October 1974, IEE Conference Publication No.120, p.223-9.

125. P E Burke, S Kuntz, G R Slemon "A Dual Linear Synchronous Motor for Maglev Vehicles" IEEE Trans. on Magnetics Vol. MAG 13, No.5, September 1977, p.1415-7.

126. R E Rhodes, B E Mulhall, E Abel, "Flying Land Vehicles using Superconducting Magnets", International Conference on Hovering Craft, Hydrofoil and Advanced Transit Systems, Brighton, 13-16 May 1974, p.157-66.

127. J P Howell, J Y Wong, R G Rhodes, B E Mulhall, "Stability of Magnetically Levitated Vehicles over a Split Guideway". IEEE Trans. on Magnetics, Vol. MAG-11, No.5, September 1975, p.1487-9.

128. R G Rhodes, B E Mulhall, E Abel, J P Howell, J L Mahtani, J Y Wong, Wolfson Progress Report to July 1975.

129. R G Rhodes, B E Mulhall, E Abel, J P Howell, M E Hunt, J L Mahtani, Wolfson Progress Report to September 1976.

130. E Abel, J L Mahtani, B E Mulhall, R G Rhodes, "An Assessment of Linear Superconducting Motors for Maglev" Second Conference on Advances in Magnetic Materials and their Applications, London, 1-3 September 1976, IEE Conference Publication No.142, p.125-7.

131. E Abel, J P Howell, J L Mahtani, R G Rhodes "Design Criteria for Rectangular Superconducting Coils for Transport Applications", Proc. Sixth International Conference on Magnet Technology (MT-6)Bratislava, 29 August - 2 September 1977, p.165-71.

132. W Leonhard "Technische Alternativen bei der Magnetschwebebahn" VDI Nach, 15 April 1977, p.42-3.

133. E Abel, "A Study of the Power Consumption of German Maglev Passenger Vehicles (EDS and EMS), Internal Memo, January 1978.

134. E Abel, R G Rhodes "Power Consumption for Alternative Maglev Systems" Electronics and Power, Vol.24, No.9, September 1978, p.673-4.

135. E Abel, J L Mahtani, R G Rhodes "Linear Machine Power Requirements and System Comparisons", IEEE Trans. on Magnetics, Vol. MAG-14, No.5, September 1978, p.918-20.

136. R G Rhodes, E Abel, J L Mahtani, "Magnetic Levitation and Linear Motor Propulsion for High Speed Vehicles" Report to the Science Research Council, January 1979.

137. E Abel, "A Cooperative Research Programme to Investigate the Application of Air Cored Linear Synchronous Machines to Advanced Ground Transport" Internal Memo, Warwick Maglev Group, December, 1978.

138. Id, "Linear Synchronous Machines as Traction Drives for Trains" Internal Memo, Warwick Maglev Group, January 1979.

139. R G Rhodes, E Abel, J L Mahtani, J H Rakels, "The Superconducting LSM for Vehicle Propulsion" Conference on Superconducting Electrical Machines, Oxford, 19-20 April, 1979, Paper No.18.

140. D S Armstrong, J W Teape, "Air Cored Linear Synchronous Motor : Model Tests", Colloquium on Advanced Ground Transportation Schemes, London 18 April 1979, IEE Digest No 1979/27, p.7.1 - 7.4.

141. H Autruffe, D Lancien, R Moulin "Les Etudes de Sustenation Magnetique a la SNCF" Rev.Gen.Chemins de Fer, Vol.94, No.9, September 1975, p.497-522.

142. D Lancien, R Moulin, "Moteur Lineaire Synchrone a Inducteur Supraconducteur" RGE, Vol.84, No. 7/8, July-August 1975, p.553-65.

143. E R Laithwaite, "Induction Machines for Special Purposes" London, Newnes, 1966.

144. S Yamamura, "Theory of Linear Induction Motors" New York, Wiley, 1972.

145. J A Wagner, "Bibliography on the Linear Induction Motor in High Speed Ground Transportation, Preprint to IEEE PES Summer Meeting, San Francisco, 9-14 July 1972, Paper C72-448-9, p.1-8.

146. E R Laithwaite, S A Nasar, "Linear Motion Electrical Machines", Proc. EEE, Vol.58, No.4, April 1970, p.531-42.

147. E R Laithwaite, "Linear Electric Machines - A Personal View", vol.63, No.2 February 1975, p.250-285.

148. M Pouloujadoff "Linear Induction Machines : I. History and Theory of Operation" IEEE Spectrum, vol.8 No.2, February 1971, p.72-80.

149. id; "Linear Induction Machines : II. Applications", ibid, vol 8, No.3, March 1971, p.79-86.

150. G P Kalman, D Irani, A Simpson "Electrical Propulsion System for Linear Induction Motor Test Vehicle", Proc.Fourth Intersociety Energy Conversion Engineering Conference, Washington, 22-26 September 1969, p.807-17.

151. K M Chirgwin "Test Results from the US Linear Induction Motor Research Vehicle Program" Conference on Linear Electric Machines, London, 21-23 October 1974, IEE Conference Publication No.120, p.236-43, plus addendum.

152. J J Stickler, "Comparison of Theories for High Speed Linear Induction Motors" IEEE Trans. on Vehicular Technology, vol. VT-29, No.1, February 1980, p.65-71.

153 R J A Bevan, G Kalman "Non Uniform Power Distribution in Linear Induction Motors due to End Effects", IEEE Trans. on Power Apparatus & Systems, vol. PAS-98, No.5, September-October 1979, p.1516-21.

154. E R Laithwaite, J F Eastham, H R Bolton, T G Fellows, "Linear Motors with Transverse Flux" Proc.IEE, Vol.118, No.12, December 1971, p.1761-7, Discussion ibid, vol.119, No.12, December 1972, p.1727-9.

155. J F Eastham, E R Laithwaite, "Linear Induction Motors as Electromagnetic Rivers" Proc. IEE, vol.121, No.10, October 1974, p.1099-1108.

156. J F Eastham, Discussion Meeting organised by the Science Research Council, London 18 January 1978.

157. W Farrer, IEE Discussion Meeting "Linear Induction Motors" London, 25 May 1978.

158. J A Ross, "ROMAG Transportation System" Proc.IEEE, vol.61, No.5, May 1973, p.617-20.

159. W J Holt, J A Ross, "New Developments in Magnetic Suspension and Propulsion for Transportation", IAS Annual, 1976, p.133-7.

160. R G Rule, R G Guilliland, "Combined Magnetic Levitation and Propulsion : the Mag-Transit Concept", IEEE Trans on Vehicular Technology, vol. VT-29, No.1, February 1980, p.41-9.

161. L del Cid, V Nene, "The Three Axial Forces of an Offset LIM" presented at Intermagnetics Conference, Florence, 9-12 May, 1978.

162. V D Nene, Private Communication, 2 August 1978.

163. R M Katz, A R Eastham, G E Dawson, D A Atherton, C L Schwalm, "Integrated Magnetic Suspension and Propulsion of Guided Ground Transportation Vehicles with a SLIM", IEEE Trans on Magnetics, vol. MAG-15, No.6, November 1979, p.1437-9, also IEEE Trans. on Vehicular Technology, vol. VT-29, No.1, February 1980, p.61-4.

164. G E Dawson, C L Schwalm, "Microcomputer Data System for Maglev Test Facility", Proc. International Symposium on Mini and Microcomputers, Montreal, 11-18 November 1977, IEEE Publ. No. 77CH134-4C, p.189-93.

165. A R Eastham, R M Katz "The Operation of a Single Sided Linear Induction Motor with Squirrel Cage and Solid Steel Reaction Rails" IEEE Trans on Magnetics, vol. MAG-16, No.5, September 1980, p.722-4.

166. G Sobolewski, D Gilmore "An Interim Report on the Development of a Light Steerable Axle Truck for Rail Passenger Vehicles", Proc. Biennial CIGGT Seminar on Railway Research, The Eighties : A New Rail Era, Kingston, 29-30 January 1978, CIGGT Report No 78-5, April 1978, p.61-72.

167. G E Brown "Linear Induction Motors for Intermediate Capacity Transit Systems" ibid, p.173-8.

168. C D English, G E Brown, "The Linear Induction Motor Propulsion System in Urban Transportation", IEEE Industry Applications Society Conference, Chicago, 11-14 October 1976, IEEE Publ.No. 76 CH 112-1-IA, p.138-44.

169. "UTDC's Test Track Completed" Railway Gazette International, vol.134, No.6, June 1978, p.382.

170. "Automated Transit Planned in Ontario" ibid, vol.134, No.11, November 1978, p.831.

171. A K Wallace, J H Parker, G E Dawson, "Slip Control for LIM Propelled Transit Vehicles" IEEE Trans. on Magnetics, vol. MAG-16, No.5, September, 1980, p.710-12.

172. "AC Motors for Traction" Brush Electrical Machines Ltd, Publicity Material, 1977.

173. J Chahal, IEE Discussion Meeting, "Linear Induction Motors" London, 25 May 1978.

174. J J Pierro, "Linear Electric Motor", US Patent 3,456, 136, 15 July 1969.

175. M Guarino, "Integrated Linear Electric Motor Propulsion Systems for High Speed Transportation", Conference on Linear Electric Motors and High Speed Electric Propulsion, Lyon 15 May 1974,Grenoble 16-17 May, 1974.

176. E Levi, "Linear Synchronous Motors for High Speed Ground Transportation" IEEE Trans. on Magnetics, vol. MAG-9, No.3, September 1973, p.242-7.

177. Id. "High Speed, Iron Cored, Synchronously Operating Linear Motors", Conference on Linear Electric Machines, London, 21-23 October 1974, IEE Conference Publication No.120, p.236-43.

178. Id. "Development of the Design for Iron Cored Synchronously Operating Linear Motors", Private communication, 7 July 1978.

179. T R Haller, W R Mischler "A Comparison of Linear Induction and Linear Synchronous Motors for High Speed Ground Transportation" IEEE Trans. on Magnetics, vol. MAG-14, No.5, September 1978, p.924-6.

180. J F Eastham "Iron Cored Linear Synchronous Machines" Electronics and Power, vol.23, No.3, March 1977, p.239-42.

181. M J Balchin "Operating Characteristics of a Heteropolar Linear Synchronous Motor" Colloquium on Advanced Ground Transportation Schemes, London, 18 April, 1979, IEE Digest No 1979/27, p. 4.1-4.4

182. A J Davis, J S Chahal, W Farrer, "A Study of Linear Synchronous Motors at Brush Electrical Machines Limited", ibid, p.5.1-5.4.

183. R M Davis, S.A.E. El-Drieny, D J Rhodes, "Linear Synchronous Motor Design and Performance" ibid, p.6.1-6.5

184. W Leitgeb, "Linearmotoren fur Fahrzeugantriebe", Siemens Zeitschrift, vol.45, 1971, p.177-80.

185. H Buchberger, W Leitgeb "Fahrzeugantriebe mit synchronen Linearmotoren", Elecktrische Bahnen, vol.46, No.4, April 1975, p.82-5.

186. W Leitgeb "Bauarten von Wanderfeldmaschinen fur den spurgebundenen Schnellverkehr" VDI-Z, vol.117, No.2, January 1975, p.57-63.

187. E Rummich "Machines Lineaires Synchrones" Bull. ASE, vol.63, No.23, 11 November 1972, p.1338-44.

188. J F Eastham, E R Laithwaite, "Linear Motor Topology", Proc. IEE, Vol.120, No.3, March 1973, p.337-43.

189. B-T Ooi, "Homopolar Linear Synchronous Motor Dynamic Equivalents" IEEE Trans. on Magnetics, Vol. MAG-13, No.5, September 1977, p.1424-6.

190. E Levi, J P Lee, F Lalezari, M Gemelos, "Computer Aided Conformal Mapping of Magnetic Fluxes in Saturated Inductor Motors" ibid, Vol. MAG-14, No.5, September 1978, p.927-9.

191. B K Bose, T A Lipo, "Control and Simulation of a Current Fed Linear Inductor Machine" IEEE Trans. on Industry Applications, Vol. IA-15, No.6, November/December 1979, p.591-600.

192. E Levi, L Birenbaum, Z Zabar, "Concerning the Design of Inductor Synchronous Motors fed by Current Source Inverters", IEEE Trans. on Magnetics, Vol. MAG-13, No.5, September 1977, p.1421-3.

193. G R Slemon, "A Homopolar Linear Synchronous Motor" International Conference on Electrical Machines, Brussels, 11-13 September 1978, p. L4/4-1 - 10.

194. I Boldea, S A Nasar, "Thrust and Normal Forces in a Segmented Linear Reluctance Motor", Proc IEE, Vol.122, No.9, September 1975, p.922-4.

195. S A Nasar, I Boldea, "Linear Motion Electric Machines" Wiley Interscience, 1976.

196. J D Edwards, A M El Antably "Segmental Rotor Linear Reluctance Motors with Large Airgaps" Proc.IEE, Vol.125, No.3, March 1978, p.209-14.

197. J S Chahal, "Linear Reluctance Machines for Urban Transport", International Conference on Electrical Machines, Brussels, 11-13 September 1978, p. L4/1-1 - 10.

198. J S Chahal, A J Davis "A Study of Linear Reluctance Machines at Brush Electrical Machines Limited" Colloqium on Advanced Ground Transportation Schemes, London, 18 April 1979, IEE Digest No 1979/27, p.5.5-5.8.

199. G Williams, J D Edwards, P Lindon, A M El-Antably, P D Luke, "Linear Reluctance Machines for Traction and Suspension of Guided Vehicles" ibid, p.8.1-8.2.

200. P Lindon, G Williams, P D Luke, A M El-Antably, J D Edwards "Closed Loop Control of Linear Reluctance Motors for Traction Applications", Second International Conference on Electrical Variable Speed Drives, London 25-27 September, 1979, IEE Conference Publication No.179, p.191-5.

201. A M El-Antably, J D Edwards, G Williams, P Lindon, P D Luke, "Steady State Performance Characteristics of Linear Reluctance Motors" IEEE Trans. on Magnetics, Vol.MAG-15, No.6 November 1979, p.1440-2.

202. D Kaye "Linear Motor for Mass Transport Improved by Pulsed Techniques" Electronic Design, Vol.19, No.10, 13 May 1971, p.30.

203. Japanese National Railways "Improvements in Propulsion Systems", UK Patent 1,360,834, 24 July 1974.

204. Y Amemiya, S Aiba, "Tractive Characteristics of DC Linear Motor with a Constant Current Applied to Ground Coil", Electrical Engineering in Japan, Vol.94, No.10, October 1974, p.97-103.

205. K Matsui, T Umemori,Y Taketsuna, Y Hosoda "DC Linear Motor Controlled by Thyristors and the Testing Equipment for its High Speed Characteristics" Conference on Linear Electric Machines, London 21-23 October 1974, IEE Conference Publication No.120, p.149-54.

206. K Matsui, T Umemori, M Toyoshima, K Katakami, S Osawa, "Ground Coil Assembly of a Linear Induction Motor with DC Levitating Armature for High Speed Vehicle", US Patent 3,855,485, 17 December 1974.

207. T Umemori, "Construction and Characteristics of Linear Thyristor Motors" Electrical Engineering in Japan, Vol.98, No.1, January-February 1978, p.28-36.

208. Id, "Power Supply and Control of Linear Thyristor Motors" ibid, p.96-105

209. T Umemori, M Kawashima, M Oda, S Otisawa, "Development of DC Linear Motor, I Fundamental Construction and Feasibility" IEEE PES Summer Meeting, Los Angeles, 16-21 July 1978, Paper F78 757-7.

210. T Umemori, Y Hosoda, M Iwasaki, M Toyoshima, "Development of a DC Linear Motor, II, Research for a Ground Coil and a Field Magnet", ibid, Paper F 78 756-9.

211. T Umemori "Construction and Characteristics of DC Linear Motor" Quarterly Reports of the Railway Technical Institute Vol.21, No.1 March 1980, p.22-8.

212. T Umemori, S Kumazawa, Y Furuto, T Kamoshida, "Study on Miniaturization of Electromagnet for DC Linear Motor" IEEE Trans. on Magnetics, Vol. MAG-16, No.5, September 1980, p.713-5.

213. G R Slemon, P E Burke, N Terzis, "A Linear Synchronous Motor for Urban Transit using Rare Earth Magnets" IEEE Trans. on Magnetics, Vol. MAG-14, No.5, September 1978, p.921-3.

214. K Murato, K Takei, Y Akihama, H Takahashi, H Akabane "Type L4 Linear Motor System Wagon Booster/Retarder for Shiohama Shunting Yard of the JNR", Hitachi Review, Vol.24, No.6, June 1975, p.269-76.

215. T Nondahl "Design Studies for Single Sided Linear Electric Motors : Homopolar Synchronous and Induction", Electric Machines and Electromechanics, Vol.5, No.1, January-February 1980, p.1-14.

216. G K O'Neill, H H Kolm, "Mass Driver for Lunar Transport and as a Reaction Engine" Journal of the Astronomical Sciences, Vol.25, No.4, October-December, 1977, p.349-63.

217. "The Electromagnetic Gun" International Defense Review, Vol.13, No.5, May 1980.

218. H H Kolm, P Mongeau, F Williams "Electromagnetic Launchers" IEEE Trans on Magnetics, Vol. MAG-16, No.5, September 1980, p.719-21.

219. A H Greene, W J Harrold, R S Kasevich, C H Tang, E Weiss, "Magneplane Linear Synchronous Motor Study" Final Report to MIT, Raytheon Company, Equipment Division, June 1973.

220. P C Sen "On Linear Synchronous Motor (LSM) for High Speed Propulsion" IAS Annual, 1975, p.261-7, and slightly modified as IEEE Trans. on Magnetics, Vol. MAG-11, No.5, September 1975, p.1484-6.

221. E Abel, "Linear Synchronous Machine Design for Minimum Terminal Rating" Technical Memo No.4, Warwick Maglev Group, March 1975, revised August 1978.

222. Id, "Flux Linkage and Induced Emf in Air Cored Machines" Technical Memo No.10, Warwick Maglev Group, February 1976, revised November 1978.

223. Id, "Fourier Analysis of Linear Machine Airgap Fluxes" Technical Memo No.13, Warwick Maglev Group, May 1975, revised November 1978.

224. B E Mulhall, D H Prothero, "Mechanical Stresses in Solenoid Coils", J Physics D, Vol.6, 1973, p.1973-7.

225. E Abel, unpublished work at University of Warwick, 1976.

226. D B Montgomery, "Solenoid Magnet Design" Wiley, New York, 1969.

227. R J Roark, "Formulas for Stress and Strain", McGraw Hill, New York, 1965.

228. D L Atherton, "Proposed Propulsion System for Magnetically Levitated Guided Ground Transportation" Proc. 1972 Applied Superconductivity Conference, Annapolis, May 1972, IEEE Conference Publication No. 72 CHOC.

229. J K Dukowicz, L O Hoppie, T C Wang "DC Magnetic Propulsion and Levitation System for High Speed Vehicles", US Patent No. 3,815,511, 11 June 1974.

230. H Weh, "Future Developments in Electromagnetic Lift, Guidance and Propulsion Systems" International Conference on Transportation Technology, Hamburg, June 1979, p.218-38.

231. E Abel, "Multilayer Region Analysis" unpublished work, University of Warwick, February 1974.

232. E M Freeman, Travelling Waves in Induction Machines : Input Impedance and Equivalent Circuits, PIEE, Vol.115, No.12, December 1968, p.1772-5.

233. R Zurek, "Methods of Levitation for Tracked High Speed Traffic", Endeavour, Vol.2, No.3, 1978, p.108-14.

234. K Glatzel, G Khurdok, D Rogg "The Development of the Magnetically Suspended Transportation System in the Federal Republic of Germany" IEEE Trans. on Vehicular Technology, Vol. VT.29, No.1, February 1980, p.3-16.

235. G Winkle, "Forschungs-und Entwicklungsstand der Elektromagnetischen Schwebetechnik in der Bundesrepublik Deutschland" ETZ-A, Vol.96, No.9, September 1975, p.367-73.

236. E Abel, "Aerodynamic Drag on German Revenue Vehicles, Internal Memo, University of Warwick, October 1977.

237. T Satow, M Tanaka, T Ogama, "AC Losses in Multifilamentary Superconducting Composites for Levitated Trains Under AC and DC Magnetic Fields" Proc. 1973 Cryogenic Engineering Conference, Atlanta, Advances in Cryogenic Engineering, Vol.19, p.154-61.

238. T K Hunt "AC Loses in Superconducting Magnets at Low Excitation Levels" J.Appl.Physics, Vol.45, No.2 February 1974, p.907-13.

239. G Ries, "AC Losses in Multifilamentary Superconductors at Technical Frequencies" IEEE Trans. on Magnetics, Vol. MAG-13, No.1, January 1977, p.524-9.

240. M E Hunt, J H Rakels, R G Rhodes, "The Effects of Magnetic Field Oscillations on Losses in Superconducting Composites", Cryogenics, Vol.22, No.7, July 1980, p.390-4.

241. J D Rogers, H J Boenig, W V Hassenzahl, R I Schermer, "Superconducting Magnetic Energy Storage For Electric Utilities and Fusion Systems", Proc.Joint Automatic Control Conference (JACC/78) Philadelphia, 18-20 October 1978, p.71-84.

242. J W H Chi "Conceptual Design of a Hollow Cable Conductor for the Large Coil Program" IEEE Trans. on Magnetics, Vol. MAG-15, No.1, January 1979, p.337-9.

243. S H Kim, S T Wang, W F Praeg, C I Krieger, M Lieberg, "Performance Tests of a 1.5 MJ Pulsed Superconducting Coil and its Cryostat" ibid, p.840-2.

244. K Kwasnitza, D Salathe, D G Howe, D U Gubser, "Pulsed Magnetic Field Losses and Critical Current Densities of V_3 Ga and Nb_3Sn Multifilament Superconductors", Cryogenics, Vol.22, No.2, February 1980, p.101-6.

245. E Abel, "Cryogenic Precooling of Coils for Pulse Operation" Technical Memo No.7, Warwick Maglev Group, August 1978.

246. W Schauer, "Conductor Materials for Cryomagnets" Proc. Fifth International Conference on Magnet Technology (MT-5), Rome, April 1975, p.629-43.

247. P H Melville, "Magnetic Propulsion for Magnetically Levitated Trains", Cryogenics, Vol.13, No.12, December 1973, p.716-7.

248. P H Melville, M N Wilson, B E Mulhall, "Propulsion of Magnetically Leviated Vehicles" ibid, Vol.15, No.5, May 1975, p.295.

249. S L Wipf "Propulsion of Magnetically Levitated Trains",ibid, Vol.16, No.5, May 1976, p.281-8.

250. H Brechna, H Kronig, "Three Phase Induction Motor with a Superconductive Cage Winding" IEEE Trans. on Magnetics, Vol.13, No.1, January 1979, p.715-8.

251. S P Bernard, D L Atherton "High Efficiency Flux Pump Power Supply Using Inductive Current Transfer" Rev.Sci.Instrm. Vol.48, No.10, October 1977, p.1250-2.

252. G J Homer, P J Houzego, C A Scott, M N Wilson, "A Thermally Switched Flux Pump" Rutherford Laboratory, Report RL-74-134, October 1974, (Also as IEEE Trans. on Magnetics Vol. MAG-11, No.2, 1975, p.576-9).

253. T C Bartram, "A Superconducting Fault Limiter : Its Construction and Testing" Conference on Superconducting Electrical Machines, Oxford 19-20 April 1979, Paper No.20.

254. "Upgrading Wheel/Rail Systems" Machine Design, Vol.51, No.9, 26 April 1979, p.52,

255. "The Bus That Will Ride Warwickshires Rails" Engineering Today Vol.5, No.17, p.17.

256. F M Russell "Mixed-μ Magnetic Levitation for Advanced Ground Transport System" Rutherford Laboratory RL-77-076/B, December 1977.

257. J D Cockroft "The Design of Coils for the Production of Strong Magnetic Fields" Phil.Trans. Royal Society, Vol.227, 31 May 1928, p.317-43.

258. D E Morris, R A Kilgore, "The Magnetic Field on the Axis of Circular Cylindrical Coils" NASA TN D-1013, April 1962.

259. G V Brown, L Flax, "Superposition Calculation of Thick Solenoid Fields from Semi-Infinite Solenoid Tables" NASA TN D-2494, September 1964.

260. F W Grover, "Inductance Calculations" Dover, New York, 1946.

261. T H Fawzi, P E Burke "The Accurate Computation of Self and Mutual Inductances of Circular Coils" IEEE Trans. on Power Apparatus and Systems, Vol. PAS-97, No.2, March/April 1978, p.464-8.

262. D B Montgomery, "Solenoid Magnet Design" Wiley Interscience, New York, 1969.

263. W Y Cheu "Interactive Computer Program for Coil Geometry Data Base Generation and Manipulation" IEEE Trans. on Magnetics, Vol. Mag-14, No.6, November 1978, p.1180-5.

264. D B Montgomery "The Generation of High Magnetic Fields" Reports on Progress in Physics, Vol.26, Institute of Physics and the Physical Society, 1963.